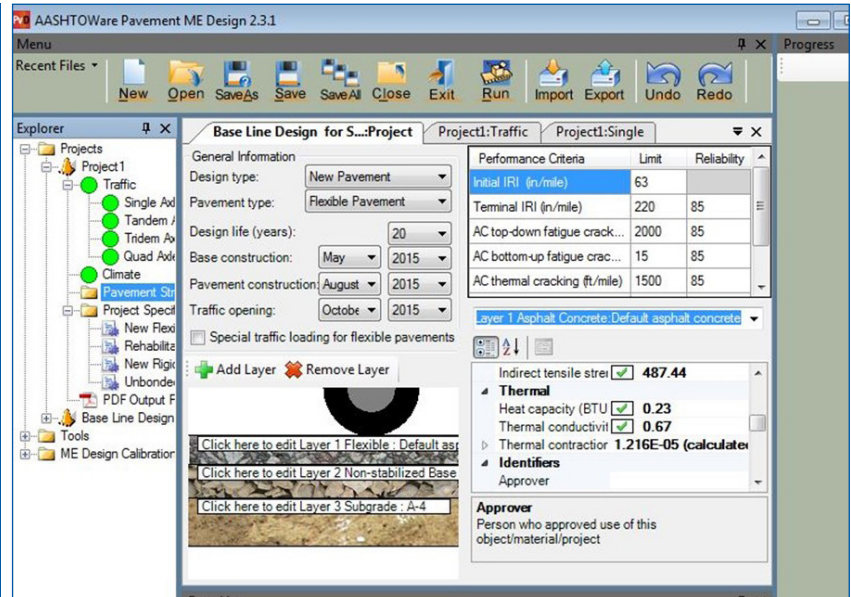# MOUNTAIN-PLAINS CONSORTIUM

MPC 19-380 | K. Ng, M. Brhanemeskel, and K. Ksaibati

Enhancement of Mechanistic-Empirical Pavement Design Guide for Roadway Design, and Construction in the State of Wyoming

MOUNTAIN-PLAINS CONSORTIUM REGION 8

Enhancement of Mechanistic-Empirical Pavement Design Guide for Roadway Design, and Construction in the State of Wyoming

Prepared by:

Kam Ng, Ph.D., P.E., Associate Professor

Melake A. Brhanemeskel, Graduate Assistant

Khaled Ksaibati, Ph.D., P.E., Professor

Department of Civil & Architectural Engineering
University of Wyoming
1000 E. University Avenue, Dept. 3295
Laramie, Wyoming 82071

March 2019

Acknowledgements

Disclaimer

The contents of this report reflect the views of the authors, who are responsible for the facts and the accuracy of the information presented. This document is disseminated under the sponsorship of the Department of Transportation, University Transportation Centers Program, in the interest of information exchange. The U.S. Government assumes no liability for the contents or use thereof.

ABSTRACT

To facilitate the implementation of Mechanistic-Empirical Pavement Design Guide (MEPDG) in Wyoming, this research investigated the relationships between subgrade resilient modulus (M_r) and the dynamic cone penetration (DCP) and the standard penetration test (SPT) results, selected three best subgrade M_r predictive models based on M_r and distress estimations, and determined the sensitivity of design parameters on pavement distresses. To enhance the prediction of pavement performance distresses, 11 subgrade M_r predictive models were evaluated, and three best models were identified and selected. All pavement distresses were found to be sensitive to asphalt concrete thickness and most distresses were found to be non-sensitive to asphalt concrete (AC) grade, base thickness, and base M_r. Finally, pavement design comparisons were made between the WYDOT 2012 user design guide and the recommended design guide based on locally calibrated properties. The average overall cost per square yard of the pavement structure designed using the WYDOT 2012 user design guide was found to be 21% higher than that based on the recommended design guide.

TABLE OF CONTENT

LIST OF TABLES

LIST OF FIGURES

1. INTRODUCTION

1.1 Overview

To account for different variables related to traffic, climate and materials, and their interactions affecting pavement performance, a research effort initiated by the National Cooperative Highway Research Program (NCHRP) has led to the development of a Mechanistic-Empirical Pavement Design Guide (MEPDG) documented in the NCHRP Report 01-37A (2004). This MEPDG method is being adapted by the Wyoming Department of Transportation (WYDOT) for roadway designs. However, the default input variables recommended in the MEPDG were developed based on national conditions that do not reflect the local Wyoming conditions. Due to potential differences between national and local conditions, and the significant influence of input data on the precision of pavement design using the MEPDG, many states have already instituted calibration procedures and developed calibration methods for partial or full calibration of the MEPDG on a local level (Hall 2010).

To optimize the effectiveness of using MEPDG in Wyoming, WYDOT funded a research project in 2013 with the main objective of characterizing representative local material properties for unbound subgrade layers to facilitate locally calibrated MEPDG implementation in the state. A comprehensive testing program was conducted by a research team at the University of Wyoming (UW) to collect pavement data from 12 locations throughout the state of Wyoming as shown in Figure 1.1 and summarized in Table 1.1. The testing program included the Dynamic Cone Penetromer (DCP) test, Standard Penetration Test (SPT), Falling Weight Deflectometer (FWD) test, R-value test using a stabilometer, soil classification, standard Proctor compaction test, and laboratory resilient modulus test. Also, a pavement distress survey was conducted at each test site in accordance with the Distress Identification Manual for the Long-Term Pavement Performance Program (Strategic Highway Research Program 1993), to document the existing pavement performance (Hellrung 2015).
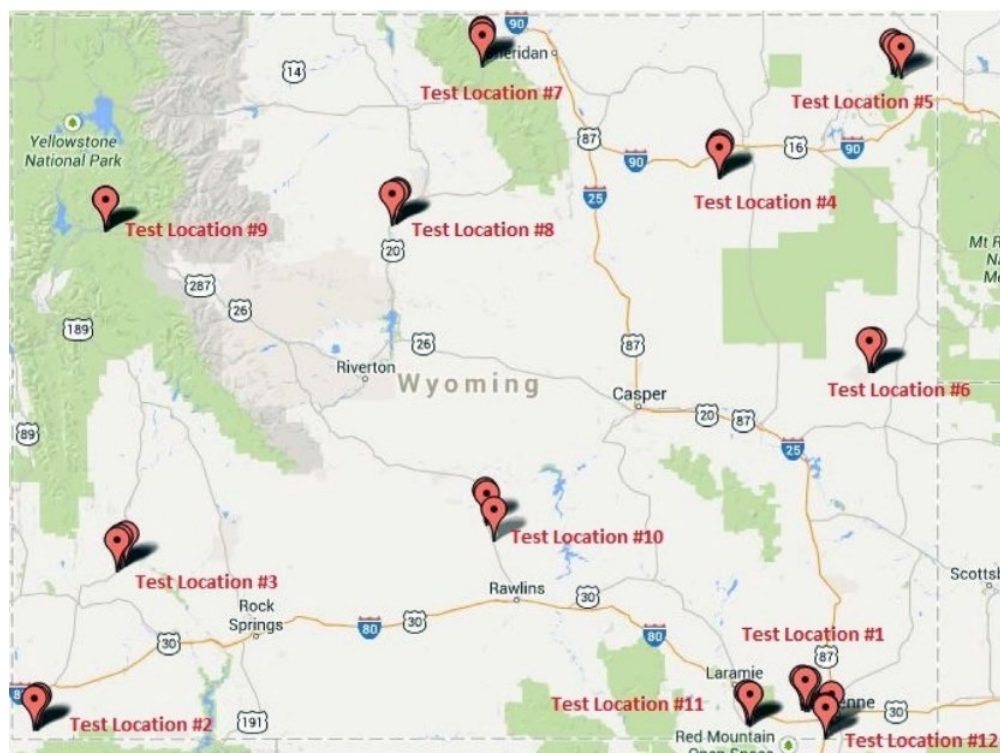
Figure 1.1 Twelve test locations on a Wyoming map (Source Ng et al. 2016)

This research focuses on correlating the representative resilient modulus (M_r) of unbound subgrade layers using field measurements from DCP and N-value obtained from SPT. Also, 11 subgrade M_r predictive models developed in past studies were evaluated. As a result, three suitable predictive models were recommended for MEPDG implementation in Wyoming. In addition, a sensitivity study was conducted to identify influential variables to pavement performance. Pavement design comparisons for typical and most common flexible pavements in Wyoming were completed. These design comparisons validated the benefits of using the locally calibrated MEPDG.

Table 1.1 Summary of test locations and test sites

Location	Name	Site	Asphalt Thickness (in.)	Base Thickness (in.)	Subgrade Soil	DCP Test	SPT Test
1	Happy Jack Road	A	12	9.5	A-6	No	Yes
		B	12	9.5	A-4		
		C	12	9.5	A-2-4		
2	Evanston South	A			A-1-b	No	No
		B	N/A	N/A	N/A		
		C			A-1-b		
3	Kemmerer – La Barge	A	13	9.5	A-6	No	Yes
		B	6.5	7	A-7-6		
		C	6	12	A-7-6		
4	Gillette – Pine Tree	A	4	12	A-6	Yes	Yes
		B	6.5	12	A-4		
		C	5	13	A-6		
5	Aladdin – Hulett	A	6	16	A-2-4	Yes	Yes
		B	6	18	A-2-4		
		C	6	12	A-6		
6	Lance Creek	A	4	10	A-7-6	Yes	Yes
		B	5	13	A-7-6		
		C	5	11	A-7-6		
7	Burgess Junction – Dayton	A	6	12	A-1-a	Yes	Yes
		B	6	12	A-1-b		
		C	5	9	A-1-b		
8	Thermopolis – Worland	A	11	13	A-2-4	Yes	Yes
		B	10	12	A-4		
		C	9	10	A-4		
9	Moran Junction – Dubois	A	4	6	A-6	Yes	Yes
		B	4	6	A-1-a		
		C	4	6	A-4		
10	Lamont – Muddy Gap	A	8	9	A-1-b	Yes	Yes
		B	8	7	A-6		
		C	7	12	A-6		
11	Laramie – Colorado St. Line	A	5	10	A-1-b	Yes	Yes
		B	5	10	A-1-b		
		C	5	10	A-2-4		
12	Cheyenne – Colorado St. Line	A			A-1-b	Yes	No
		B	Concrete Pavement	N/A	A-6		
		C			N/A		

N/A – Not Available; DCP – Dynamic Cone Penetrometer; and SPT – Standard Penetration Test

1.2 Background

The AASHTO 1993 Guide has many limitations in the design of pavement, including failing to include some factors and the variation of factors with time. Climate and environmental impact, increase in traffic volume and loading, and type of material used are factors that failed to be included in the AASHTO 1993 design guide.

In 2004, an extensive research initiated by the National Cooperative Highway Research Program (NCHRP) led to development of the MEPDG with the supporting software DARWin-ME™. The MEPDG requires over 100 total inputs for concrete and flexible pavement. Approximately 15 total inputs are considered in the AASHTO (1993) Guide. All the MEPDG inputs describe the climate, traffic, and material properties. Modulus values and thermal properties of each pavement material contribute to material factors. Specific site climate contributes to climate factors. Local data on the number of axels, which are classified by traffic weight and type, contribute to the traffic inputs. The MEPDG accommodates all these inputs through the software-based program and produces predicted pavement distresses during its lifetime by evaluating climate, traffic, and material properties.

Many state Departments of Transportation (DOTs) have already instituted calibration procedures and developed calibration methods for partial or full calibration of the MEPDG on a local level (Hall, 2010). Local calibration has been made particularly in North Carolina (Muthadi and Kim 2008), Washington (Li et al. 2009), Colorado (Mallela et al. 2012), Iowa (Kim et al. 2010), Utah (Darter et al. 2009), Montana (Von Quintus et al. 2007), Arizona (Darter et al. 2012), and Michigan, Ohio, and Wisconsin (Kang and Adams 2007). Dzotepe and Ksaibati (2010) identified that adequate funding is one of four critical components in the basic step toward a successful implementation of the MEPDG. Hence, millions of dollars have been invested by the above-mentioned state DOTs to support full implementation of the MEPDG.

Likewise, WYDOT has invested over $500,000 on implementation of the MEPDG (Kam and Ksaibati 2013). As a result, enhancement on the implementation of MEPDG has been made in Wyoming. After evaluating data from the several weigh-in-motion (WIM) stations placed in Wyoming, Applied Research Associates, Inc. (ARA) developed the required traffic inputs for Wyoming. Traffic characteristics, including axle load distributions, vehicle class distributions, monthly adjustment factors (MAF), and hourly truck distributions were determined for various roadway classifications including primary and secondary highways. Also, specific climate inputs were established as an essential input for the MEPDG by verifying and adjusting data from the National Climatic Data Center Wyoming. In addition, Dzotepe and Ksaibati (2010) recommended inclusion of three additional weather stations in Wyoming.

To characterize representative and local unbound subgrade material properties, research works were completed by UW and ARA. Henrichs (2015) conducted laboratory experiments to measure the representative resilient modulus (M_r) of subgrade materials and developed design charts and regression models. Hellrung (2015) established a back-calculation testing protocol and developed a predictive model for estimating the resilient modulus of subgrade soils in Wyoming. Hutson (2015) developed multi-regression models in terms of moisture content and R-values to effectively estimate M_r-values for subgrade layers. Mebrahtom (2017) characterized local base material properties and developed M_r predictive models for these base materials.

1.3　Problem Statement

Since the subgrade resilient modulus is an essential parameter for computing stresses and deformations induced in the pavement structure by applied traffic loads, correlation studies have been conducted to develop predictive models to estimate the resilient modulus as summarized in Table 1.2. However, similar predictive models based on DCP and SPT have not been developed in Wyoming. Such models would be a valuable tool for in-situ quantification of the resilient modulus of an existing subgrade material in a road rehabilitation project. Additionally, it is important to quantitatively compare and contrast different predictive models in terms of their respective pavement performance estimations to provide transportation agencies, like WYDOT, necessary recommendations for choosing the most accurate predictive model. Also, these data and results can be included into the existing Wyoming Pavement Management System (PMS) to facilitate full implementation of the MEPDG in Wyoming.

Table 1.2 Summary of predictive models for subgrade resilient modulus

Predictive Model	Description
A	Model Based on DCP from Task 1
B	Model Based on SPT from Task 1
C	Constitutive Models by Henrichs (2015)
D	Correlation Models Based on Back-Calculated Resilient Modulus using FWD Data by Hellrung (2015)
E	Design Tables of Resilient Modulus by Henrichs (2015)
F	Correlation Models based on R-value Measurements by Hutson (2015)
G	Correlation Models by Farrar et al. (1991)
H	Other Models by Applied Research Associates (ARA), Inc.
I	Correlation Models based on R-value Measurements by Hutson (2015)
J	Correlation Model by Farrar et al. (1991)
K	Constitutive Model by Applied Research Associates (ARA), lnc.
L	Correlation Model Based on Back-Calculated Mr using FWD Data by Applied Research Associates (ARA), lnc. (C-factor model)

Although ongoing research provides locally calibrated input parameters for MEPDG pavement design, it is indispensable to evaluate the sensitivity of influential variables of pavement materials on pavement performance predictions. This additional study will help designers and engineers optimize their pavement designs and facilitate the iterative design process while using the MEPDG design software known as AASHTOWare. Knowledge from the ongoing research and results from this proposed research should be integrated and presented through a series of trial pavement design examples that systematically articulate the whole pavement design process. This proposed research will enhance the pavement design procedure and efficiency, overcome shortcomings of the ongoing research, and expedite full implementation of locally calibrated MEPDG in Wyoming.

1.4　Objectives

This research focuses on calibrating local material properties for unbound subgrade layer and serves as a supplementary study to enhance the full implementation of the MEPDG in Wyoming, including rehabilitation roadway projects. This research project has the following principal objectives:
1) Evaluate the relationships between subgrade resilient modulus (M_r) and the dynamic cone penetration (DCP) and standard penetration test (SPT) results.
2) Select three best subgrade M_r predictive models based on M_r and distress estimations.
3) Determine sensitivity of the design parameters on pavement distresses in Wyoming.

4) Compare new flexible pavement design outcomes based on WYDOT MEPDG pavement design user's guide (2012) and the locally calibrated pavement input parameters from recent research studies.

1.5   Tasks

The research objectives were accomplished by completing the five research tasks described below.

1.5.1   Task 1. Evaluation of the Relationships between Subgrade M_r and DCP and SPT Results

This task focused on evaluating the relationship between resilient modulus of unbound subgrade layers and field measurements from DCP and SPT through a recently completed testing program. The correlation study used a multivariate regression method to relate the measured resilient modulus of subgrades to the Dynamic Cone Penetration Index (DCPI) and N-values obtained from SPT tests. A correlation model between M_r and DCPI was developed. No evidence was found to describe the linear relationship between M_r and SPT N-value. The developed model is intended for MEPDG Level 2 design and calibration.

1.5.2   Task 2. Assessment of Subgrade M_r Predictive Models

The two predictive models for subgrade resilient modulus, developed in the first task with other predictive models and summarized in Table 1.2, were evaluated to determine their relative accuracy on the estimation of flexible pavement performance using the software AASHTOWare. Predicted pavement distresses were generated by maintaining constant local traffic, climate conditions and pavement material, but employing different subgrade M_r values, which were estimated from the different predictive models developed from the testing program. The predicted pavement distresses were compared with actual pavement defects at each test site measured from the distress survey documented by Hellrung (2015). Quantitative assessment of predictive models provided the required foundation for developing pavement designs using the AASHTOWare considered in the fourth task. Finally, the three best predictive models were recommended for MEPDG implementation in Wyoming.

1.5.3   Task 3. Sensitivity Study

This task identified influential variables to pavement performance. Sensitivity analysis was performed to evaluate the effects of input parameters on MEPDG performance measures (cracking, rutting and smoothness). These variables included annual Average Daily Truck Traffic (AADTT), asphalt thickness, base thickness and modulus, subgrade modulus, climate, AC air void (%), and AC binder grade. They were selected because some distresses were found to be sensitive to these variables in the sensitivity studies completed by DOTs (Mallela et al. 2013 for CDOT, Schwartz et al. 2011 for IADOT, and Darter et al. 2009 for UDOT). The average input values used in Wyoming were taken as baseline values, and sensitivity analysis was performed considering one variable at a time. The completion of this task provided pavement designers a better understanding on the effect of the MEPDG input parameters that should be carefully quantified and adjusted to achieve a desired pavement performance in a pavement design process.

1.5.4   Task 4. Pavement Design Comparison

Using the knowledge and methods gained from previous tasks, several trial designs of flexible pavements were developed and conducted using the AASHTOWare. To cover a wide range of roads in Wyoming, interstate, primary, and secondary roads were selected for the pavement design comparison. The comparisons were conducted by selecting three projects and designing them using two different approaches. The first design approach (denoted as Design Approach 1) followed every step described in the WYDOT 2012 user design guide, and the second design approach (denoted as Design Approach 2) employed the locally calibrated M_r values for subgrade and base materials and locally calibrated distress coefficients. A cost analysis was performed to compare design approaches. This design comparison validates the benefits of using the locally calibrated subgrade material, base material, and distress coefficients in the MEPDG. The completion of this task facilitates implementation of the locally calibrated MEPDG in Wyoming.

1.5.5   Task 5. Conclusions and Recommendations

This task was accomplished by providing conclusion about the findings from this research. Recommendations for WYDOT engineers and designers for the proper utilization of this research outcome are also provided.

1.6   Report Focus and Organization

This report focuses on enhancement of the mechanistic-empirical pavement design guide for roadway design and construction in the state of Wyoming. All the elements covered in this report will enable designers and engineers to use the MEPDG in an effective way. Section 1 presents the background, objectives and tasks of this research. A literature review follows in Section 2. Section 3 focuses on the correlation study. Section 4 describes the selection of predictive models for resilient modulus of subgrade. Section 5 presents the sensitivity studies. Section 6 summarizes the design comparison. Finally, recommendations and conclusions are given in Section 7, which is followed by the references and appendices.

2. LITERATURE REVIEW

2.1 Introduction

This section presents the literature review of Mechanistic-Empirical Pavement Design Guide (MEPDG) at the national level, in Wyoming and other state DOTs. To implement the level 2 design input value for MEPDG, correlation studies between resilient modulus (M_r) and dynamic cone penetration test (DCP) completed by some states are described. Sensitivity study and its outcomes accomplished by different agencies are also described in this section. In addition, comparisons between American Association of State Highway and Transportation Officials (AASHTO) 1993 and MEPDG design guides for new flexible pavement are included.

2.2 MEPDG Development

AASHTO 1993 pavement design procedures have served as the main design guide for the past years. However, the design procedures were insufficient due to its limitations when considering increase in traffic volumes, effect of climate and other environmental parameters on pavement performance, and implementation of new materials. To eradicate the limitations, research was initiated by the National Cooperative Highway Research Program (NCHRP) in 2004 to develop a new pavement design guide known as the Mechanistic-Empirical Pavement Design Guide (MEPDG). The MEPDG considers the input parameters that influence pavement performances, such as traffic, climate, and pavement structure materials.

2.2.1 MEPDG in Wyoming

Due to potential differences between national and local conditions and the significant influence of input data on precision of the MEPDG, many states have already instituted calibration procedures and developed calibration methods for partial or full calibration of the MEPDG on a local level (Hall, 2010). Likewise, Wyoming Department of Transportation (WYDOT) has been working toward a full implementation of MEPDG and conducting many research works to optimize and enhance the effectiveness of MEPDG and to calibrate the local conditions in Wyoming.

A comprehensive testing program was completed on 12 locations. Each have three sites throughout the state. Subgrade soil samples were collected from the 36 sites for standard laboratory tests and resilient modulus (M_r) test. Representative resilient modulus (M_r) of the subgrade materials was determined in relation to the subgrade properties. Regression models and design charts for estimating resilient modulus of subgrade layers were developed using statistical methods for the state of Wyoming (Henrichs, 2015). Similarly, a comprehensive study on base materials was completed by Mebrahtom (2017).

Even though Level 1 design input for MEPDG requires laboratory testing of resilient modulus, it is costly, tedious, and time-consuming to measure the representative resilient modulus of each required site in the laboratory. Therefore, Level 2 input using correlated M_r with other material properties, such as California Bearing Ratio (CBR) and Resistance value (R-value), can be done to make use of M_r in MEPDG. In summer 2013, Falling Weight Deflectometer (FWD) tests were performed at 32 sites throughout the state of Wyoming to collect pavement deflection data for development of a back-calculation protocol for M_r of the subgrade soils. Additionally, two linear regression models were developed to correct the back-calculation resilient modulus to laboratory-measured M_r (Hellrung, 2015).

To facilitate future calibrations and optimize effectiveness of MEPDG in the state of Wyoming, an electronic database designated as *WYOMEP* and correlation models were developed. Data collected from

33 field test sites and corresponding laboratory tests were effectively stored and organized in *WYOMEP* and were developed using Microsoft® Access (Hutson 2015). Moreover, Bhattacharya et al. (2015) locally calibrated the distress transfer coefficients for the global MEPDG distress functions to estimate pavement distresses.

2.2.2 MEPDG in Other States

2.2.2.1 Kansas

Kansas Department of Transportation (KDOT) is moving toward implementation of the new Mechanistic-Empirical Pavement Design Guide (MEPDG) for pavement designs. Understanding the advantage and benefits of MEPDG over the AASHTO 1993 design guide, many research works were completed to enhance and facilitate full implementation of MEPDG in the state of Kansas. The major task in implementing MEPDG is validating and calibrating the national distress coefficients to local distress coefficients. Sun et al. (2015) did research to calibrate the Mechanistic-Empirical Pavement Design Guide for Kansas. To achieve the research objective, researchers evaluated and compared the actual pavement performance data obtained from the pavement management system (PMS) of the selected pavement projects with the MEPDG-predicted performance of the same projects. In this research, 60 projects were selected comprised of 28 flexible pavement and 32 rigid pavement projects. The projects were strategically selected so each project consisted of unique material properties, climate conditions and traffic capacities (Volume). For new flexible pavements, significant biases were existed between the measured and predicted distresses such as transverse cracking, longitudinal cracking, rutting and IRI. For new rigid pavements, the mean measured joint faulting was found to be very low as compared with the default MEPDG threshold value.

Due to large differences between the actual and MEPDG-predicted performance, the need for calibration of the MEPDG models to reflect the Kansas conditions was verified and local calibration was completed subsequently. Furthermore, Sufian (2016) completed research to update and locally calibrate MEPDG distress models for Kansas.

2.2.2.2 Iowa

Iowa Department of Transportation (IDOT) is one of the state DOTs that has invested millions of dollars to support full implementation of the MEPDG. A preliminary sensitivity study was initially performed by Kim et al. (2007) to evaluate the comparative effect of design input parameters of traffic, material properties and climate on the performance of two existing flexible pavements in Iowa. Twenty input parameters were assessed by evaluating the influence of each input variable on predicted distresses such as rutting, thermal cracking, top to bottom cracking, alligator cracking and IRI. Top to bottom cracking and total rutting were sensitive to most input variables. On the other hand, thermal cracking, IRI and alligator cracking were non-sensitive to most input variables.

Following the preliminary study, additional sensitivity studies were conducted by Ceylan et al. (2009) using the MEPDG software considering input variables (AC layer thickness, nominal maximum size, PG grade, base thickness, base Mr and.etc), which are particularly sensitive to flexible pavements in Iowa. Longitudinal cracking was found sensitive to most of the input parameters while alligator cracking was found non-sensitive to most of the input parameters. Furthermore, nationally calibrated MEPDG predicted distress models were assessed and evaluated. Then after the assessment and evaluation, huge biases and error were observed between the measured and predicted distresses. As a result, the local distress coefficients of MEPDG were calibrated and resulted in improving the accuracy of distress model prediction. For rigid pavement, the locally calibrated models for faulting and transverse cracking yielded better prediction with less biases and standard errors. For flexible pavements, although both locally and

nationally calibrated rutting predictive models give good prediction of total rutting, the locally calibrated rutting resulted in a better prediction than the nationally-calibrated model. No change was made to the nationally-calibrated model for alligator cracking as it provides acceptable prediction. (Ceylan et al. 2013).

2.2.2.3 Louisiana

Since the introduction of MEPDG developed under the NCHRP Project 1-37A, Louisiana Department of Transportation and Development (LADOTD) has started employing the MEPDG accompanied by DARWin 3.1 design software. Since the MEPDG distress prediction models were nationally calibrated, preliminary local calibration for rutting prediction model was completed and local calibration for the fatigue cracking prediction model was recommended (Wu and Yang 2012). Continuing the above research project, further local calibration was conducted on the nationally-calibrated distress models, which were found with large variation and bias. The outcome of the studies enabled LADOTD to have calibrated coefficients to implement the latest MEPDG software in their design and analysis of new and rehabilitated pavement structures in Louisiana (Wu and Xiao 2016).

2.3 Subgrade M_r Correlation

Resilient modulus (Mr) is an important and fundamental property of materials used in the design of unbound pavement structures. To provide mechanistically based design or analysis for pavements, it is necessary to determinate the resilient modulus of pavement materials. MEPDG allows three levels of inputs based on the type of project, availability of the resources, and access to the required information. For the highest level of accuracy, Level 1 inputs are used. To achieve this level of input, laboratory or field testing of the input parameter will be needed. Level 2 inputs provide a medium level of accuracy and could be obtained from limited test programs or could be estimated through correlated models. For providing the lowest level of accuracy, Level 3 is employed, and it allows the use of accepted values.

Applying level 1 for M_r value input is time-consuming and costly; therefore, engineers and designers prefer to use level 2 design input. In level 2 input, M_r value is correlated with other soil index properties such as California Bearing Ratio (CBR), Resistance value (R), dynamic cone penetration test index (DCPI), and numbers of blows taken from standard penetration test (SPT-N). This study focuses on the correlation of M_r-value with DCPI and SPT N-values.

2.3.1 Development of M_r Prediction Models from DCP Test Results

Since the DCP test is a relatively easy and simple field test, many researchers have correlated the DCPI value with M_r-value. Some correlations of M_r-value and DCPI are presented.

2.3.1.1 Louisiana Department of Transportation and Development

In the development of M_r prediction models from DCP test results, nine overlay rehabilitation pavement projects in Louisiana were selected. Each location consisted of three sites — 27 sites were selected in this investigation. DCPI, Log (DCPI), 1/DCPI, dry unit weight (γ_d), water content (w), and the ratio $\frac{\gamma_d}{w}$ were the variables considered in a multiple regression analysis. The M_r-value was plotted versus all selected variables to determine their respective correlations (Mohammad et al, 2007).

Based on the correlation matrix presented in Table 2.1, M_r and 1/DCPI showed a strong agreement with $R^2 = 0.87$ and p-value less than 0.001. In addition, dry unit weight (γ_d), water content (w), and the ratio γ_d/w were also found to have a significant relationship with M_r. The 1/DCPI, γ_d, w, and γ_d/w were further

9

used in the stepwise selection analysis. As a result of the statistical analysis, two models were developed. The first model correlates M_r directly to the measurements of DCPI, and the other includes some soil properties in addition to the DCPI (Mohammad et al. 2007).

Table 2.1 A correlation matrix for the DCP test results (Mohammad et al. 2007)

Soil para-meters	Coefficient of Determination (R² value)											
	γ_d	w	M_r	DCPI	γ_d/w	#200	%Silt	% Clay	LL	PI	Log (DCPI)	1/ DCP
γ_d	1.00	-0.89	0.42	-0.49	0.75	-0.52	0.10	-0.45	-0.49	-0.42	-0.43	0.34
w	-0.89	1.00	-0.48	0.5	-0.86	0.49	-0.11	0.44	0.48	0.43	0.45	0.36
M_r	0.42	-0.48	1.00	-0.76	0.56	-0.14	0.08	-0.27	-0.18	-0.13	-0.85	0.87
DCPI	-0.49	0.50	-0.76	1.00	-0.42	0.15	-0.004	-0.1	-0.24	0.29	0.96	-0.85
γ_d/w	0.75	-0.86	0.56	-0.42	1.00	-0.62	-0.03	-0.4	-0.47	-0.42	-0.39	0.33
#200	-0.52	0.49	-0.14	0.15	-0.62	1.00	0.29	0.4	0.46	0.37	0.14	-0.13
%Silt	0.10	-0.11	0.08	-0.004	-0.03	0.29	1.00	-0.76	-0.60	-0.64	-0.22	0.09
%Clay	-0.45	0.44	-0.27	-0.10	-0.40	0.4	-0.76	1.00	0.88	0.86	-0.31	-0.17
LL	-0.49	0.48	-0.18	-0.24	-0.47	0.46	-0.60	0.88	1.00	0.95	0.23	-0.09
PI	-0.42	043	-0.13	0.29	-0.42	0.37	-0.64	0.86	0.95	1.00	0.17	-0.04
Log (DCPI)	-0.43	0.45	-0.85	0.96	-0.39	0.14	-0.22	0.31	0.23	0.17	1.00	-0.97
1/DCP	0.34	0.36	0.87	-0.85	0.33	-0.13	0.09	-0.17	-0.09	-0.04	-0.97	1.00

DCPI- Dynamic cone penetration index, γd- Dry unit weight, ω- water content, PI- Plasticity index,
LL- Liquid limit, #200- Percent passing #200 sieve, %Silt- Percentage of silt, and %Clay- Percentage of clay

The first model, which shows the direct correlation between M_r and DCP, is given by Equation (2.1), and the second model, which includes the measurement of DCP and the physical properties of tested soil, is given by Equation (2.2)

$$M_r = \frac{151.8}{DCPI^{1.096}} \qquad R^2 = 0.91 \text{ \& RMSE} = 0.88 \text{ ksi} \tag{2.1}$$

$$M_r = 165.5\left(\frac{1}{DCPI^{1.147}}\right) + 0.0966\left(\frac{\gamma d}{w}\right) \quad R^2 = 0.92 \text{ and RMSE} = 0.86 \tag{2.2}$$

where,

M_r = resilient modulus (ksi),
DCPI = dynamic cone penetration index (mm/blow),
γ_d = dry unit weight,
w = water content (%),
R^2 = the coefficient of determination, and
RMSE = the root-mean-square error.

2.3.1.2 Mississippi

Intensive research was done to correlate the representative laboratory resilient modulus (M_r) with automated Dynamic Cone Penetration Index (DCPI) in the state of Mississippi. A total 180 test cylinders of soils were considered to determine the representative M_r value. Dynamic cone penetration tests were conducted in 12 locations, and soil index properties, such as dry density and water content of the locations, were also determined. The soil samples were classified into two groups: fine-grain and coarse-grain soils, in accordance with AASHTO M145-87. To determine variables to be included in the regression models as independent variables in addition to the DCPI, some basic soil properties were evaluated. Addition of important variables in the regression analysis enhances accuracy of the prediction

models. The variables considered in the analysis were dry density (γ_d), moisture content (w), liquid limit (LL), plasticity index (PI), percentage passing the #200 sieve, and uniformity coefficient (c_u). When each variable was plotted versus M_r value, some of these variables yielded poor correlation and were excluded from further considerations, including the PI for fine-grain soils and the percentage passing the #200 sieve for coarse-grain. All regression analyses were executed using the Statistical Package for the Social Sciences (SPSS) program. Finally, two regression models were developed for fine-grained and coarse-grained soils given by Equation (2.3) and (2.4), respectively (Rahim and George 2002)

$$M_r = a_o\,(DCPI)^{a_1}\left[\gamma_{dr}^{a_2} + \left(\frac{LL}{w}\right)^{a_3}\right] \quad R^2 = 0.71 \text{ and RMSE} = 31.6 \tag{2.3}$$

$$M_r = b_o\,\left(\frac{DCPI}{\log c_u}\right)^{b_1}\left[\gamma_{dr}^{b_2} + w^{b_3}\right] \quad R^2 = 0.72 \text{ and RMSE} = 12.1 \tag{2.4}$$

where,

    R^2 = the coefficient of determination,
    RMSE = the root-mean-square error,
    γ_{dr} = actual density / standard Proctor maximum density,
    w = actual moisture content/optimum moisture content, and
    $a_o, a_1, a_2\ a_3, b_o\ b_1, b_2, b_3$ = coefficiens given in Table 2.2.

Table 2.2 Summary of coefficients for two soil models

Soil Type	Coefficient	Value	t*	F*	RMSE	R^2
Fine-grained	a_o	27.86	4.33	46.5^a	31.45	0.71
	a_1	-0.114	2.05			
	a_2	7.82	4.60			
	a_3	1.925	10.81			
Coarse-grained	b_o	90.68	9.99	31.82^b	12.12	0.72
	b_1	-0.305	10.48			
	b_2	-0.935	1.98			
	b_3	0.674	2.17			

[a]–Critical F = 2.50; [b]–Critical F = 2.55, t*–Statistics, F*– Statistics, RMSE– root-mean-square error, and R^2– coefficient of determination.

2.4   Sensitivity Analysis by Other DOT's

A sensitivity analysis is the process of varying model input parameters (e.g., Hot Mix Asphalt or HMA, thickness, subgrade type, base type, Average Annual Daily Truck Traffic or AADTT, etc.) over a practical range and observing the relative change in model responses (e.g., cracking, rutting and smoothness). Most state DOTs conducted sensitivity analyses to identify influential variables in the design of pavement structures. The input variables selected by state DOTs for the sensitivity analysis and their outcomes for MEPDG flexible pavements are summarized in Table 2.3.

Table 2.3 Summary of input sensitivity results for MEPDG flexible pavements

State DOTs	HMA Pavement Input		Level of Sensitivity for Flexible Pavement Outputs				
	General Group	Parameter Selected	Alligator Cracking	Total Rutting	Transverse Cracking	IRI (Roughness)	Long. Cracking
Colorado Department of Transportation (CDOT) (Mallela et al. 2013)	Material	HMA thickness	VS	VS	VS	VS	-
		Base thickness	S	NS	NS	NS	-
		Sub base thickness.	NS	NS	NS	NS	-
		AC volumetric binder content	S	S	NS	NS	-
		AC air voids content	S	S	NS	VS	-
		Asphalt binder type	NS	VS	VS	VS	-
	Traffic	AADT	S	VS	NS	VS	-
	Climate	Climate	NS	VS	VS	VS	-
Iowa Department of Transportation (IADOT) (Schwartz et al. 2011)	Material	Performance grade (PG)	S	S	VS	NS	VS
		AC layer thickness	VS	VS	NS	NS	S
		Base layer thickness	S	S	NS	NS	S
		Type of base (Mr – moduli	VS	S	NS	S	VS
		Nominal max size	NS	NS	NS	NS	S
		AC volumetric properties	NS	NS	VS	NS	S
		Thermal conductivity	NS	NS	S	NS	NS
		Poisson's ratio	NS	S	NS	NS	NS
	Traffic	Tire pressure	NS	NS	NS	NS	S
		AADTT	NS	VS	NS	NS	S
		Traffic distribution	NS	NS	NS	NS	S
		Traffic velocity	NS	S	NS	NS	S
	Climate	Climate data	NS	S	VS	S	S

Long.−longitudinal, IRI−International Roughness Index, VS−very sensitivity, S−sensitivity, and NS−non-sensitivity

Table 2.3 Summary of input sensitivity results for MEPDG flexible pavements (continued)

| State DOTs | HMA Pavement Input | | Level of Sensitivity for Flexible Pavement Outputs | | | | |
	General Group	Parameter Selected	Alligator Cracking	Total Rutting	Transverse Cracking	IRI (Roughness)	Long. Cracking
Utah Department of Transportation (UDOT) (Darter et al. 2009)	Material	HMA thickness	-	S	-	-	-
		Base type	-	S	-	-	-
		Subgrade type	-	VS	-	-	-
		HMA air voids	-	VS	-	-	-
		HMA binder type	-	S	-	-	-
	Climate	Climate	-	S	-	-	-
Ohio Department of Transportation (ODOT) (Glover & Mallela 2009)	Material	HMA thickness	-	S	-	S	-
		Subgrade type	-	S	-	S	-
		Base type	-	S	-	S	-
		HMA air voids	-	S	-	S	-
	Climate	Climate	-	S	-	S	-
Maryland State Highway Administration (MDSHA) (Carvalho and Schwartz 2006)	Material	HMA thickness	S	S	-	-	-
		Base thickness	S	S	-	-	-
		Binder grade	S	S	-	-	-
		Binder content	S	S	-	-	-
		Base type	S	S	-	-	-
		Subgrade type	S	S	-	-	-
		Air void	S	S	-	-	-
	Traffic	AADT	S	S	-	-	-
		Vehicle class	S	S	-	-	-
		Vehicle class distributions	S	S	-	-	-
	Climate	Climate	S	S	-	-	-

Long.−longitudinal, IRI−International Roughness Index, VS−very sensitivity, and S−sensitivity

2.5   Design Comparison of AASHTO 1993 Guide and MEPDG

Since the evolution of MEPDG initiated by NCHRP Project 1-37A in 2004, many agencies have made a comparison between MEPDG and AASHTO 1993 Pavement Design Guide to validate the MEPDG. Many researchers like Carvalho et al. (2006) have explained the difficulty in directly comparing MEPDG and AASHTO 1993 due to the inequality in the number and feature of design inputs needed by the two methods. More than 100 input are required for the MEPDG while about 15 inputs are needed for the AASHTO 1993 guide. AASHTO 1993 guide uses the ESALS (Equivalent Single Axle load) as a traffic input while MEPDG uses the actual AADTT. In the climatic input, MEPDG uses the actual climate data from the weather stations placed on the site while AASHTO 1993 incorporates the environmental effect in terms of drainage coefficients, serviceability loss and effective M_r value of subgrade that considers seasonal variation. The way they assess performance of the pavement structure also differs. The AASHTO 1993 guide expresses the pavement performance in PSI (present serviceability index), and this PSI is the cumulative result of individual performance criterion. However, the performance criterion is assessed individually in MEPDG.

Therefore, Carvalho et al. (2006) used the empirical distress models that convert PSI into the individual structural distresses. In this case, permanent deformation and alligator fatigue cracking are used for comparison purpose. With the assumption that the nationally-calibrated MEPDG method is more sophisticated and believing that its performance prediction is accurate, the AASHTO 1993 guide was evaluated on how individual structural distresses differ in relation to environmental conditions and traffic for the selected sites. The following conclusions were made, based on the investigation:
- For flexible pavement in a warm climate and high traffic loading (i.e. 55 million ESALs), the AASHTO 1993 design guide underestimated bottom-up fatigue cracking and rutting.
- For pavements with low traffic loading and low to moderate temperatures, the AASHTO 1993 designs showed low variability in predicted pavement structural distresses.

Ahammed et al. (2011) examined results obtained from the design of flexible pavement using AASHTO 1993 design guide and using the nationally-calibrated MEPDG in Manitoba. This research was done on a flexible pavement, which consisted of all four layers of the pavement and analyzed for four different loading conditions (4.3 million ESALs, 8.6 19 million ESALs, 17.3 million ESALs, and 28.8 million ESALs). Manitoba axle load distribution was used for the traffic input, and Winnipeg climate station was used for the climate data input for the MEPDG. The same 90% reliability was employed for both methods. As a result, all the pavements designed using AASHTO 1993 yielded overestimated pavement performance compared to the result produced by the nationally-calibrated MEPDG. Permanent deformation and terminal IRI were taken to compare the above design results.

Li et al. (2010) made a comparison among the historical pavement performance of empirical AASHTO 1993 and MEPDG in Washington state. The pavement thicknesses for all the selected sections designed using empirical AASHTO 1993 design guide were found to be overdesigned.

2.6   Summary

This section presents the literature review of Mechanistic-Empirical Pavement Design Guide (MEPDG) at the national level, in Wyoming and other state DOTs. The development of resilient modulus (M_r) predictive models based on the dynamic cone penetration test (DCP) results by other states DOT's was described. Sensitivity analyses completed by different agencies were also described in this section. In addition, comparisons between AASHTO 1993 and MEPDG design guides for new flexible pavements were included.

3. EVALUATION OF THE RELATIONSHIPS BETWEEN SUBGRADE RESILIENT MODULUS AND DCP AND SPT RESULTS

3.1 Introduction

Resilient modulus (M_r) is an important and fundamental property of materials used in the design of unbound pavement structures. To provide mechanistically based design or analysis for pavements, it is necessary to determine the resilient modulus of pavement materials. The MEPDG allows three input levels based on the type of project, availability of resources, and access to the required information. Level 1 yields the highest level of accuracy. To achieve this level of input, laboratory or field measurement of the input parameters is needed. Level 2 provides a medium level of accuracy and could be either obtained from limited test programs or estimated through prediction models. Level 3 is employed for the lowest level of accuracy.

Applying Level 1 for M_r value input is time-consuming and costly. Hence, engineers and designers prefer to use Level 2 design input. For Level 2 input, the M_r value is correlated with other soil index properties, such as California Bearing Ratio (CBR), Resistance value (R), dynamic cone penetration test index (DCPI), and the number of hammer blows taken from a standard penetration test (SPT N-value). Correlation studies have been conducted to develop predictive models to correlate resilient modulus and many laboratory and field-measured subgrade soil parameters as summarized in Table 2.1. However, similar predictive models based on DCPI and SPT have not been developed in the state of Wyoming, and they would be a valuable tool for in-situ quantification of the resilient modulus of an existing subgrade material in a road rehabilitation project. This study focuses on the correlation of M_r-value with dynamic cone penetration test index (DCPI) and SPT N-value. The model development was done separately since both field tests were performed with different instruments and by different technicians.

3.2 Data Collection

To facilitate this correlation study, a comprehensive testing program was completed on 12 locations throughout the state of Wyoming, and each test location had three sites named as A, B, and C. Subgrade soil samples were collected from the 36 sites, and standard laboratory resilient modulus (M_r) tests were conducted (Henrichs, 2015). Although 36 M_r test results were prepared, only 26 DCP results were available. Due to large cobble and concrete equivalent materials, the DCP test was not performed in Test Location #2 (Evanston South). Likewise, test locations #1 and #3 failed to fulfill the standardized field-testing procedure of a DCP test, so no result was provided for these locations. Additionally, the DCP test was not performed at test location #12 Site C, because the pavement was concrete (Hutson, 2015). Similarly, 29 SPT results were available. Due to the presence of large cobbles and rigid pavement in test locations #2 and #12, the SPT test was not conducted. In addition, the SPT N-value for Site A in test location #1 was 0, which was found to be unrealistic because the SPT N-value cannot be 0. Thus, this site was discarded from analysis. Table 3.1 shows the laboratory and field test results of these test locations.

Based on correlation studies previously completed by other state DOTs, a range of variables were employed in the regression analysis. However, in this study, maximum dry unit weight (γ_d) and optimum water content (*w*), which are the most common variables, are only considered in addition to

the main independent variables of Dynamic Cone Penetration Index (DCPI) and SPT-N value to enhance the model prediction for resilient modulus.

Table 3.1 Laboratory and field test results

Test Location Name	Pro. No	M_r (psi)	SPT N-value	DCPI (in/blow)	w (%)	γ_d (pcf)	R-value
Happy Jack Road	0107-A	20081	NA	NA	11.2	121.1	14
Happy Jack Road	0107-B	10424	50	NA	23.2	93.5	47
Happy Jack Road	0107-C	10023	10	NA	21.1	100.3	19
Evanston South	2100-A	15646	NA	NA	6.1	132.9	73
Evanston South	2100-B	NA	NA	NA	NA	NA	NA
Evanston South	2100-C	16966	NA	NA	7.5	129.5	55
Kemmerer - La Barge	0P11-A	15246	11	NA	14.7	113.3	10
Kemmerer - La Barge	0P11-B	10976	20	NA	17	104.9	12
Kemmerer - La Barge	0P11-C	11909	6	NA	17	105.9	15
Gilette - Pine Tree	0300-A	10442	16	0.78	16.4	109.4	18
Gilette - Pine Tree	0300-B	14830	17	0.45	12.8	114.9	43
Gilette - Pine Tree	0300-C	10638	14	0.87	15.3	112.1	10
Aladdin - Hulett	0601-A	11847	26	0.28	8.3	117.2	67
Aladdin - Hulett	0601-B	10186	57	0.18	6.6	100.7	61
Aladdin - Hulett	0601-C	14707	27	1.08	15.6	108.7	18
Lance Creek	1401-A	9433	11	0.78	18.5	99.4	13
Lance Creek	1401-B	5994	28	0.40	23.4	93.8	11
Lance Creek	1401-C	5017	50	0.26	28.4	90.4	13
Burgess Junction - Dayton	0N37-A	12173	10	0.60	8.2	126.5	76
Burgess Junction - Dayton	0N37-B	16431	45	0.24	6.1	127.5	72
Burgess Junction - Dayton	0N37-C	14186	50	0.26	6.3	129.5	75
Thermopolis - Worland	0N34-A	7938	6	0.64	12.2	116.8	74
Thermopolis - Worland	0N34-B	14859	13	0.43	10.9	120.1	47
Thermopolis - Worland	0N34-C	10329	10	0.54	11.7	120	26
Moran Junction - Dubios	0N30-A	8936	11	0.76	14.7	113.8	14
Moran Junction - Dubios	0N30-B	16962	5	0.80	6.4	129.1	65
Moran Junction - Dubios	0N30-C	13880	18	0.47	11.8	119.7	35
Lamont - Muddy Gap	0N21-A	9083	45	0.27	7.8	120.5	73
Lamont - Muddy Gap	0N21-B	12825	11	0.27	14.9	111.2	12
Lamont - Muddy Gap	0N21-C	11014	12	0.87	13.5	116.8	12
Laramie-Colorado State Linez	0N23-A	12991	100	0.18	6.3	125.6	79
Laramie-Colorado State Linez	0N23-B	12321	100	0.36	5.2	126.6	75
Laramie-Colorado State Linez	0N23-C	16436	33.00	0.16	8.5	123.1	59
Cheyenne-Colorado State Line	I025-A	16354	NA	0.21	6.6	129.2	86
Cheyenne-Colorado State Line	I025-B	2836	NA	1.24	21.1	106	22
Cheyenne-Colorado State Line	I025-C	NA	NA	NA	NA	NA	NA

M_r−resilient modulus, SPT N-value−standard penetration test blow count, DCPI−dynamic cone penetration test index, w−optimum moisture content, γ_d−maximum dry unit weight, R-value−resistance value, and NA−not available.

3.3 Regression Analysis

3.3.1 Evaluation of Relationship between M_r and DCPI

All analyses in this section are based on 26 available DCP test results summarized in Table 3.1. The first step in the regression analysis is to prepare a correlation matrix, which describes the degree of relationship between individual variables. It helps to determine the independent variables (DCPI, maximum dry density and optimum moisture content) that have high degree of correlation with the dependent variable (M_r value), and it is a good indicator of possible multicollinearity that may exist between independent variables. Large correlation coefficients show the potential for multicollinearity. In this study, three correlation matrices were prepared for three groups of subgrade materials. Table 3.2 shows the correlation matrix and its coefficient of correlation (r) for all soil types, while Table 3.3 and Table 3.4 were prepared for soils with R-values less than or equal 50 and greater than 50, respectively. The closer absolute r-value to 1, the stronger linear relationship between the variables. An absolute r-value greater than 0.8 between the independent variables indicates that there is multi-collinearity between the variables. Figure 3.1 shows the scatter plot matrix of M_r, DCPI, optimum moisture content, and maximum dry density.
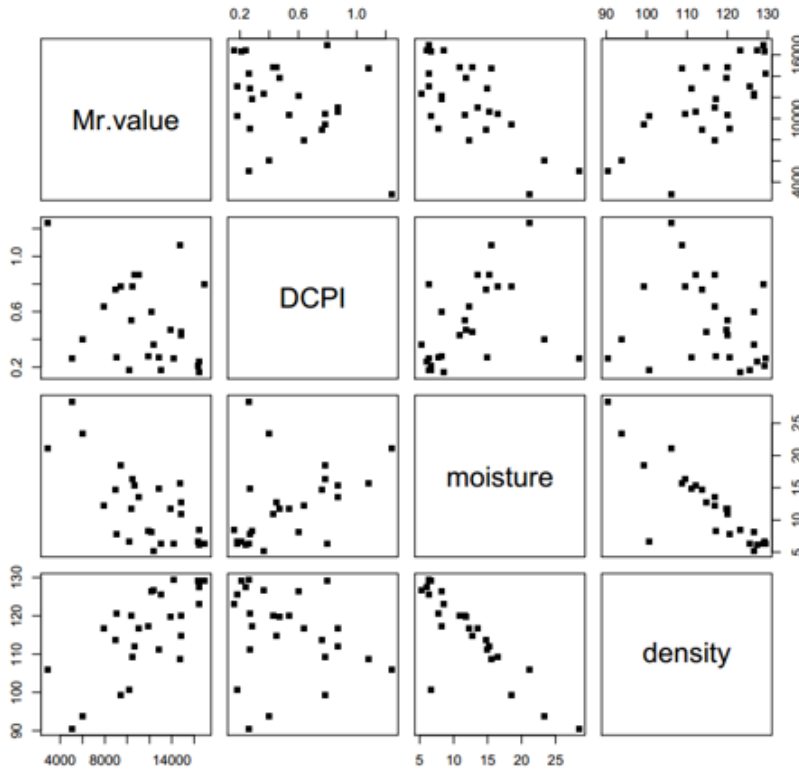
Figure 3.1 Scatter plot matrix of M_r, DCPI, optimum moisture content, and maximum dry density

Table 3.2 Summary of DCP r-value based on the correlation matrix for all soil types

Variable	r (coefficient of correlation)			
	M_r	DCPI	w	γ_d
M_r	1.000	-0.321	-0.706	0.711
DCPI	-0.321	1.000	0.413	-0.228
w	-0.706	0.413	1.000	-0.854
γ_d	0.711	-0.228	-0.854	1.000

M_r−resilient modulus, DCPI−dynamic cone penetration test index, w−optimum moisture content, and γ_d−maximum dry unit weight.

Table 3.3 Summary of DCP r-value based on the correlation matrix for soils with R-value ≤ 50

Variable	r (coefficient of correlation)			
	M_r	DCPI	w	γ_d
M_r	1.000	-0.198	-0.803	0.676
DCPI	-0.198	1.000	-0.049	0.087
w	-0.803	-0.049	1.000	-0.955
γ_d	0.676	0.087	-0.955	1.000

M_r−resilient modulus, DCPI−dynamic cone penetration test index, w−optimum moisture content, and γ_d−maximum dry unit weight.

Table 3.4 Summary of DCP r-value based on the correlation matrix for soils with R-value >50

Variable	r (coefficient of correlation)			
	M_r	DCPI	w	γ_d
M_r	1.000	-0.088	-0.524	0.628
DCPI	-0.088	1.000	0.349	0.200
w	-0.524	0.349	1.000	-0.302
γ_d	0.628	0.200	-0.302	1.000

M_r−resilient modulus, DCPI−dynamic cone penetration test index, w−optimum moisture content, and γ_d−maximum dry unit weight.

Negligible correlation coefficients (-0.321,-0.198, 0.088) were observed in Table 3.2 through Table 3.4 between the response variable (M_r-value) and the regressor (DCPI). In addition, a potential multicollinearity problem (r =0.854, r =0.955) was found for independent variables of optimum moisture content and maximum dry density when all soils and soils with R-value less than 50 are considered in the analysis. Model selection was conducted using hypothesis tests described in Section 3.3.2, and a best subset model selection described in Section 3.2.3.

3.3.2 Hypothesis Test (Using p-values to select model)

The linear relationship between M_r-value and DCPI was evaluated using the t-test with a significance level of 0.05. Variables considered in this study were DCPI, optimum moisture content, maximum dry density, and the interaction of DCPI with optimum moisture content and maximum dry density. In the hypothesis test with interaction, only the p-values of the interactive terms were evaluated. Table 3.5 shows the p-values for both interactive terms (i.e., DCPI:w and DCPI:γ_d) and main variables (i.e., DCPI, γ_d and w). The p-values for DCPI:w and DCPI:γ_d were found to be 0.0149 and 0.037,

respectively. These p-values show that the coefficients of the interactive term are statistically significant at 0.05 level. This means there is 95% confidence that the dependent and independent variables have a linear relationship. The developed regression model is given by Equation (3.1) and formulated by making the estimates in Table 3.5 as the coefficients of their respective variable. The coefficient of determination (R^2) of the developed model was found to be 0.67 and the adjusted R^2 was found to be 0.59.

Table 3.5 Summary of t-test results based on 26 samples from DCP

Variable	Estimate	Standard Error	t value	p-value
(Intercept)	-33128.7	18233.6	-1.817	0.0842
DCPI	120804.7	51733.4	2.335	0.0301
w	264.9	236.0	1.122	0.2750
γ_d	357.6	137.6	2.599	0.0172
DCPI:w	-1744.4	655.0	-2.663	0.0149
DCPI:γ_d	-846.8	379.1	-2.234	0.0371

DCPI−dynamic cone penetration test index, w−optimum moisture content, and γ_d−maximum dry density.

$$\widehat{Mr} = -33128.7 + 120804.7 \times (DCPI) + 264.9 \times (w) + 357.6 \times (\gamma_d) - 1744.4 \quad (3.1)$$
$$\times (DCPI \times w) - 846.8 \times (DCPI \times \gamma_d)$$

3.3.3 Best Subset Selection Model

Best subset selection was also employed to determine other potential models for estimating M_r. Best subset regression uses the model selection criteria, such as adjusted R-Square, Mallows C_p, Akaike information criterion (AIC), and Bayesian information criterion (BIC). A best model has a large adjusted R-Square (R_{sq-adj}), and low AIC, BIC, and C_p values. However, the model selection process must be restricted to proper models in which models with interaction terms contain all corresponding main variables. Models can be ranked by different model selection criteria values. The result of best subset selection is given in Table 3.6. The fifth model with the largest R_{sq-adj} of 0.585, C_p value of 6.00, AIC of 408.93, and BIC of 416.479 was the best model. This selected model is the same as Equation (3.1) determined based on the hypothesis test. However, according to the BIC criterion only, the first model, which includes maximum dry density, was the best model.

Table 3.6 Best subsets regression for DCP

N	(Inter.)	x1	x3	x4	x1:x3	x1:x4	R_{sq}	R_{sq-adj}	C_p	AIC	BIC
1	1	0	0	1	0	0	0.505	0.484	7.824	487.104	490.878
1	1	0	1	0	0	0	0.499	0.478	8.215	487.443	491.217
2	1	0	1	1	0	0	0.541	0.501	7.639	487.126	492.158
2	1	1	0	1	0	0	0.532	0.491	8.211	487.658	492.690
4	1	1	1	1	1	0	0.585	0.506	8.989	488.505	496.054
5*	1	1	1	1	1	1	0.668	0.585	6.000	484.715	493.521

N-number of variables in the model, Inter.-Intercept, x1-DCPI, x3-Optimum Moisture content, x4-Maximum Dry Density, x1:x3-DCPI×Optimum Moisture Content, x1:x4-DCPI× Maximum Dry Density, R_{sq}-R-squared, R_{sq-adj}-R-Square (adjusted), C_p-Mallowa Cp statistics, AIC-Akaike information criterion, BIC-Bayesian information criterion, 1-The variable is included in the model, and 0-the variable is not included in the model.

3.4   Evaluation of the Relationship between M_r and SPT N-value

The relationship between SPT N-value and M_r was evaluated using 29 SPT samples (see Table 3.1). In addition to SPT N-value, optimum moisture content, and maximum dry density were considered in the analysis. A scatter plot matrix for all the considered variables is shown in Figure 3.2. Table 3.7 through Table 3.9 show the correlation matrices of all the variables considered in this analysis. The relatively low r-values indicate no good correlation between M_r value and SPT N-value.
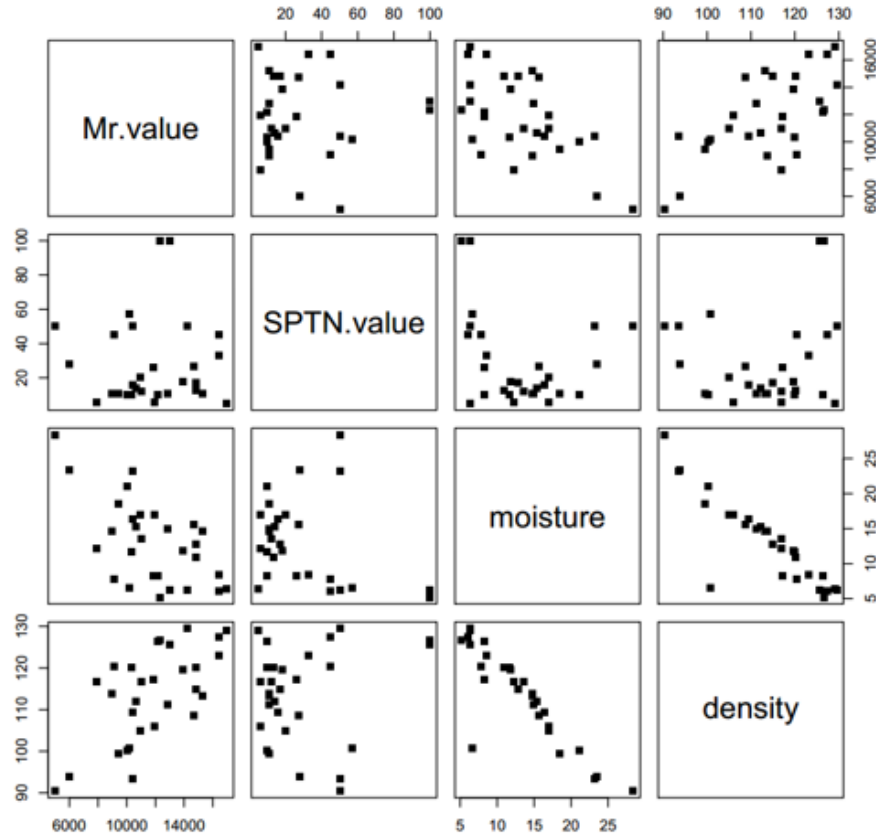
Figure 3.2 Scatter plot matrix of M_r, SPT N-value, optimum moisture content, and maximum dry density for all soils

Table 3.7 Summary of SPT r-value based on the correlation matrix for all soil types

Variable	r (coefficient of correlation)			
	M_r	SPT N	w	γ_d
M_r	1.00	-0.008	-0.607	0.658
SPT N-value	-0.008	1.00	-0.294	0.133
w	-0.607	-0.294	1.00	-0.880
γ_d	0.658	0.133	-0.880	1.00

M_r−resilient modulus, SPT N−standard penetration test number of blows, w−Optimum moisture content, and γ_d−maximum dry unit weight.

Table 3.8 Summary of SPT r-value Based on the correlation matrix for soils with R-value ≤ 50

Variable	r (coefficient of correlation)			
	M_r	SPT N	w	γ_d
M_r	1.000	-0.420	-0.755	0.686
SPT N-value	-0.420	1.000	0.718	-0.664
w	-0.755	0.718	1.000	-0.969
γ_d	0.686	-0.664	-0.969	1.000

M_r−resilient modulus, SPT N−standard penetration test number of blows, w−Optimum moisture content, and γ_d−maximum dry unit weight.

Table 3.9 Summary of SPT r-value based on the correlation matrix for soils with R-value >50

Variable	r (coefficient of correlation)			
	M_r	SPT N	w	γ_d
M_r	1.000	-0.021	-0.513	0.596
SPT N-value	-0.021	1.000	-0.633	0.027
w	-0.513	-0.633	1.000	-0.280
γ_d	0.596	0.027	-0.280	1.000

M_r−resilient modulus, SPT N−standard penetration test number of blows, w−Optimum moisture content, and γ_d−maximum dry unit weight.

The same procedure and test methods were employed to determine the linear relationship between M_r-value and SPT N-value value. The correlation study was conducted to consider the following variables: SPT N-value, optimum moisture content, maximum dry density, and the interactions of SPT N-value value and both optimum moisture and maximum dry density.

In the hypothesis test, variables with p-value greater than a significance level of 0.05 were dropped from the analysis. The analysis was continued with the remaining variables until all variables had p-values less than 0.05. Unfortunately, based on the t-test results given in Table 3.10, the p-values of the interaction terms were found to be 0.488 and 0.522. Therefore, both interaction terms were dropped from the analysis. The analysis continued to evaluate the significance of SPT N-value. Nevertheless, as indicated in Table 3.11, no independent variable was found statistically significant at the 0.05 level. SPT N-value was dropped from the analysis and this implies that there is no linear relationship between M_r-value and SPT N-value based on the t-test.

Table 3.10 Summary of t-test results based on 29 samples from SPT

Variable	Estimate	Standard Error	t value	p-value
(Intercept)	27072.11	43079.40	0.628	0.536
SPT N-value	-569.757	835.67	-0.682	0.502
w	-539.295	626.91	-0.860	0.399
γ_d	-66.429	305.66	-0.217	0.830
SPT N:w	8.462	12.00	0.705	0.488
SPT N:γ_d	-596.53	6.01	0.651	0.522

Table 3.11 Summary of t-test results based on 29 samples from SPT without interaction terms

Variable	Estimate	Standard Error	t value	p-value
(Intercept)	-511.12	12050.15	-0.042	0.967
SPT N-value	-16.45	19.04	-0.864	0.396
w	-116.99	169.37	-0.691	0.496
γ_d	126.09	86.72	1.454	0.158

Since a linear relationship between M_r value and SPT N-value cannot be found using the hypothesis test, best subset model selection was used. With this method, SPT N-value cannot be considered in any models to satisfy the selection criteria. Instead, as shown in Table 3.12, the first model included only the maximum dry density was selected as the best predictive model with the R_{sq-adj} of 0.412, C_p of -0.651, AIC of 452.838, and BIC of 456.94. Thus, the subset selection revealed no good relationship between M_r value and SPT N-value.

Table 3.12 Best subsets regression for SPT

N	(Inter.)	x1	x2	x3	x1:x2	x1:x3	R_{sq}	R_{sq-adj}	C_p	AIC	BIC
1*	1	0	0	1	0	0	0.433	0.412	-0.651	535.136	539.238
1	1	0	1	0	0	0	0.368	0.345	2.122	538.263	542.365
2	1	0	0	1	0	1	0.443	0.399	0.935	536.638	542.107
2	1	1	0	1	0	0	0.442	0.399	0.949	536.656	542.125
3	1	1	1	1	0	0	0.453	0.387	2.500	538.108	544.944
4	1	1	1	1	1	0	0.455	0.364	4.423	540.012	548.215
5	1	1	1	1	1	1	0.464	0.348	6.000	541.483	551.054

N-number of variables in the model, Inter.-Intercept, x1-SPT-N, x2-Moisture, x3-Density, x1:x3-SPT N×Moisture, x1:x4-SPT-N×Density, R_{sq}-R-squared, R_{sq-adj}-R-Square (adjusted), C_p-Mallowa Cp statistics, AIC-Akaike information criterion, BIC-Bayesian information criterion, 1-The variable is included in the model, and 0-The variable is not included in the model.

3.5   Evaluation of Relationship between M_r value, and SPT-N and DCPI at In-situ Conditions

It is believed that the statistical relationship between M_r value and the DCPI and SPT N-value will be improved if the correlation study is conducted by considering all the dependent and independent parameters at in-situ conditions. Therefore, additional correlation analyses were conducted to examine the linear relationships between M_r value measured at in-situ condition and DCPI and SPT N-value. Table 3.13 summarizes the measured M_r value, DCPI, and SPT N-value at the in-situ condition (Henrichs, 2015).

The analyses were performed using 13 DCPI and 16 SPT N-values. However, poor correlation results were obtained based on the hypothesis tests. The correlation matrices summarized in Table 3.14 and Table 3.15 show that relatively low coefficients of correlation were obtained. Similarly, the p-values of all the variables presented in Table 3.16 and Table 3.17 were greater than the 0.05 level of significance. In conclusion, a good relationship cannot be obtained between in-situ measured M_r values and the field-measured DCP and SPT values.

Table 3.13 Summary of measured M_r value, DCPI and SPT N-value results at in-situ condition

Test Location Name	Pro.No	M_r (psi)	SPT N value	DCPI (in/blow)	w (%)	γ (pcf)	R-value
Kemmerer - La Barge	0P11-A	3814	11	NA	14.7	113.3	10
Kemmerer - La Barge	0P11-B	11903	20	NA	17	104.9	12
Kemmerer - La Barge	0P11-C	5101	6	NA	17	105.9	15
Gilette - Pine Tree	0300-A	11846	16	0.78	16.4	109.4	18
Gilette - Pine Tree	0300-B	5809	17	0.45	12.8	114.9	43
Gilette - Pine Tree	0300-C	6902	14	0.87	15.3	112.1	10
Aladdin - Hulett	0601-A	4931	26	0.28	8.3	117.2	67
Aladdin - Hulett	0601-C	14061	27	1.08	15.6	108.7	18
Lance Creek	1401-A	9374	11	0.78	18.5	99.4	13
Lance Creek	1401-B	7083	28	0.40	23.4	93.8	11
Burgess Junction - Dayton	0N37-A	13723	10	0.60	8.2	126.5	76
Burgess Junction - Dayton	0N37-C	13848	50	0.26	6.3	129.5	75
Thermopolis - Worland	0N34-B	15593	13	0.43	10.9	120.1	47
Thermopolis - Worland	0N34-C	11014	10	0.54	11.7	120	26
Moran Junction - Dubios	0N30-A	3690	11	0.76	14.7	113.8	14
Lamont - Muddy Gap	0N21-B	14207	11	0.27	14.9	111.2	12

M_r−resilient modulus measured in situ condition, SPT N−standard penetration test blow count, DCPI−dynamic cone penetration test index, w−in situ moisture content, γ_d−in situ dry unit weight, R-value−resistance value.

Table 3.14 Summary of correlation matrix for all soil types for M_r, DCPI, w, and γ_d

Variable	r (coefficient of correlation)			
	M_r	DCPI	w	γ_d
M_r	1.000	-0.039	-0.263	0.333
DCPI	-0.039	1.000	0.377	-0.311
w	-0.263	0.377	1.000	-0.958
γ_d	0.333	-0.311	-0.958	1.000

M_r−resilient modulus, DCPI−dynamic cone penetration test index, w−in situ moisture content, and γ_d−in situ dry unit weight.

Table 3.15 Summary of correlation matrix for all soil types for M_r, SPT N-value, w, and γ_d

Variable	r (coefficient of correlation)			
	M_r	SPT N	w	γ_d
M_r	1.00	0.232	-0.270	0.303
SPT N-value	0.232	1.000	-0.267	0.202
w	-0.267	0.377	1.00	-0.959
γ_d	0.303	-0.202	-0.959	1.00

M_r−resilient modulus, SPT N−standard penetration test number of blows, w−in situ moisture content, and γ_d−in situ dry unit weight.

Table 3.16 Summary of t-test results based on 16 SPT-N samples

Variable	Estimate	Standard Error	t value	p-value
(Intercept)	-33484.48	62828.61	-0.533	0.604
SPT N	81.37	108.92	0.747	0.469
Moisture	437.63	952.51	0.459	0.654
Density	314.89	438.78	0.718	0.487

Table 3.17 Summary of t-test results based on 13 DCP samples

Variable	Estimate	Standard Error	t value	p-value
(Intercept)	-44297.7	64092.3	-0.691	0.507
DCPI	191.7	5314.6	0.036	0.972
Moisture	590.3	987.2	0.598	0.565
Density	407.7	455.2	0.896	0.394

3.6   Summary

This section discusses assessment of relationships between subgrade M_r and the Dynamic Cone Penetration (DCP) and the Standard Penetration Test (SPT) test results. A model to predict M_r value based on DCP results was developed. The coefficient of determination (R^2) of this model was 0.67, and the adjusted R^2 was 0.59. However, the similar hypothesis test yields a low correlation between SPT N-value and M_r. Therefore, no linear relationship was found for SPT to estimate M_r value at a significance level of 0.05.

4. ASSESSMENT OF RESILIENT MODULUS PREDICTIVE MODELS

4.1 Introduction

One predictive model for subgrade resilient modulus was developed in Section 3. The model based on Dynamic Cone Penetration (DCP) developed in Section 3 and other predictive models developed from previous MEPDG research (Ng et al., 2016) are summarized in Table 4.1. These models were evaluated for their relative accuracy on the estimation of flexible pavement performance using the software AASHTOWare. The model developed and based on DCP from Task 1 was excluded in this assessment due to missing DCPI at the test sites selected for the comparison. Predicted pavement distresses were generated by keeping traffic, climate, and pavement material constant while employing different subgrade M_r values estimated using the different predictive models. Quantitative assessment of predictive models was done to provide the required foundation for developing pavement design comparisons using the AASHTOWare considered in Section 6. Finally, the three best predictive models that predicted closer distress performance to the actual measured distress of the sites are recommended for MEPDG implementation in Wyoming.

Table 4.1 Summary of predictive models for subgrade resilient modulus

Predictive Model	Description	Equation/ Table
A	Model Based on DCP from Task 1	Eq. (3.1)
B	Constitutive Models for all type of soils by Henrichs (2015)	Eqs. (4.1) and (4.2)
C	Constitutive Models for soils with different R-value by Henrichs (2015)	Eqs. (4.3), (4.4) and (4.5)
D	Design Tables of Resilient Modulus by Henrichs (2015)	Tables 4.5 and 4.6
E	Correlation Models Based on Back-Calculated Resilient Modulus using FWD Data- intercept model by Hellrung (2015)	Eq. (4.6)
F	Correlation Models Based on Back-Calculated Resilient Modulus using FWD Data –C factor model by Hellrung (2015)	Eq. (4.7)
G	Correlation Models based on R-value Measurements by Hutson (2015)	Eq. (4.8)
H	Correlation Model by Farrar et al. (1991)	Eq. (4.9)
I	Constitutive Model by Applied Research Associates (ARA), lnc. (k1, k2…)	Eq. (4.11)
J	Correlation Model Based on Back-Calculated M_r using FWD Data by Applied Research Associates (ARA), lnc. (C-factor model)	Eq. (4.12)
K	Correlation model Based on R-value Measurements by Applied Research Associates (ARA), lnc.	Eq. (4.13)

4.2 Subgrade M_r Predictive Models Developed by Different Researchers

4.2.1 Subgrade M_r Predictive Models and Design Tables Developed by Henrichs (2015)

Henrichs (2015) conducted a regression analysis to locally calibrate the generalized constitutive triaxial stress model developed as a result of a Joint Transportation Research Program (JTRP). The constitutive triaxial stress model was modified by selecting significant parameters to enhance the prediction of subgrade M_r values in the state of Wyoming. As per the t-test, the confining pressure and deviator stress were the most significant parameters and the developed model is given in Equation (4.1). Similarly, without sorting the data based on resistance value (R-value) of the subgrade soils, regression analysis was performed to yield a single Equation (4.2) for k_4 coefficient.

$$\widehat{M_r} = k_4 \times \left(\sigma_c / P_a\right)^{k_5} \times \left(\sigma_d / P_a\right)^{k_6} \times P_a \qquad (4.1)$$

$$k_4 = 10^{\left[b_0 + b_1\gamma + b_2w + b_3R_{cat} + b_4R_{cat}\gamma_d + b_5R_{cat}w + b_6\left(\sigma_c / P_a\right)b_7\left(\sigma_d / P_a\right)\right]} \qquad (4.2)$$

where,

$\widehat{M_r}$ = predicted resilient modulus (psi),
σ_c = confining stress (psi),
σ_d = deviator stress (psi),
P_a = atmospheric pressure = 14.696 psi,
γ_d = maximum unit weight,
w = optimum moisture content,
R_{cat} = 0 for R > 50 and 1 for R ≤ 50,
k_4, k_5, and k_6 = regression coefficients, and
b_0, b_1, b_2, b_3, b_4, b_5, b_6 and b_7 = constants summarized in Table 4.2.

The regression coefficients b_0 to b_7, k_5 and k_6 for all soil types are shown in Table 4.2.

Table 4.2 Regression estimates for all soils

Regression Coefficient	Estimates	Standard Error	t-value	p-value
b_0	2.95733	0.935056	3.163	0.00539
b_1	0.00895	0.003311	2.702	0.01460
b_2	-0.02973	0.018522	-1.605	0.12583
b_3	3.44703	1.624022	2.123	0.04792
b_4	-0.02540	0.011350	-2.380	0.03812
b_5	-0.02341	0.028974	-0.808	0.42966
b_6	-9.57986	6.456833	-1.484	0.15519
b_7	0.81530	0.333305	2.446	0.02494
k_5	0.82712	0.493717	1.675	0.11116
k_6	-0.77521	0.283459	-2.735	0.01361

Additionally, Henrichs (2015) grouped the data in terms of R-value greater than 50 and less than 50. Regression analysis was performed to develop two equations for k_4 coefficient. Equation (4.4) was developed for soils with R-value greater than 50, and Equation (4.5) was developed for soils with R-value less than 50. Equation (4.3) is the locally calibrated constitutive model, which is the same as Equation (4.1).

$$\widehat{M_r} = k_4 \times \left(\sigma_c/P_a\right)^{k_5} \times \left(\sigma_d/P_a\right)^{k_6} \times P_a \tag{4.3}$$

where,

σ_c = confining stress (psi),
σ_d = deviator stress (psi),
P_a = atmospheric pressure = 14.696 psi,
k_5 and k_6 = regression coefficients given in Table 4.3 for soils with R>50 or Table 4.4 for soils with R≤50, and
k_4 = regression coefficient determined using Equation (4.4) for soils with R>50 or Equation (4.5) for soils with R≤50.

$$k_4 = 10^{\left[b_0+b_1\gamma d+b_2\left(\sigma_c/P_a\right)b_3\left(\sigma_d/P_a\right)\right]} \tag{4.4}$$

where,

γ_d = maximum dry density; and
b_0, b_1, b_2, and b_3 = constants given in Table 4.3.

$$k_4 = 10^{\left[b_0+b_1w+b_2\left(\sigma_c/P_a\right)b_3\left(\sigma_d/P_a\right)\right]} \tag{4.5}$$

where,

w = optimum moisture content; and
b_0, b_1, b_2, and b_3 = constants given in Table 4.4.

Table 4.3 Regression estimates for soils with R > 50

R > 50	b_0	b_1	b_2	b_3	k_5	k_6
Estimates	4.16331	0.00883	-22.45321	0.94778	1.55845	-0.95736
Std. Error	0.49982	0.00161	2.71585	0.29956	0.20526	0.29636
t-value	8.330	5.485	-8.267	3.164	7.593	-3.230
Pr(> |t|)	0.00114	0.00583	0.00117	0.03406	0.00161	0.03196

Table 4.4 Regression estimates for soils with R ≤ 50

R ≤ 50	b_0	b_1	b_2	b_3	k_5	k_6
Estimate	2.877041	-0.026380	4.001782	0.561017	0.098897	-0.353928
Std. Error	3.083768	0.007289	19.936303	1.038287	2.051692	0.60020
t-value	0.933	-3.362	0.201	0.540	0.048	-0.590
Pr(> |t|)	0.36923	0.00352	0.84427	0.59885	0.96235	0.56635

Moreover, Henrichs (2015) developed design charts to estimate M_r values of different subgrade soils based on flexible pavement and crushed base structures. The design charts consist of typical asphalt and crushed base thicknesses used in Wyoming for new highway and interstate pavement designs. In addition, maximum dry density was required to determine the M_r values of subgrade soils with R-value greater than 50, and optimum moisture content for subgrade soils with R-value less than 50, as summarized in Table 4.5 and Table 4.6, respectively.

4.2.2 Subgrade M_r Predictive Models Developed by Hellrung (2015)

Falling weight deflectometer (FWD) field tests were completed by Hellrung (2015) to back-calculate the subgrade resilient modulus (M_r) using deflection data collected from 25 test sites in Wyoming. Two correlation models were developed to correct the back-calculated M_r value to the laboratory measured equivalent values. The model with an intercept is given by Equation (4.6) and the model with zero intercept is given by Equation (4.7).

$$\widehat{M_r}(\text{psi}) = 0.0776 \times M_{r\text{-back-calculated}} \text{ (psi)} + 9804 \qquad \textbf{(4.6)}$$

$$\widehat{M_r}(\text{psi}) = 0.3775 \times M_{r\text{-back-calculated}} \text{ (psi)} \qquad \textbf{(4.7)}$$

4.2.3 Subgrade M_r Predictive Model Developed by Hutson (2015)

Hutson (2015) developed a multivariate predictive model for subgrade M_r in terms of R-value and optimum moisture content. The estimates and intercepts were prepared for specific deviator and confined stresses as summarized in Table 4.7. The developed regression model is given by Equation (4.8).

$$\widehat{M_r}(\text{psi}) = \alpha i + \beta i \times R + \mu i \times w \qquad \textbf{(4.8)}$$

where,

       R   = resistance value,
       w   = optimum moisture content, and
       αi, βi, and μi = regression coefficient estimates given in Table 4.7.

Table 4.5 Design chart of resilient modulus for subgrade soils (R>50)

Estimated Resilient Modulus (psi) for R > 50														
Base Thickness (in)	Asphalt Thickness (in.) and Corresponding Maximum Dry Unit Weight (pcf)													
	4			5			6			7			8		
	γ = 129.6	γ = 123.9	γ = 119.6	γ = 129.6	γ = 123.9	γ = 119.6	γ = 129.6	γ = 123.9	γ = 119.6	γ = 129.6	γ = 123.9	γ = 119.6	γ= 129.6	γ= 123.9	γ = 119.6
6	16592	15443	14615	15938	14392	13231	15508	13718	12365	-	-	-	-	-	-
8	16095	14641	13556	15621	13894	12589	15299	13397	11958	15051	13018	11483	-	-	-
10	15745	14089	12839	15372	13509	12099	15120	13122	11613	14919	12819	11236	14766	12590	10953
12	15455	13637	12262	15173	13204	11716	14967	12891	11326	14813	12661	11041	14691	12478	10817
14	15222	13279	11809	15013	12960	11411	14841	12702	11092	14721	12523	10871	14617	12368	10682
16	-	-	-	14881	12762	11166	14741	12553	10908	14647	12412	10736	14568	12295	10593
18	-	-	-	-	-	-	14669	12445	10776	14582	12317	10620	14470	12150	10417

*γ−Maximum dry unit weight

Table 4.6 Design chart of resilient modulus for subgrade soils (R≤50)

Estimated Resilient Modulus (psi) for R ≤ 50														
Base Thickness (in)	Asphalt Thickness (in.) and Corresponding Optimum Moisture Content (%)													
	4			5			6			7			8		
	w = 11.5	w = 16.9	w = 22.6	w = 11.5	w = 16.9	w = 22.6	w = 11.5	w = 16.9	w = 22.6	w = 11.5	w = 16.9	w = 22.6	w = 11.5	w = 16.9	w = 22.6
6	12471	9332	6218	12832	9904	6710	13084	10313	7067	-	-	-	-	-	-
8	12743	9761	6586	13017	10203	6970	13210	10521	7250	13365	10780	7478	-	-	-
10	12944	10083	6866	13166	10448	7185	13322	10707	7414	13449	10921	7604	13547	11088	7754
12	13116	10365	7112	13288	10651	7364	13418	10869	7558	13517	11036	7707	13585	11172	7829
14	13258	10600	7320	13389	10820	7514	13499	11006	7680	13577	11138	7799	13635	11256	7904
16	-	-	-	13473	10962	7641	13564	11116	7779	13626	11222	7874	13668	11312	7955
18	-	-	-	-	-	-	13611	11197	7851	13668	11295	7940	13734	11426	8057

*w−Optimum moisture content

Table 4.7 Summaries for the estimated multivariate multi-regression model

Sequence	σ_c (psi)	σ_d (psi)	R-value β_i	R-value p-value	w_{opt} (%) μ_i	w_{opt} (%) p-value	α_i	R^2
1		2	-75.28	0.0985	-902.34	0.0001	32709	0.4662
2		4	-31.24	0.4114	-897.49	0.0000	30969	0.6228
3	6	6	-3.60	0.9192	-884.26	0.0000	29119	0.6931
4		8	14.94	0.6643	-883.68	0.0000	27846	0.7350
5		10	31.60	0.3512	-883.24	0.0000	26944	0.7665
6		2	-87.28	0.0255	-763.56	0.0001	29007	0.4292
7		4	-62.39	0.0691	-763.13	0.0000	27389	0.5290
8	4	6	-41.52	0.1955	-776.39	0.0000	26414	0.6085
9		8	-17.2	0.5672	-770.85	0.0000	25320	0.6789
10		10	4.71	0.8741	-775.10	0.0000	24622	0.7264
11		2	-90.41	0.0044	-540.66	0.0004	23086	0.3496
12		4	-75.1	0.0076	-577.50.	0.0000	22492	0.4476
13	2	6	-56.37	0.0303	-602.29	0.0000	22041	0.5382
14		8	-34.46	0.1576	-617.61	0.0000	21524	0.6272
15		10	-13.29	0.5814	-625.61	0.0000	21038	0.6858

σ_c–confining stress; σ_d–deviator stress; α_i, β_i, and μ_i–regression coefficient estimates; p-value–p-value from partial ANOVA test; R^2–Coefficient of determination; and w_{opt}–optimum moisture content.

4.2.4 Subgrade M_r Predictive Model Developed by Farrar and Turner (1991)

Farrar and Turner (1991) conducted a study to determine the M_r value of Wyoming subgrade soils. They developed a subgrade M_r predictive model in terms of soil index properties, and deviator and confining stresses. The developed model is given by Equation (4.9), and the percent of saturation (S) can be determined by Equation (4.10).

$$\widehat{M_r} = 30280 - 359 \times S\% - 325 \times \sigma_d + 237 \times \sigma c + 86 \times PI + 107 \times P_{200} \tag{4.9}$$

where,

σ_c = confining stress,
σ_d = deviator stress,
S% = degree of saturation in percentage,
PI = plasticity Index, and
P_{200} = percent passing No. 200 sieve.

$$S = \frac{w_{opt} \times G_s}{e} \tag{4.10}$$

where:

w_{opt} = optimum moisture content;
G_s = specific gravity; and
e = void ratio and is assumed as 0.8.

4.2.5 Subgrade M_r Predictive Models Developed by Applied Research Associates (ARA) Inc.

Using the subgrade test data collected in Wyoming, ARA performed a regression analysis to locally calibrate the generalized M_r constitutive model given by Equation (4.11). This model was originally developed in 2004 to estimate M_r in MEPDG while the coefficients can be calibrated to represent local materials. The calibrated k_1, k_2, and k_3 for all soil types are given in Table 4.8.

$$\widehat{M_r} = k_1 \times P_a \left(\theta/P_a\right)^{k_2} \times \left(\tau_{oct}/P_a + 1\right)^{k_3} \tag{4.11}$$

where,

M_r = resilient modulus (psi);

θ = bulk stress, psi = $\sigma_1 + \sigma_2 + \sigma_3$ (sum of major, intermediate and minor principal stresses);

τ_{oct} = octahedral shear stress, psi = $\sqrt{\dfrac{(\sigma_1-\sigma_2)^2+(\sigma_2-\sigma_3)^2+(\sigma_3-\sigma_1)^2}{3}}$;

P_a = normalizing stress (equal to atmospheric pressure); and

k_1, k_2, k_3 = regression constants obtained from fitting resilient modulus data in Table 4.8.

Table 4.8 Summary of resilient modulus constitutive model coefficients

Soil Class	WYDOT Sections			LTPP Sections		
	Mean k_1	Mean k_2	Mean k_3	Mean k_1	Mean k_2	Mean k_3
Base	—	—	—	665.8	0.481	-0.332
A-1-a	1,544.8	0.626	-0.527	—	—	—
A-1-b	1,505.6	0.619	-1.063	635.3	0.370	-1.205
A-2-4	1,131.2	0.483	-1.056	570.2	0.551	-1.146
A-2-6	—	—	—	843.4	0.1549	-0.6828
A-4	1,003.6	0.52	-0.356	711.7	0.270	-1.284
A-6	801.6	0.294	0.443	712.9	0.243	-1.482
A-7-6	520.4	0.264	0.651	—	—	—

Similarly, using the deflection data collected using the falling weight deflectometer in Wyoming, ARA determined the correlation factor (C-factor) between the back-calculated M_r values and laboratory measured M_r values. The average C-factor was 0.49, as given by Equation (4.12). Additionally, ARA completed a regression analysis to correlate the in-situ pavement resilient modulus and R-values of subgrade soils in Wyoming given by Equation (4.13).

$$\widehat{M_r}(psi) = 0.49 \times M_{r\text{-back-calculated}}\ (psi) \tag{4.12}$$

$$\widehat{M_r}(psi) = 9713.91 + 61.56 \times R\text{-value} \tag{4.13}$$

4.3 Site Selection for M_r Model Comparisons

In this study, 36 sites were identified for comparing the 11 M_r models. However, conducting the comparison over the 36 sites would be time consuming and cumbersome. Thus, only eight sites, at five test locations, which represent different conditions in terms of subgrade soil type, distress type and PCI value, were selected, as summarized in Table 4.9. These sites were selected to examine the accuracy of each predictive model for different soil types and distress types. Soil types: A-1-a, A-1-b, A-2-4, A-4, A-6, and A-7-6 were included in the comparison. Similarly, longitudinal and transverse cracking, patch and rutting, and bleeding were the distresses considered in the assessment.

Table 4.9 Summary of eight sites of five locations selected for comparison

Test Loc.	Project Name	Proj. No.	Site	Sub-grade Soil Type	Distress Data		PCI
					Distress Type	Measured Distress values	
3	Kemmerer-La Barge (WYO 189)	0P11	B	A-7-6	Longitudinal Crack	445 (ft/mile)	98
			C	A-7-6	Longitudinal Crack	965.5 (ft/mile)	93
5	Aladdin-Hulett (WYO 24)	0601	A	A-2-4	Patch & Rutting	0.5 (in)	58
			C	A-6	Rutting	0.25 (in)	78
8	Thermopolis – Worland (US 20)	0N34	C	A-4	Transverse Crack	905.1(ft/mile)	96
9	Moran Junction (US 26)	0N30	A	A-6	None	0	100
			B	A-1-a	None	0	100
11	Laramie-CO. St. Line (US 287)	0N23	B	A-1-b	Bleeding	-	98

Loc.-Location, Proj.-Project, Thk− thickness, and PCI−pavement condition index

4.4 Resilient Modulus Calculation

The M_r value of each site selected was calculated using the predictive models. At first, all necessary input variables for all predictive models were identified. Accordingly, most input values were obtained from the WYOMEP database, and input variables for the model developed by ARA were obtained from 2015 ARA report. For the Model H developed by Hutson (2015), some linear interpolations were applied to estimate M_r values for a specific deviator stress of the site that is different from the standard deviator stresses. Similarly, Model D developed by Henriches (2015) (Table 4.5 and Table 4.6), linear interpolations were used for estimating the M_r value based on the respective maximum dry densities or optimum moisture contents. For other predictive models, M_r-values were calculated directly. The input parameters for Model H, Model E, Model F, Model J and Model K are summarized in Table 4.10. Input values for other M_r predictive models are given in Appendix A. The calculated M_r values from all the models are summarized in Table 4.11.

Table 4.10 Input parameters for Model H, Model E, Model F, Model J and Model K

Project No.	Sites	σ_c (psi)	σ_d (psi)	PI (%)	P200 (%)	S (%)	Pa (psi)	R-Value	Hellrung Back calculated M_r-value	ARA Back calculated M_r-value
0P11	C	0.8	3.8	22	54.6	58.4	14.696	15	15385	13000
O601	A	0.8	3	17	16.5	28.5	14.696	67	54496	41000
0N34	C	0.6	2.6	2	39.5	40.2	14.696	26	15805	28000
0N30	A	0.4	9.9	8	56.3	50.5	14.696	14	18589	25000
0N30	B	0.5	9.9	1	9.3	22.0	14.696	65	37893	35000
0N23	B	0.3	5.4	1	7.5	17.9	14.696	75	31349	34000
0P11	B	0.6	4.9	28	82.9	58.4	14.696	12	33355	21000
O601	C	0.7	3.8	17	41.2	53.3	14.696	18	20222	29000

σ_c–confined pressure, σ_d–deviator stress, PI–plasticity index, P200– percent of passing in sieve #200, and Pa–atmospheric pressure

4.5 Model Comparison Based on Measured and Predicted M_r Values

The accuracy of the models was evaluated by comparing the predicted M_r values verses the measured laboratory M_r values. The best models were those that have a smaller sum of square error than the others. The total sum of square error of each model is summarized under each model in Table 4.11. Based on the smallest sum of square errors, Model G, Model C and Model K were found to be three best models, respectively.

4.6 Model Comparison Based on Pavement Distress Prediction

4.6.1 Estimation of Pavement Distresses Using AASHTOWare Software

The objective of determining all M_r values of the selected sites was to use them as input for the MEPDG software (AASHTOWare) shown in Figure 4.1. The MEPDG software requires three main inputs, namely the traffic, material, and climate data as summarized in Table 4.12. Based on the main line (ML) number and milepost of the segments where the sites are located, the AADTT was obtained from the 2014 Vehicle Miles Book provided as a reference by WYDOT. The material data consists of the M_r values determined using different models for the subgrade layer. The M_r values of the base materials were taken from back calculation results by Hellrung (2015). The thickness of the base and asphalt layer were taken from pavement coring results reported by Henrichs (2015). The material property of the asphalt and other input constants required by the AASHTOWare software were obtained from the WYDOT AASHTO DARWin-ME Pavement Design User's Guide (2012) prepared by ARA. Some climate data of the sites selected for comparison were obtained based on the closest weather station near the site. If the site was located between two weather stations, then the virtual climate station was employed in the analysis.

33

Table 4.11 Summary of M$_r$-values calculated by Model B to Model L

Project No.	Sites	Estimated Resilient Modulus, M$_r$ (psi)										Laboratory Measured Resilient Modulus, M$_r$ (psi)
		Model B	Model C	Model D	Model E	Model F	Model G	Model H	Model I	Model J	Model K	
0P11	C	16826	11005	10869	10996	5798	11664	15989	6898	6370	10637	11909
O601	A	21345	10646	10908	14033	20572	12610	22479	8710	20090	13838	11847
0N34	C	22575	13400	13547	11031	5966	13805	19537	7486	13720	11315	10329
0N30	A	4108	11201	10611	11247	7017	11724	15696	13172	12250	10576	8936
0N30	B	6750	16638	16491	12745	14305	16126	20364	24397	17150	13715	16962
0N23	B	9629	13203	15987	12237	11834	14432	23067	9910	16660	14331	12321
0P11	B	11406	9499	10417	12392	12592	11477	19127	7270	10290	10453	10976
O601	C	16600	11106	11482	11373	7634	12238	15953	8739	14210	10822	14707
$\sqrt{SSE}$		20074	5732	6285	6508	14005	5656	21335	13093	11861	6260	

SSE– Sum of square errors for each model

Table 4.12 Asphalt thickness, base thickness and AADTT of the selected sites

Test Loc.	Project Name	Project No.	County	Sites	Asphalt/ Base Thk.(in)	ML number	Mile Post		AADTT (during opening of a road)
							Beg MP	End MP	
3	Kemmerer-La Barge (WYO 189)	0P11 (P1103(024))	Lincoln	A	13/9.5	ML 11B	59	68	150
				B	6.5/7				
				C	6/12.0				
5	Aladdin-Hulett (WYO 24)	0601 (FH-0601(29))	Crook	A	6/16	ML 601B	31	32	90
				B	6/18				
				C	6/12				
8	Thermopolis – Worland (US 20)	0N34 (M6-0N34-03(033))	Washakie	A	11/13	ML 34B	150.7	156.6	350
				B	10/12				
				C	9/10				
9	Moran Junction (US 26)	0N30 (N30101S)	Teton	A	4/6	ML 30B	8	9	104
				B	4/6				
				C	4/6				
11	Laramie-CO. St. Line (US 287)	0N23 (0N23-02(045))	Albany	A	5/10	ML 23B	417.4	425.4	598
				B	5/10				
				C	5/10				

Thk–thickness, ML–main line, Beg MP–beginning mile post, End MP–ending mile post, and AADTT–annual average daily truck traffic
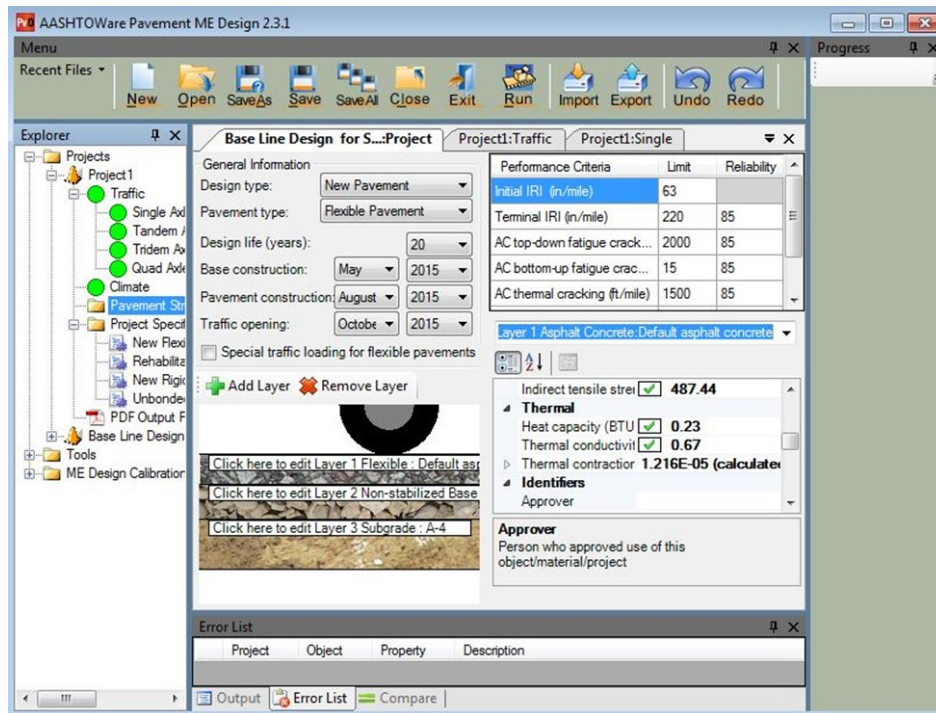
Figure 4.1 Interface of AASHTOWare pavement ME design version 2.3.1

Base construction, pavement construction, and traffic opening dates of the road segments were established. The pavement design user-guide recommends the use of different design reliabilities based on the functional classification of the roadways (interstate roads, primary roads and secondary roads). Since the objective of this study was to compare distresses as a function of M_r values estimated by the predictive models, both 90% reliability and a design life of 15 years were used in this study for all sites.

After imputing all the MEPDG input parameters, the AASHTOWare software was used to run the pavement analysis and determine distresses at the end of the design life presented in a tabular form as shown in Figure 4.2 and in a graphical form in Figure 4.3.
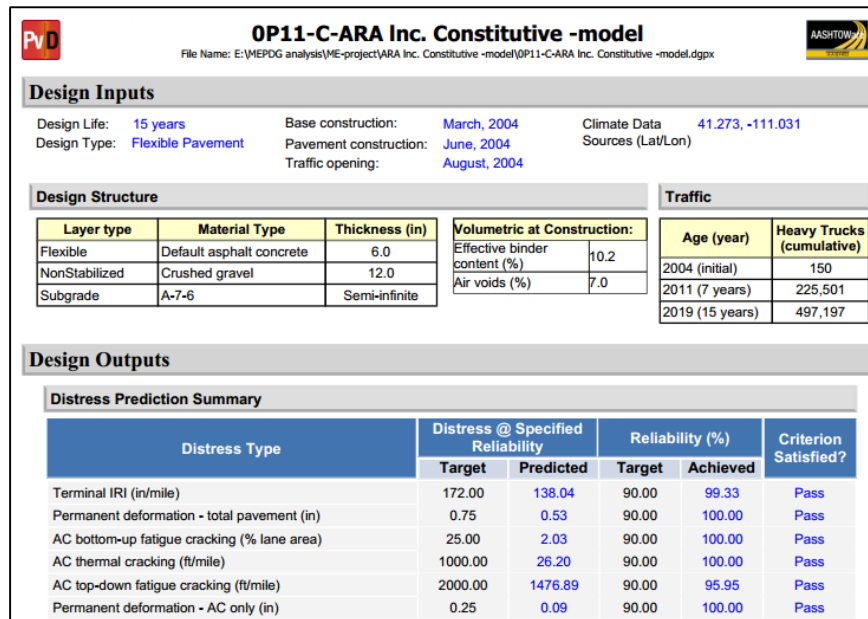
Figure 4.2 AASHTOWare pavement ME design outputs in a table
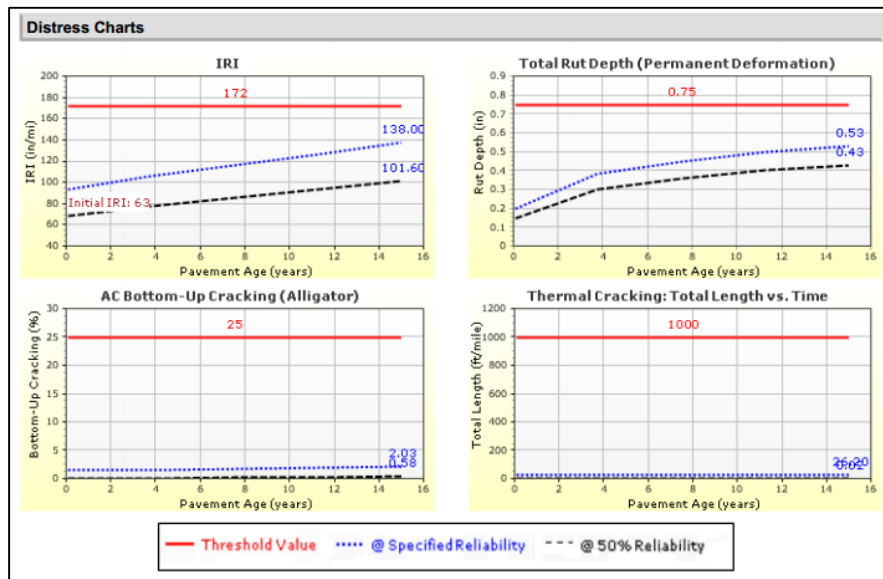
Figure 4.3 AASHTOWare pavement ME design distress outputs in graphical form

36

The distress survey was conducted in June 2013 by Hellrung (2015). Thus, the pavement distresses predicted in June 2013 were taken from the distress outputs obtained from the AASHTOWare output for comparison. Initially, during the site selection process, four distresses were included: longitudinal cracking, transverse cracking, rutting, and bleeding. Bleeding was excluded from the comparison because it was not among the distresses predicted by AASHTOWare. Also, transverse (thermal) cracking was excluded because AASHTOWare provides an equal prediction of transverse cracking for all the subgrade M_r values, because thermal cracking was insensitive to subgrade M_r values. The difference between the distress predicted from the MEPDG analysis and actual surveyed distress was determined for each site. Table 4.13 summarizes the surveyed distresses, the distresses predicted by MEPDG analysis using Model I (i.e., constitutive model by ARA), the difference (i.e., predicted minus measured distresses) expressed as an error for each site, and the total sum of errors. Similar distress comparisons for the remaining models are included in Appendix B.

Table 4.13 Comparison of distresses measured on site and predicted by ME (AASHTOWare) software using Model I

Project No	Sites	Longitudinal Crack (ft/mile)			Rutting Depth (inch)		
		Measured	Predicted	Error	Measured	Predicted	Error
0P11	C	965.49	1116.28	150.79	0.00	0.48	0.48
O601	A	0.00	285.70	285.70	0.50	0.39	0.11
0N34	C	0.00	303.57	303.57	0.00	0.64	0.64
0N30	A	0.00	1460.32	1460.32	0.00	0.31	0.31
0N30	B	0.00	905.66	905.66	0.00	0.26	0.26
0N23	B	0.00	1937.5	1937.5	0.00	0.52	0.52
0P11	B	445.00	580.65	135.65	0.00	0.41	0.41
O601	C	0.00	966.67	966.67	0.25	0.474	0.22
Total Sum of Errors				**6145.86**			**2.95**

4.6.2 Comparison of M_r Predictive Models

The best M_r predictive model was the model that was able to predict the distress values closest to the surveyed distresses. In other words, the best model is the one with the smallest total sum of errors in all distresses. However, since the longitudinal cracking (ft/mile) and rutting depth (inch) have different units of measurement, both total sums of errors cannot be added directly. Each distress error was normalized into a dimensionless quantity (z) using Equation (4.14). Table 4.14 summarizes the sum of distress errors and their normalized distress errors. The model with the smallest normalized distress error, considering positive and negative values, was considered the best model. Figure 4.4 through Figure 4.6 show the graphical presentation of the total sum of longitudinal cracking errors, total sum of rutting errors, and cumulative normalized errors for both longitudinal cracking and rutting.

$$ z = \frac{x - \bar{x}}{s} $$

(4.14)

where,

        z   = the normalized distress error,
        x   = distress value to be normalized,

$\bar{x}$ = mean value of all distress errors, and

s = standard deviation of the distress errors.

Table 4.14 Sum of distress errors in both standard and normalized forms

Model	Longitudinal Crack		Rutting		All
	Total Sum of Error	Normalized Error	Total Sum of Error	Normalized Error	Total Normalized Error
B	8555.02	0.965	2.978	0.917	1.882
C	7572.38	-0.099	2.643	-0.507	-0.605
D	7676.54	0.014	2.56	-0.860	-0.846
E	7639.8	-0.026	2.728	-0.146	-0.171
F	6675.36	-1.070	3.236	2.014	0.944
G	7922.46	0.280	2.6203	-0.603	-0.323
H	9458.18	1.943	2.421	-1.451	0.492
I	6145.86	-1.643	2.942	0.764	-0.879
J	7140.1	-0.567	2.721	-0.175	-0.742
K	7848.925	0.201	2.773	0.046	0.247
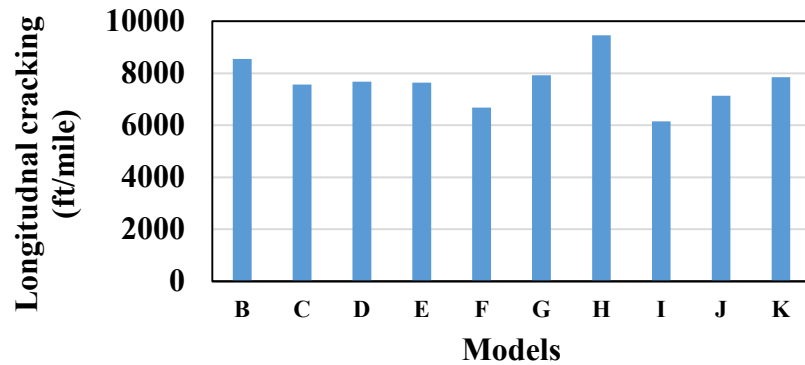
Figure 4.4 Total sum of longitudinal cracking errors
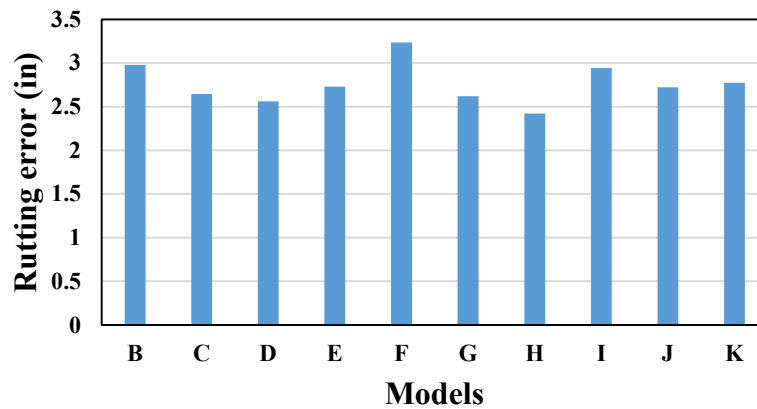
Figure 4.5 Total sum of rutting errors
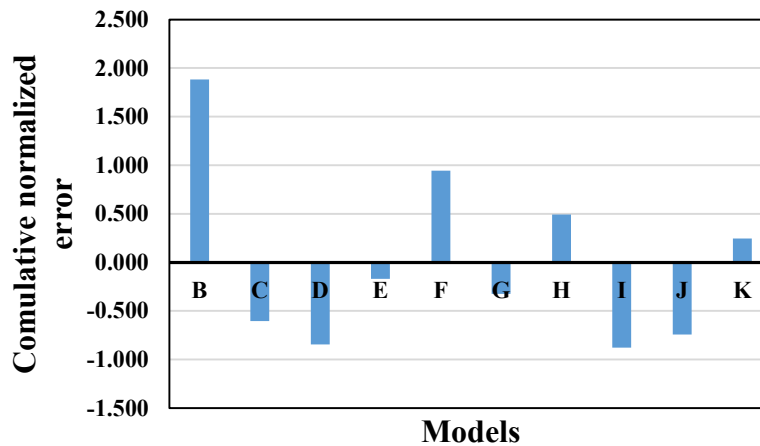
Figure 4.6 Cumulative normalized errors considering both longitudinal crack and rutting

Based on the cumulative normalized error of longitudinal crack and rutting summarized in Table 4.14 and shown in Figure 4.6, the three best predictive models with the lowest normalized errors of -0.879, -0.846 and -0.742 are Model I, Model D and Model J, respectively. These models were selected for the pavement design comparison described in Section 6.

4.7   Summary

This section describes the procedure for selecting the best subgrade resilient modulus (M_r) predictive models. Ten subgrade M_r models for subgrade soils in Wyoming were evaluated for their relative accuracy on their predicted resilient modulus and estimated flexible pavement performance in terms of distresses using the software AASHTOWare. Finally, based on the distress performance comparison, three best predictive models that predicted a closer distress performance to the actual measured distress on the site were recommended for MEPDG implementation in Wyoming. These models are constitutive model by ARA (Model I), M_r design tables by Henrichs (Model D), and c-factor model by ARA (Model J).

5. SENSITIVITY ANALYSIS OF FLEXIBLE PAVEMENTS USING LOCALLY CALIBRATED MEPDG MODELS

5.1 Introduction

A sensitivity analysis is the process of varying model input parameters (e.g., asphalt concrete (AC) thickness, subgrade type, base type, Annual Average Daily Truck Traffic (AADTT)) over a practical range and observing the relative change in distress model responses (e.g., cracking, rutting, and smoothness) over the entire design life of the pavement. WYDOT and other state DOTs have conducted sensitivity analyses to identify the influential variables in the design of pavement structures. The first sensitivity analysis completed by WYDOT was using the old locally calibrated distress coefficients, and results were provided in the AASHTO DARWin-ME Pavement Design User's Guide of WYDOT published on September 2012.

This sensitivity study employs locally calibrated MEPDG distress coefficients documented in the WYDOT 2015 report on local calibration (Byattacharya et al., 2015), and only new flexible (HMA) pavement was considered. In addition, input parameters, which have significant, moderate, or no influence in the design of new flexible pavement in Wyoming, were identified.

5.2 Sensitivity Analysis

To proceed with the sensitivity analysis, baseline design parameters were initially selected to represent the typical (mean) values of the site conditions (material, traffic, and climate) used in the state of Wyoming. The input parameters selected in this analysis are AC thickness, AC air void, AC grade, base thickness, base M_r, subgrade M_r, AADTT, and climate. These variables were selected because they were very sensitive to some distresses in the sensitivity studies completed by DOTs (Mallela et al. 2013 for CDOT, Schwartz et al. 2011 for IADOT, and Darter et al. 2009 for UDOT). The lower, baseline, and the upper values of the input variables are given in Table 5.1. The lower and upper values were selected by referring to user manuals, reports, and field collected data.

Table 5.1 Lower, baseline and upper input values used for sensitivity analysis of new flexible pavements

Input	Lower Value	Baseline Value	Upper Value
AC Thickness (in)	2	6	12
AC Air void (%)	3	7	9
AC Grade	PG 58-28	PG 64-28	PG 70-28
Base Thickness (in)	3	7	12
Base M_r (psi)	20,000	30,000	40,000
Subgrade M_r (psi)	8,000 (A-7-6)	12,000 (A-4)	15,000 (A-1-a)
Traffic: AADTT	250	2,000	5,000
Climate: Temperature	Low (Big Piney)	Medium (Cody)	High (Torrington)

AC−Asphalt concrete, M_r−Resilient modulus, PG−Performance grade, and AADT−Annual average daily truck traffic

Generally, sensitivity analyses have been completed using initial triage, extensive one-at-a-time (OAT) sensitivity analyses, and comprehensive global sensitivity analyses (GSA) by many DOTs. The initial triage was mainly performed based on experience and past studies. The OAT analyses were conducted by varying each selected sensitive design parameter over a practical range to examine the change in the MEPDG predicted distresses. In contrast to the OAT analyses, the GSA was used to vary all the design input parameters simultaneously across the given range (Schwartz et al 2011).

In this research, only the OAT method was employed because this is the most common sensitivity analysis approach, and it is the first step in performing GSA. The Normalized Sensitivity Index (NSI) was adopted to quantify and determine sensitivity of each design parameter. According to Schwartz et al. (2011), the NSI is defined as the percentage change of predicted distress (e.g., total rutting) relative to its design limit (e.g., 0.75 inches) caused by a given percentage change in the design input (e.g., granular base resilient modulus). Four sensitive categories were defined based on the calculated NSI values using Equation (5.1). They are hypersensitive ($|NSI| > 5$), very sensitive ($1 < |NSI| < 5$), sensitive ($0.1 < |NSI| < 1$), and non-sensitive ($|NSI| < 0.1$). The positive or negative value of NSI shows the decrease or increase in distress due to the change in input values.

$$NSI = \frac{\Delta Y}{\Delta X} \times \frac{X_{baseline}}{DL} \qquad (5.1)$$

where,
ΔY = change in distress,
ΔX = change in input variable,
$X_{baseline}$ = baseline input variable, and
DL = distress limit.

An NSI calculation example was used to examine sensitivity of alligator cracking to AC thickness (X). When a two-inch AC thickness (X_1) resulting in 100% alligator cracking (Y_1) increased to 12 inches, the alligator cracking reduced to 1.91%. Six inches AC thickness ($X_{baseline}$) at baseline design and 15% alligator cracking distress limit (DL) at lifetime was used. Using these values, the absolute NSI value of 3.92 determined using Equation (5.2) indicates as very sensitive.

$$NSI = \frac{\Delta Y}{\Delta X} \times \frac{X_{baseline}}{DL} = \frac{(Y_2 - Y_1)}{(X_2 - X_1)} \times \frac{X_{baseline}}{DL} = \frac{(1.91 - 100)}{(12 - 2)} \times \frac{6}{15} = -3.92 \qquad (5.2)$$

The sensitivity analyses were performed based on 20 years of design life of the pavement. In this study, the sensitivity result of longitudinal cracking was not considered, because local calibration of a longitudinal cracking distress model for longitudinal cracking was not performed. The sensitivity results for four pavement distresses (i.e., International Roughness Index (IRI), total rutting, alligator cracking, and transverse cracking) are summarized in Table 5.2. However, the detailed explanation of these results are provided in Section 5.3. Calculated NSI values and the distress results over the design life of the pavement due the individual input variable are presented in Appendix C. Figure 5.1 through Figure 5.4 present the sensitivity plots for new flexible pavement distresses and IRI. In these plots, the lower, baseline and upper values verses their respective distress results were indicated. The red dash line indicates the baseline values and corresponding calculated distress values.

Figure 5.1 and Figure 5.4 show no consistent trend in distress results on the bar charts. For example, as shown in Figure 5.4, when the base thickness was increased from three inches to seven inches followed by 12 inches, the transverse cracking increased from 2586.75 ft/mile at three inches to

highest 3002.62 ft/mile at seven inches and later reduced to 2750.52 fit/mile at 12 inches. The consistent increasing or decreasing trend of transverse cracking values was not observed as the base thickness increased. This observation could be due to the interaction of the base thickness and other input variables. Hence, a pavement designer should consider the interactive effect among the input variables to yield a more efficient design with reasonable predicted distresses when designing a new flexible pavement using the ME software.

Table 5.2 Overall summary of sensitivity analysis results

HMA Pavement Input		Level of Sensitivity for Flexible Pavement			
General Group	Parameters	Alligator Cracking	Transverse Cracking	Total Rutting	IRI (Roughness)
Material	AC Thickness (in)	VS	S	S	S
	AC Air void (%)	HS	NS	S	S
	AC Grade	S	NS	NS	NS
	Base Thickness (in)	VS	NS	NS	NS
	Base M_r (psi)	VS	NS	NS	NS
	Subgrade M_r (psi)	VS	NS	NS	S
Traffic	Traffic: AADTT	VS	NS	S	S
Climate	Climate	S	NS	S	NS

AC−asphalt concrete, M_r−resilient modulus, AADT−annual average daily truck traffic, IRI−international roughness index, S−Sensitive, NS−non- sensitive, VS−very sensitive, and HS−hyper sensitive

5.3   Sensitivity Results

5.2.1 Alligator Cracking

In the sensitivity analysis, alligator cracking was found to be hypersensitive, very sensitive, or sensitive to all the selected input parameters. These results were consistent with that determined from the sensitivity analysis described in the WYDOT AASHTO DARWin-ME Pavement Design User's Guide (2012). However, the differences in level of sensitivity were attributed to the local calibration coefficients used in this study and the global calibrated coefficients in the WYDOT Guide (2012). Table 5.3 shows that sensitivity results based on AC thickness, AC grade and base M_r agreed with that by other DOTs (e.g., Mallela et al., 2013; Schwartz et al., 2011).

Alligator cracking was found to be hypersensitive to AC air void content. The change in AC air void from lower value (3%) to upper value 9% led to an increase in the alligator cracking from 7 to 100 percent lane area. AC thickness, base thickness, base M_r, AADTT, and subgrade M_r were variables very sensitive to the alligator cracking. The AC grade and climate were also found to be sensitive variables.
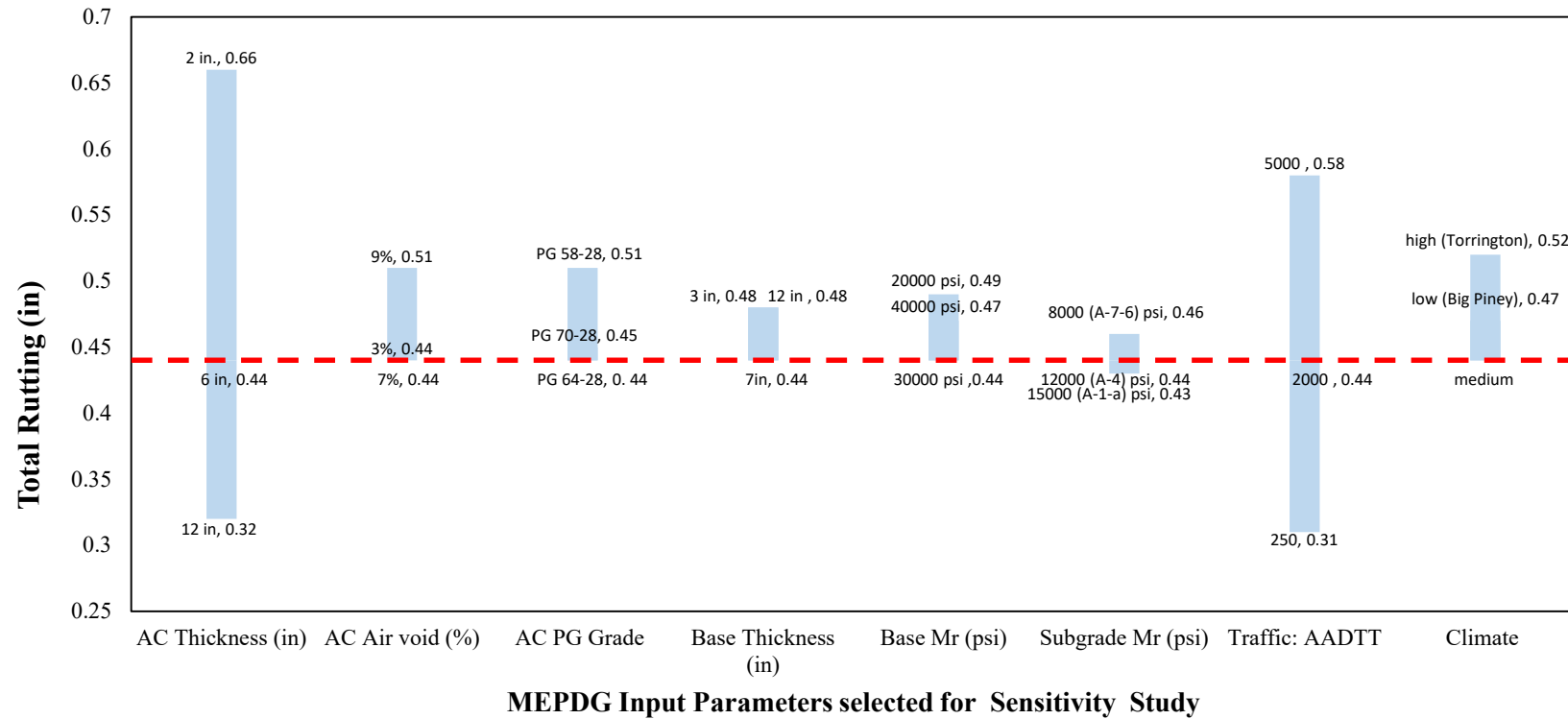
Figure 5.1 Summary of sensitivity results for new flexible pavement based on total rutting
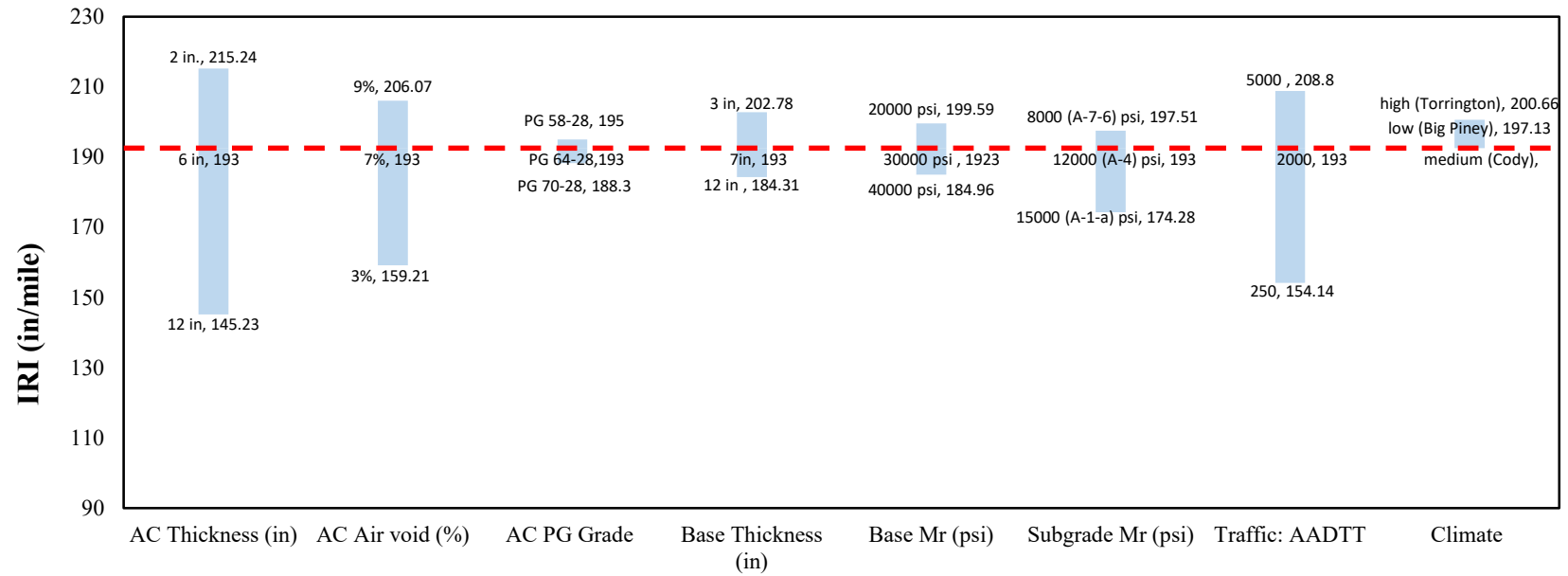
Figure 5.2 Summary of sensitivity result for new flexible pavement based on IRI
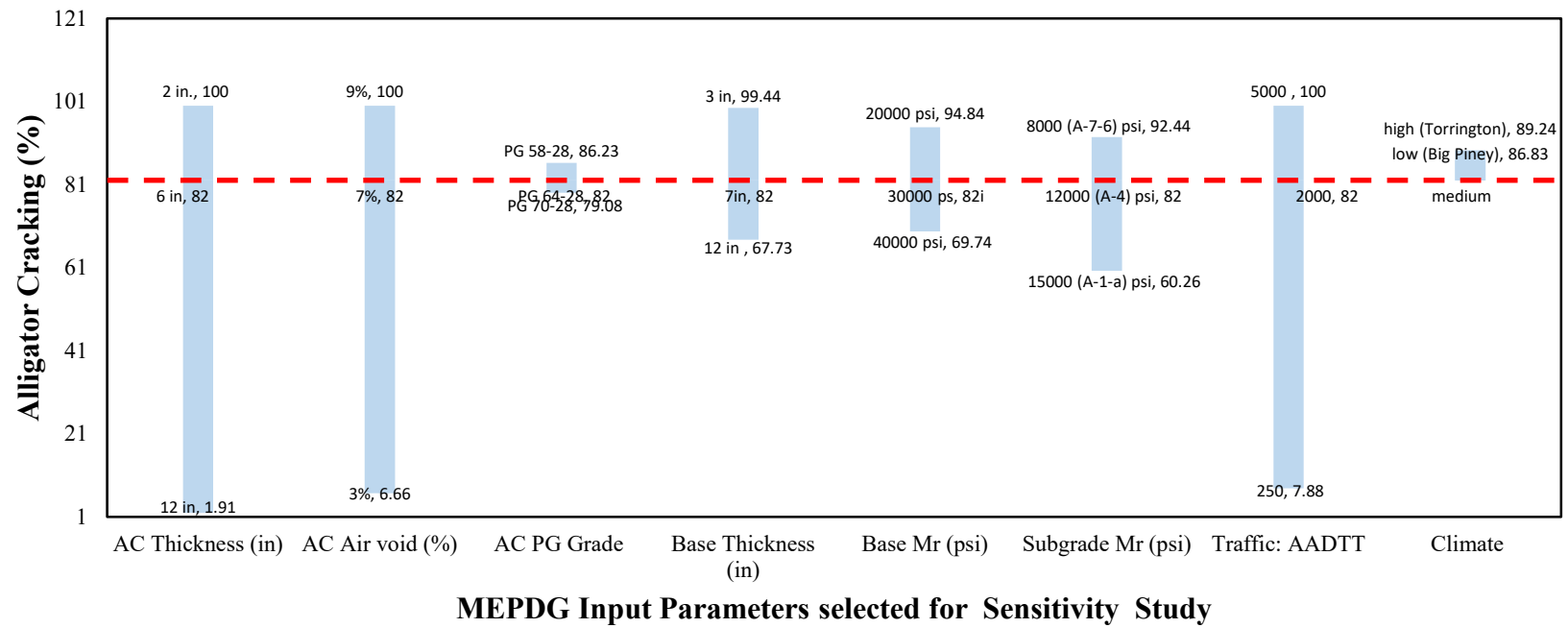
Figure 5.3 Summary of sensitivity results for new flexible pavement based on alligator cracking
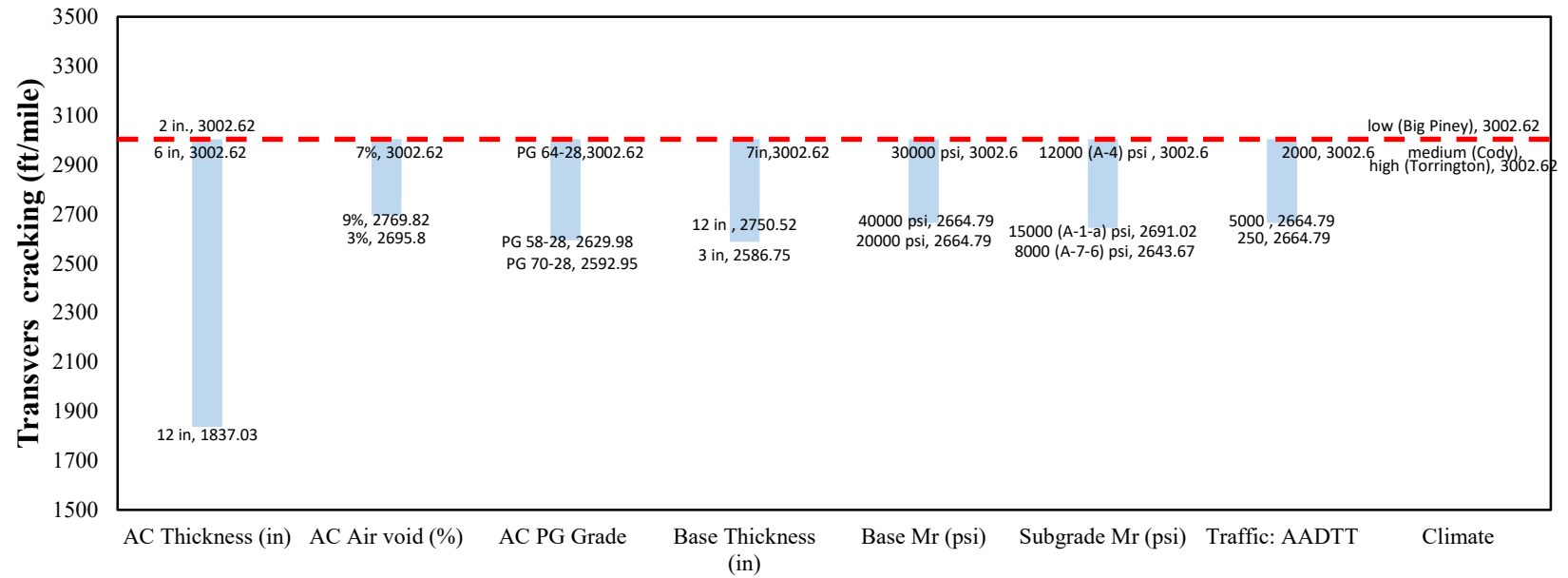
Figure 5.4 Summary of sensitivity results for new flexible pavement based on transvers cracking

Table 5.3 Comparison for alligator cracking level of sensitivity

Parameters	Alligator Cracking Level of Sensitivity			
	This Study	**WYDOT 2012**	**Mallela et al. 2013 (CDOT)**	**Schwartz et al. 2011 (IADOT)**
AC Thickness (in)	VS	HS	VS	VS
AC Air void (%)	HS	HS	S	NS
AC Grade	S	VS	NS	S
Base Thickness (in)	VS	S	S	S
Base M_r (psi)	VS	HS	-	VS
Subgrade M_r (psi)	VS	VS	-	-
Traffic: AADTT	VS	HS	S	NS
Climate	S	VS	NS	NS

AC−asphalt concrete, Mr−resilient modulus, AADT−annual average daily truck traffic, S−Sensitive, NS−non-sensitive, VS−very sensitive, and HS−hyper sensitive

5.2.2 Transverse (Thermal) Cracking

This sensitivity analysis concluded that thermal cracking was non-sensitive to all input variables except AC thickness (Table 5.2). Table 5.4 shows that thermal cracking was sensitive to AC grade, climate and AC thickness based on the sensitivity studies by other DOTs. However, in this analysis, AC grade and climate were listed as non-sensitive. These differences could be attributed to the small variation between the low (37.1ºF), medium (43.4ºF), and high (49.1ºF) mean annual air temperatures considered in this sensitivity analysis. In addition, the typical AC grades used in Wyoming (i.e., PG 52-28, PG 64-28, and PG 70-28) for this sensitivity analysis have the same lowest low temperature resistance of -28º C. Due to the similarity in low temperature (transverse) cracking, a small difference in transverse cracking was observed in this sensitivity analysis. Therefore, the small variation in thermal cracking indicates its non-sensitivity to the input parameters in this analysis. Nevertheless, thermal cracking is a serious pavement performance in Wyoming. All the considered climates (low, medium, and high) resulted in a large thermal cracking defect, which is about 3000 ft/ mile in 20 years design life of the pavement. This is about two times the distress limit or design criteria of thermal cracking of a pavement in its design life.

Table 5.4 Comparison for thermal cracking level of sensitivity

Parameters	Thermal Cracking Level of Sensitivity			
	Result of this study	**WYDOT 2012**	**Mallela et al. 2013 (CDOT)**	**Schwartz et al. 2011 (IADOT)**
AC Thickness	VS	S	VS	NS
AC Grade	NS	HS	VS	VS
Climate	NS	HS	VS	VS

AC−asphalt concrete, Mr−resilient modulus, AADT−annual average daily truck traffic, S−Sensitive, NS−non-sensitive, VS−very sensitive, and HS−hyper sensitive

5.2.3 Total Rutting

Total rutting is the sum of rut depths of the asphalt concrete, base and subgrade layers created by repeated traffic loads. The sensitivity analysis results showed that total rutting was sensitive to AC thickness, AC air void, AADTT, and climate. Pavements in hot climate areas can experience a higher

rutting than pavements in colder areas. In addition, pavements with higher traffic loads in their design life have a larger amount of rutting than those with lower traffic loads while keeping other parameters (AC thickness, AC air void, and AC grade) constant. Total rutting was found to be non-sensitive to AC grade, base thickness, base M_r and subgrade M_r. This could be due to the relatively thick AC layer of six inches used in the baseline design.

5.2.4 International Roughness Index (IRI)

IRI is the measure of smoothness of a pavement surface, and it is the summation of all the distresses. IRI was found to be sensitive to AC thickness, AC air void, subgrade M_r, and AADTT. On the other hand, IRI was found to be non-sensitive to AC grade, base thickness, base Mr and climate. These results agree with the sensitivity analysis result of the WYDOT Guide (2012) and other sensitivity results completed by CDOT (Mallela et al. 2013).

5.4 Summary

This section describes the analysis and result of sensitivity study completed using locally calibrated distress coefficients. In this research, only the one at a time (OAT) method was employed because this is the most common sensitivity analysis approach, and it is the first step in performing a global sensitivity analysis (GSA). The sensitivity analyses were completed based on a pavement structure design life of 20 years. The sensitivity result of longitudinal cracking was not considered, because local calibration of a longitudinal cracking distress model was not performed. The pavement distresses were sensitive to asphalt concrete thickness, and most distresses were non-sensitive to asphalt concrete (AC) grade, base thickness, and base M_r value.

6.   PAVEMENT DESIGN COMPARISON

6.1   Introduction

WYDOT has been using MEPDG pavement design User Guide (ARA, 2012) to design all pavement types (flexible and rigid). The WYDOT 2012 user design guide provides representative traffic, material and climate data of the state of Wyoming. These data can be easily inputted to the AASHTOWare software to design pavement structures. In addition, the user design guide has locally calibrated for distress coefficients. These calibrated coefficients were further updated and documented by Byattacharya, et al. (2015). However, the default subgrade and base material M_r values provided in the WYDOT 2012 user design guide were not calibrated to reflect local materials in Wyoming. To illustrate the benefits of local calibration of materials completed in recent research studies, the best-predictive M_r model from Section 3 was used to determine the M_r values of subgrade soils while the laboratory measured M_r values were used for the base material (Mebrahtom 2017) in new flexible pavement design comparisons presented in this section. The comparisons were conducted by selecting three projects and designing them using two different approaches. The first design approach (denoted as Design Approach 1) was by following every step described in the WYDOT 2012 user design guide. The second design approach (denoted as Design Approach 2) was by employing the locally calibrated M_r values for subgrade and base materials and locally calibrated distress coefficients. Cost analysis was performed to compare both design approaches.

To cover a wide range of roads in Wyoming, interstate, primary, and secondary roads were selected for the pavement design comparisons. Interstate road is the road, which runs from state to state continuously. This road was designed with the highest reliability and standard. Primary road has a high traffic volume (capacity) within the state while secondary road has a low traffic volume. The projects selected in this comparison study are:
> Project #1: New Flexible Pavement Design on Highway I-80 (JCT I 25)
> Project #2: New Flexible Pavement Design on Highway WY 78 (JCT I 80)
> Project #3: New Flexible Pavement Design on Highway WY 352 (JCT US 191)

6.2   Project #1: New Flexible Pavement Design on Highway I-80 (JCT I 25)

Project#1 represents a new flexible pavement design on the route of I-80, section JCT I-25, in Laramie County, WY. This project started at mile post 359.599 and ended at mile post 362.037. According to the 2014 mile book, this road had an average annual daily traffic (AADT) of 9,062 and average annual daily truck traffic (AADTT) of 4,199.

6.2.1 Design Approach 1: Based on WYDOT 2012 User Design Guide

This project was designed for 15 years of design life. The threshold values of distresses in this given design life are 10% alligator cracking, 0.5-inch total rutting, 1000 ft/mi transverse (thermal) cracking, and 170 in/mile International Roughness Index (IRI). These values are specified in the WYDOT 2012 user design guide as design criteria for interstate roads. For the interstate highways, 95% reliability is used for the pavement design. A climate station positioned in Cheyenne was employed to input the climate data for this project.

Every input required for this project was adopted primarily from WYDOT 2012 user design guide. Accordingly, the M_r values of the subgrade soil (A-7-6) and crushed gravel were taken as 3,864 psi and 4,500 psi, respectively. Moreover, the user design guide also recommends the ratio of a base or sub base M_r to subgrade M_r to be less than 3, and hence, the M_r value of the base material in this project was assigned as 11,592 psi.

The properties of the asphalt layer were taken from the WYDOT 2012 user design guide. The effective binder content and asphalt grade can be changed based of the environmental condition of the site. If thermal cracking is predicted during the design process of the flexible pavement, it can be mitigated by increasing the asphalt grade used in the design.

The distress coefficients in WYDOT 2012 user design guide were calibrated to the local conditions of Wyoming. Some of the calibrated coefficients were further updated in 2015. However, in this design the old calibrated coefficients were used.

After performing many trial design runs, a pavement structure shown in Figure 6.1 was found to satisfy the design criteria except the thermal cracking. In this design, the commonly used asphalt grade, PG 76-28, with 11.5 % binder content and 5.5% air void, was used in the upper asphalt concrete (AC) layer. For the lower AC layer, PG 70-28 with 10.2 % binder content and 7% air void was selected. However, the predicted thermal cracking of 1,355.98 ft/mile exceeded the design limit of 1,000 ft/mile. Therefore, the upper asphalt grade was upgraded to PG 76-34 to reduce thermal cracking to 166.75 ft/mile as shown in Figure 6.2.

To compare design approaches in terms of cost, cost estimation for pavement structures was performed. Average unit prices of the materials were taken from WYDOT 2016 weighted average bid prices. The unit price of a hot plant mix was listed as $43.33 per ton. This cost does not include the cost for asphalt, but only for aggregates, mixing, and placing. Since the unit cost for an asphalt binder changes daily, different unit prices were prepared for the different asphalt grades. For asphalt binder PG 64-28, the unit price was $438.94 per ton. For PG 70-28 and PG 76-28, the prices per ton were $443.76 and $463.89, respectively. The price for the crushed base was $32.53 per cubic yard (CY) which is equivalent to $1.2 per cubic foot.

Since the asphalt binder content and the hot mix plant used in this design was mixed by volume, the prices per tone of the material provide above were converted to prices per volume. A density of 135 pcf was assumed for the hot plant mix and 64.6 pcf for the asphalt binder. The conversion process was performed by dividing the mass of the material by its density. For example, one ton (2,000 lb) of the hot mix plant was divided by its density (135 pcf) to yield a volume of 14.8 ft^3. Therefore, the price for 14.8 ft^3 of the hot mix plant was $43.33, and this can be converted to its equivalent price of $2.93 per cubic foot. Following the same procedure, the prices for a cubic foot asphalt binder were found to be $14.18 for PG 64-28, $14.33 for PG 70-28, and $14.98 for PG 76-28. In this cost estimation process, the price for asphalt binder PG76-34 was not provided; therefore, the same price as PG 76-28 was assumed.

Design Inputs

Design Life: 15 years
Design Type: Flexible Pavement

Base construction: May, 2014
Pavement construction: June, 2014
Traffic opening: September, 2014

Climate Data Sources (Lat/Lon): 41.158, -104.807

Design Structure

Layer type	Material Type	Thickness (in.):	Volumetric at Construction:	
Flexible	Default asphalt concrete	4.0	Effective binder content (%)	11.5
Flexible	Default asphalt concrete	17.0	Air voids (%)	5.5
NonStabilized	Crushed gravel	4.0		
Subgrade	A-7-6	Semi-infinite		

Traffic

Age (year)	Heavy Trucks (cumulative)
2014 (initial)	4,199
2021 (7 years)	5,664,610
2029 (15 years)	12,526,400

Design Outputs

Distress Prediction Summary

Distress Type	Distress @ Specified Reliability		Reliability (%)		Criterion Satisfied?
	Target	Predicted	Target	Achieved	
Terminal IRI (in./mile)	150.00	117.61	95.00	99.89	Pass
Permanent deformation - total pavement (in.)	0.50	0.49	95.00	96.49	Pass
AC bottom-up fatigue cracking (percent)	10.00	2.10	95.00	100.00	Pass
AC thermal cracking (ft/mile)	1000.00	1355.98	95.00	72.31	Fail
AC top-down fatigue cracking (ft/mile)	2000.00	329.39	95.00	100.00	Pass
Permanent deformation - AC only (in.)	0.50	0.23	95.00	100.00	Pass

Distress Charts
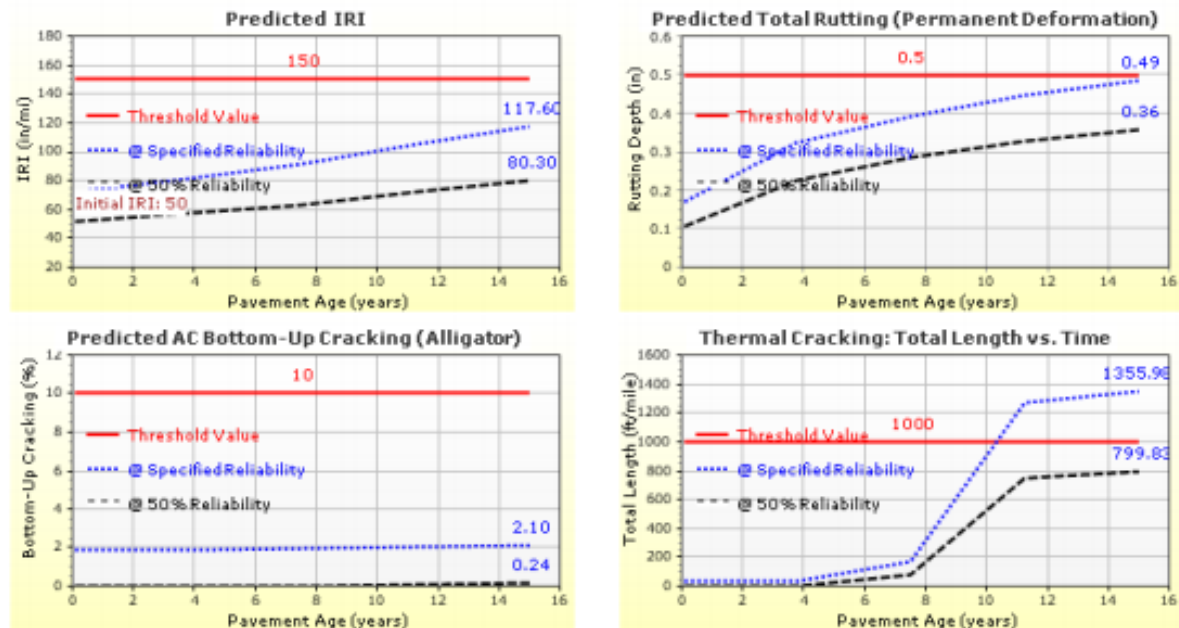
Figure 6.1 Pavement structure and predicted distresses of Project #1 based on Design Approach 1 using PG 76-28 as the upper AC layer

51

Design Inputs

Design Life: 15 years
Design Type: Flexible Pavement

Base construction: May, 2014
Pavement construction: June, 2014
Traffic opening: September, 2014

Climate Data 41.158, -104.807
Sources (Lat/Lon)

Design Structure

Layer type	Material Type	Thickness (in.):
Flexible	Default asphalt concrete	1.0
Flexible	Default asphalt concrete	6.0
Flexible	Default asphalt concrete	17.0
NonStabilized	Crushed gravel	4.0
Subgrade	A-7-6	Semi-infinite

Volumetric at Construction:

Effective binder content (%)	10.2
Air voids (%)	7.0

Traffic

Age (year)	Heavy Trucks (cumulative)
2014 (initial)	4,199
2021 (7 years)	5,664,610
2029 (15 years)	12,526,400

Design Outputs

Distress Prediction Summary

| Distress Type	Distress @ Specified Reliability		Reliability (%)		Criterion Satisfied?
	Target	Predicted	Target	Achieved	
Terminal IRI (in./mile)	150.00	115.65	95.00	99.93	Pass
Permanent deformation - total pavement (in.)	0.50	0.50	95.00	95.48	Pass
AC bottom-up fatigue cracking (percent)	10.00	1.94	95.00	100.00	Pass
AC thermal cracking (ft/mile)	1000.00	166.75	95.00	100.00	Pass
AC top-down fatigue cracking (ft/mile)	2000.00	332.40	95.00	100.00	Pass
Permanent deformation - AC only (in.)	0.50	0.28	95.00	100.00	Pass

Distress Charts
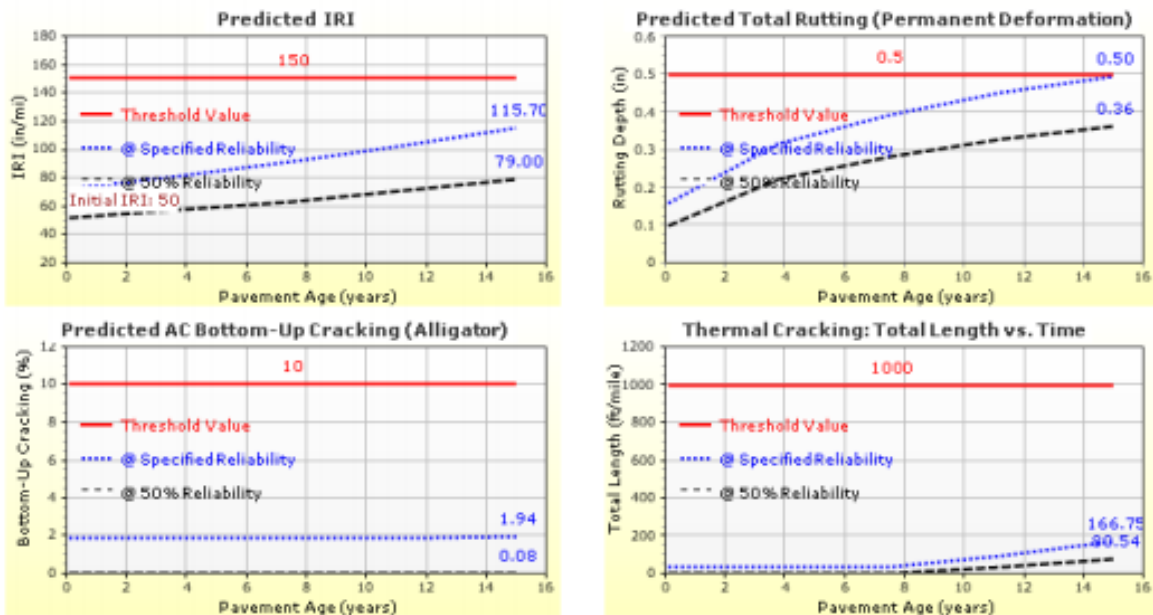
Figure 6.2 Layer structure and predicted distresses of project#1 based on Design Approach 1 using PG 76-34 as the upper AC layer

52

The cost calculations were completed as follows. First, the layer thickness was multiplied by one square yard (9 ft^2) to determine volume of total mix per square yard area. From the design output, the percent of asphalt binder was determined. Then, subtracting the percent of asphalt from 100%, the volume of aggregate was determined. Multiplying the total volume of the mix by the individual material percent produced individual volume of the materials. Costs of each material was determined by multiplying the volume of the material with its unit price. Finally, the individual cost of the materials were added to give the cost per layer. The material take off for the revised design to satisfy thermal cracking is summarized in Table 6.1.

Table 6.1 Material and cost estimation for the pavement structure design in Figure 6.2

Pave-Layers thickness	Vol. per sy (ft^3)	Material	Cost per cf (ft^3)	Percent of total mix (%)	Vol. per material (ft^3)	Cost per Vol. of material	Cost per layer
A	B	C	D	E	F= E × B	G= D × F	H
1 in (0.0833 ft)	0.75	Asphalt (PG 76-34)	14.98	10.2	0.077	1.12	3.09
		Hot plant mix	2.93	89.8	0.674	1.97	
6 in (0.5 ft)	4.5	Asphalt (PG 76-28)	14.98	11.5	0.52	7.79	19.45
		Hot plant mix	2.93	88.5	3.98	11.66	
17 in (1.42 ft)	12.78	Asphalt (PG 70-28)	14.33	10.2	1.3	18.63	52.27
		Hot plant mix	2.93	89.8	11.48	33.64	
4 in (0.333 ft)	3	Crushed base	1.2	100	3	3.6	3.6
Total cost per square yard for the overall pavement structure							**$78.4**

sy – square yards, cf – cubic foot, and Vol.-Volume

6.2.2 Design Approach 2: Based on Locally Calibrated Material Properties

For the Design Approach 2, the following adjustments were made to the aforementioned Design Approach 1.

1. Instead of employing the default subgrade M_r values provided in the WYDOT 2012 user design guide, the M_r value was calculated using the best selected subgrade predictive model. The best model was the ARA constitutive model given by Equation (4.11) determined in Section 4. This model requires the determination of deviator and confining stresses on top of the subgrade soil. To determine these stresses, the asphalt and base thicknesses should be assumed based on the designer experience. Assuming these thicknesses require understanding of the functional type of roadway (interstate, primary or secondary) and the AADTT. Once thicknesses are assumed, the vertical stress due to overburden pavement materials on top of the subgrade layer can be calculated using average unit weights of 140 pcf and 135 pcf for the asphalt concrete layer and base material, respectively. Then, the confining stress can be determined by multiplying the vertical stress with an assumed coefficient of lateral pressure of 0.5. To determine an induced vertical stress from a vehicle load, 100-psi tire pressure, five-inch contact radius, and elastic moduli of 500,000 psi, 40,000 psi and 12,000 psi for asphalt, base and subgrade materials, respectively, were assumed. Using the above inputs, computer software KENPAVE or Bitumen Stress Analysis in Roads (BISAR) was used to determine the total deviator stress on the subgrade. The deviator stresses for combined thicknesses of asphalt and base layers have been documented by Henrichs (2015). Next, the estimated confining and deviator stresses were used to determine bulk and orthogonal shear stresses. Subsequently, k_1, k_2 and k_3 regression constants for the constitutive M_r model were determined from Table 4.8. Finally, the M_r value of the subgrade was estimated using Equation (4.11). The procedure of estimating M_r value of the subgrade layer used in Project#1 is described as follows:

Step 1: Assume asphalt and base thicknesses:

For the given amount of AADTT and interstate road, 10-inch asphalt and 16-inch crushed gravel were assumed.

Step 2: Determine confined and deviator stresses on the subgrade:

Confining stress (σ_c) = vertical stress (σ_v) × coefficient of lateral presure (k_o)

$$\sigma_c = (h_1 \times \gamma_1 + h_2 \times \gamma_2) \times k_o = \left(\left(\frac{10}{12}\right) ft \times 140 \ pcf + \left(\frac{16}{12}\right) \times 135 \ pcf\right) \times 0.5$$
$$= 1.16 \ psi$$

Deviator stress is found to be 1.68 psi using the KENPAVE software package based on the combined vehicle tire pressure and overburden pressure.

Step 3: Determine bulk and octahedral shear stresses:

Bulk Stress $(\theta)(psi) = \sigma_1 + \sigma_2 + \sigma_3$

where σ_1, σ_2 and σ_3 are the major, intermidate and minor principal stresses.

$\sigma_1 = 1.16 + 1.68 = 2.84 \ psi, \quad \sigma_2 = 1.16 \ psi, \quad \sigma_3 = 1.16 \ psi$

Bulk Stress $(\theta)(psi) = \sigma_1 + \sigma_2 + \sigma_3 = 2.84 + 1.16 + 1.16 = 5.16 \ psi$

$$Octahedral \ Shear \ Stress \ (\tau_{Oct})(psi) = \sqrt{\frac{(\sigma_1 - \sigma_2)^2 + (\sigma_3 - \sigma_2)^2 + (\sigma_3 - \sigma_1)^2}{3}}$$

$$\tau_{Oct} \ (psi) = \sqrt{\frac{(2.84 - 1.16)^2 + (1.16 - 1.16)^2 + (1.16 - 2.84)^2}{3}} = 1.37 \ psi$$

Step 4: The k_1, k_2 and k_3 regression constants for A-7-6 subgrade soils are given in Table 6.2:

Table 6.2. Regression constants for A-7-6 soils.

Soil Type	k_1	k_2	k_3
A-7-6	520.4	0.264	0.651

Step 5: Calculate M_r value of the subgrade layer using the ARA constitutive model:

$$\widehat{M_r}(psi) = k_1 P_a \left(\frac{\theta}{P_a}\right)^{k_2} \left(\frac{\tau_{Oct}}{P_a} + 1\right)^{k_3}, P_a = Atmospheric \ presure \ (14.696 psi)$$

$$\widehat{M_r}(psi) = 520.4 \times 14.696 \times \left(\frac{5.16}{14.696}\right)^{0.264} \left(\frac{1.37}{14.696} + 1\right)^{0.651} = 6,142.85 psi$$

2. The M_r values of the base material (i.e., 45,000 psi) provided in the WYDOT 2012 user guide were very high compared with laboratory-measured M_r value. Thus, representative laboratory-measured M_r value for the base material by Mebrahtom (2017) was used in the design. According to Mebrahtom 2017, 12 base material sources in the state of Wyoming were identified and used for M_r testing. Since this project was located in Laramie County, the base material source from the same county was used. The M_r value of the base material at optimum moisture content at 34,460 psi was used for this project.
3. The locally calibrated coefficients, updated in the WYDOT 2015 report on local calibration (Byattacharya, et al., 2015), were also included in addition to the calibrated coefficients documented in the WYDOT 2012 user guide.

Following the aforementioned adjustments in the pavement design and employing the commonly used asphalt binder, the design outcome is shown in Figure 6.3. Asphalt grade, PG 70-28, with 11.5 % and 10.2% by volume of binders, was used for the upper and lower asphalt layers. All predicted distresses were below the target limits except for the thermal cracking of 2,022.07 ft/mile, which exceeded the target design limit of 1,000 ft/mile. To meet the design limit, the upper asphalt grade was changed to PG 70-34. As a result, thermal cracking was reduced to 54.94 ft/mile as illustrated in Figure 6.4.

To evaluate the cost comparison between the design using WYDOT 2012 guide and the adjusted design, cost estimation for the overall pavement structures was performed following the method described in Section 6.2.1. Table 6.3 shows the cost analysis for the pavement structure designed based on the Design Approach 2.

Table 6.3 Material and cost estimation for pavement structure given in Figure 6.4

Pave-Layers thickness	Vol. per sy (yd²)	Materials	Cost per cf (ft³)	% of total mix	Vol. per material	Cost per Vol. of material	Cost per layer
A	B	C	D	E	F= E × B	G= D × f	H
3 in (0.25 ft)	2.25	Asphalt (PG 70-34)	14.33	11.5	0.26	3.73	9.56
		Hot plant mix	2.93	88.5	1.99	5.83	
8in (0.67 ft)	6.03	Asphalt (PG 70-28)	14.33	10.2	0.615	8.81	24.66
		Hot plant mix	2.93	89.8	5.41	15.85	
18 in (1.5 ft)	13.5	Crushed base	1.2	100	13.5	16.2	16.2
Total cost per square yards for the overall pavement structure							**$50.4**

sy – square yards, and cf – cubic foot

Design Inputs

Design Life:	15 years
Design Type:	Flexible Pavement

Base construction:	May, 2014
Pavement construction:	June, 2014
Traffic opening:	September, 2014

Climate Data Sources (Lat/Lon)	41.158, -104.807

Design Structure

Layer type	Material Type	Thickness (in.):
Flexible	Default asphalt concrete	2.0
Flexible	Default asphalt concrete	8.0
NonStabilized	Crushed gravel	10.0
NonStabilized	Crushed gravel	8.0
Subgrade	A-7-6	Semi-infinite

Volumetric at Construction:

Effective binder content (%)	11.5
Air voids (%)	5.5

Traffic

Age (year)	Heavy Trucks (cumulative)
2014 (initial)	4,199
2021 (7 years)	5,664,610
2029 (15 years)	12,526,400

Design Outputs

Distress Prediction Summary

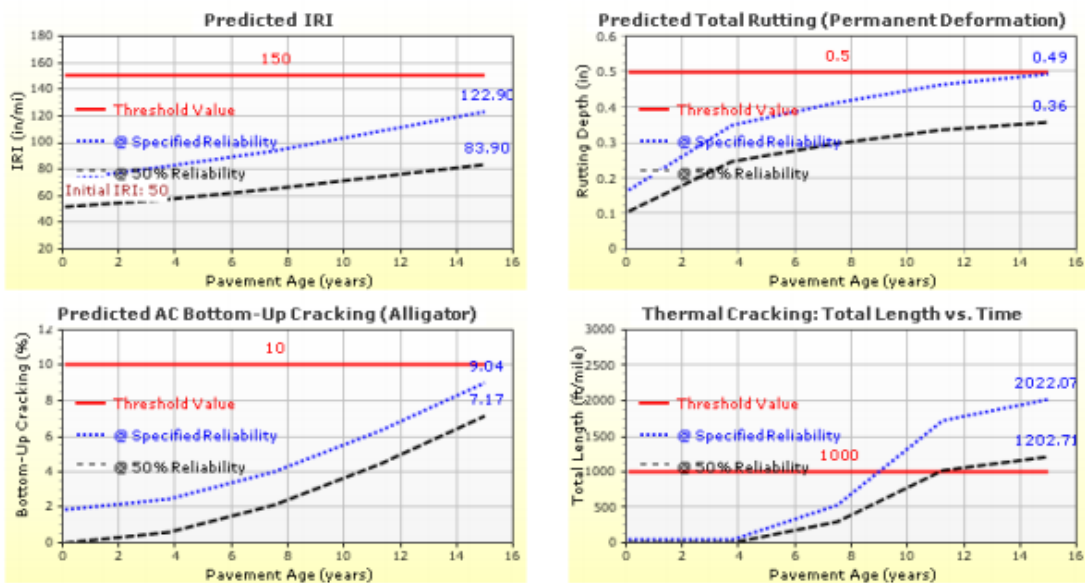| Distress Type	Distress @ Specified Reliability		Reliability (%)		Criterion Satisfied?
	Target	Predicted	Target	Achieved	
Terminal IRI (in./mile)	150.00	122.93	95.00	99.73	Pass
Permanent deformation - total pavement (in.)	0.50	0.49	95.00	95.69	Pass
AC bottom-up fatigue cracking (percent)	10.00	9.03	95.00	99.37	Pass
AC thermal cracking (ft/mile)	1000.00	2022.07	95.00	34.20	Fail
AC top-down fatigue cracking (ft/mile)	2000.00	335.92	95.00	100.00	Pass
Permanent deformation - AC only (in.)	0.50	0.31	95.00	100.00	Pass

Distress Charts

Figure 6.3 Pavement structure and predicted distresses for project#1 based on Design Approach 2 using PG 70-28 as the upper AC layer

56

Design Inputs

Design Life: 15 years
Design Type: Flexible Pavement

Base construction: May, 2014
Pavement construction: June, 2014
Traffic opening: September, 2014

Climate Data Sources (Lat/Lon): 41.158, -104.807

Design Structure

Layer type	Material Type	Thickness (in.):	Volumetric at Construction:	
Flexible	Default asphalt concrete	3.0	Effective binder content (%)	11.5
Flexible	Default asphalt concrete	8.0	Air voids (%)	5.5
NonStabilized	Crushed gravel	10.0		
NonStabilized	Crushed gravel	8.0		
Subgrade	A-7-6	Semi-infinite		

Traffic

Age (year)	Heavy Trucks (cumulative)
2014 (initial)	4,199
2021 (7 years)	5,664,610
2029 (15 years)	12,526,400

Design Outputs

Distress Prediction Summary

| Distress Type	Distress @ Specified Reliability		Reliability (%)		Criterion Satisfied?
	Target	Predicted	Target	Achieved	
Terminal IRI (in./mile)	150.00	117.18	95.00	99.90	Pass
Permanent deformation - total pavement (in.)	0.50	0.48	95.00	97.47	Pass
AC bottom-up fatigue cracking (percent)	10.00	5.64	95.00	100.00	Pass
AC thermal cracking (ft/mile)	1000.00	54.94	95.00	100.00	Pass
AC top-down fatigue cracking (ft/mile)	2000.00	332.15	95.00	100.00	Pass
Permanent deformation - AC only (in.)	0.50	0.30	95.00	100.00	Pass

Distress Charts
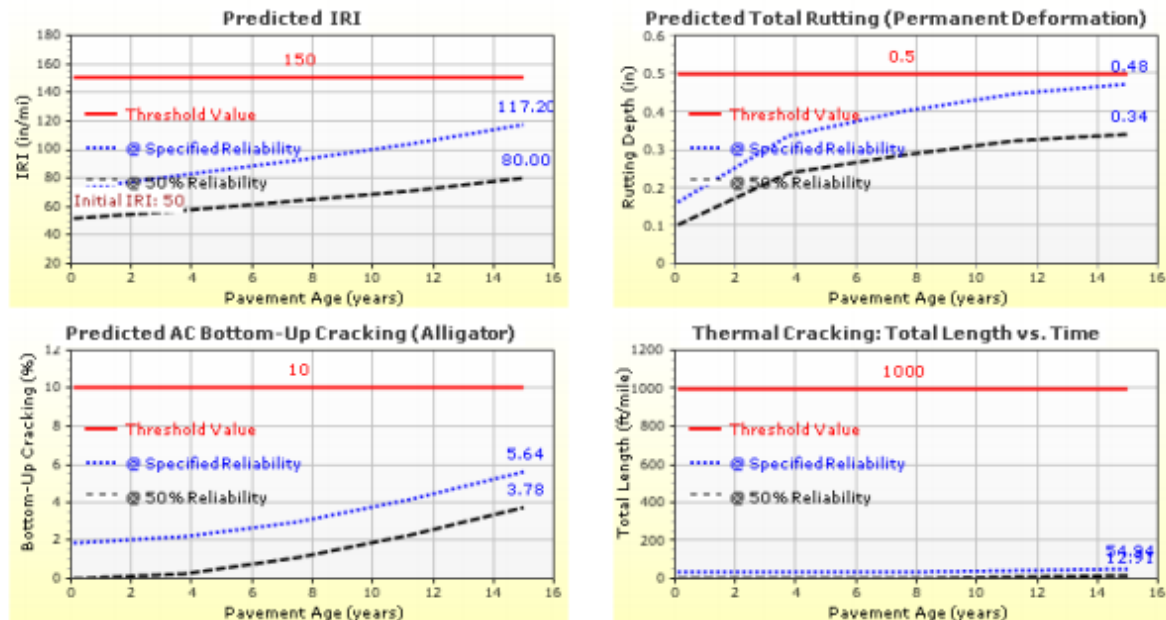
Figure 6.4 Pavement structure and predicted distresses for project#1 based on modified Design Approach 2 using PG 70-34 as the upper AC layer.

57

6.3 Project #2: New Flexible Pavement Design on Highway WY 78 (JCT I 80)

Project#2 represents a primary road with a new flexible pavement design in Carbon County, WY. The project is located in section JCT I 80 (THAYER INT) and has 0.152 starting and 0.4 ending mile posts. According WYDOT 2014 mile book, this section has AADT of 4268 and AADTT of 1259.

6.3.1 Design Approach 1: Based on WYDOT 2012 User Design Guide

The design criteria are different for different road classifications. For a primary road, the design criteria for 20 years of design life are given as 15% alligator cracking, 0.5-inch total rutting, 1,500 ft/mile transverse (thermal) cracking, and 170 in/mi IRI. For this project, 85% of design reliability was used as per the recommendation of WYDOT 2012 user design guide. Climate station positioned in Rawlins, WY was used for inputting the climate data for this project.

A-6 subgrade soil was assumed for this project, and the recommended M_r value was 5,810 psi as per WYDOT 2012 user design guide. The M_r value of the base layer was taken as 17,430 psi, which was equivalent to three times the subgrade M_r value. In this design process, the old calibrated distress coefficients were used.

Figure 6.5 shows the best outcome of the pavement structure, predicted distresses, and corresponding reliability based on the WYDOT 2012 user design guide. Asphalt grade, PG 70-28, was used for the two-inch thick upper asphalt layer, while PG 64-28 for the 10-inch thick lower layer. To overcome the excessive thermal cracking, the upper asphalt binder was changed to PG 70-34 and the lower to PG 70-28. Figure 6.6 shows the design outcome of the pavement structure and predicted distresses based on the modified Design Approach 1. Cost estimates are summarized in Table 6.4.

Table 6.4 Material and Cost Estimation for the Pavement Structure Given in Figure 6.6

Pave-Layers thickness	Vol. per sy (yd²)	Materials	Cost per cf (ft³)	% of total mix	Vol. per material	Cost per Vol. of material	Cost per layer
A	B	C	D	E	F= E × B	G= D × f	H
2 in (0.167 ft)	1.5	Asphalt (PG 70-34)	14.33	11.5	0.173	2.5	6.4
		Hot plant mix	2.93	88.5	1.33	3.9	
10 in (0.833 ft)	7.5	Asphalt (PG 70-28)	14.33	10.2	0.765	10.96	30.71
		Hot plant mix	2.93	89.8	6.74	19.75	
4 in (0.333ft)	3	Crushed base	1.2	100	3	3.6	3.6
Total cost per square yards for the overall pavement structure							**$40.7**

sy – square yards, and cf – cubic foot

Design Inputs

Design Life: 20 years
Design Type: Flexible Pavement

Base construction: May, 2016
Pavement construction: June, 2017
Traffic opening: September, 2017

Climate Data Sources (Lat/Lon): 41.806, -107.2

Design Structure

Layer type	Material Type	Thickness (in.):	Volumetric at Construction:	
Flexible	Default asphalt concrete	2.0	Effective binder content (%)	11.5
Flexible	Default asphalt concrete	10.0	Air voids (%)	5.5
NonStabilized	Crushed gravel	4.0		
Subgrade	A-6	Semi-infinite		

Traffic

Age (year)	Heavy Trucks (cumulative)
2017 (initial)	1,259
2027 (10 years)	2,348,680
2037 (20 years)	5,318,160

Design Outputs

Distress Prediction Summary

| Distress Type	Distress @ Specified Reliability		Reliability (%)		Criterion Satisfied?
	Target	Predicted	Target	Achieved	
Terminal IRI (in./mile)	170.00	120.05	85.00	99.84	Pass
Permanent deformation - total pavement (in.)	0.50	0.50	85.00	85.75	Pass
AC bottom-up fatigue cracking (percent)	15.00	3.86	85.00	100.00	Pass
AC thermal cracking (ft/mile)	1500.00	1990.86	85.00	57.23	Fail
AC top-down fatigue cracking (ft/mile)	5000.00	210.92	85.00	100.00	Pass
Permanent deformation - AC only (in.)	0.50	0.18	85.00	100.00	Pass

Distress Charts
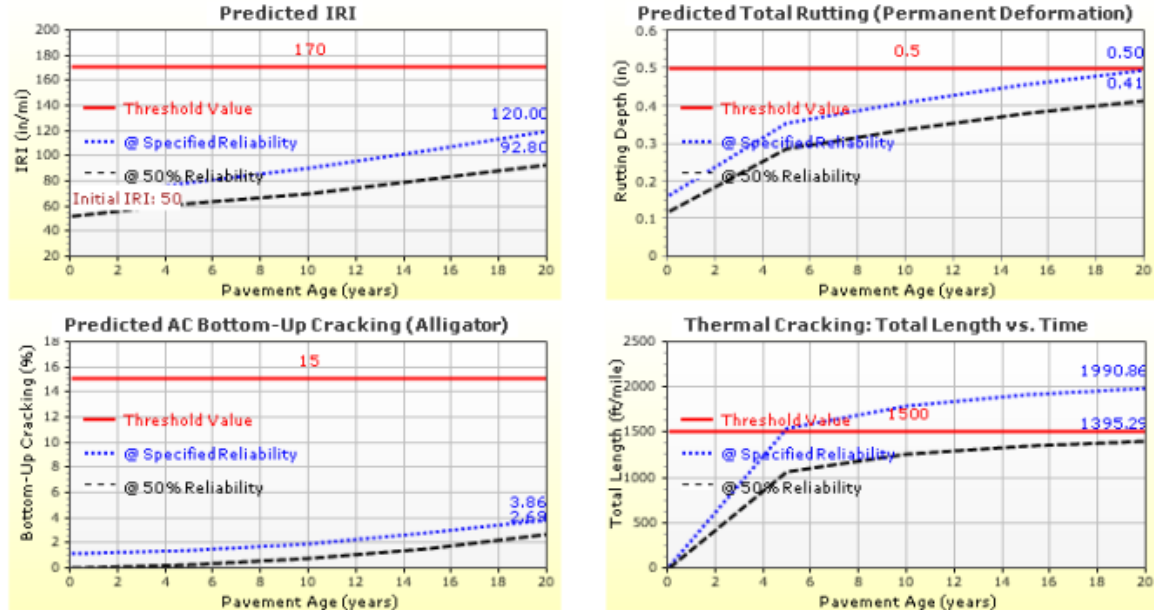
Figure 6.5 Pavement structure and predicted distresses for project#2 based on Design Approach 1 using PG 70-28 and PG 64-28 as the upper and lower AC layers.

Design Inputs

Design Life: 20 years
Design Type: Flexible Pavement

Base construction: May, 2016
Pavement construction: June, 2017
Traffic opening: September, 2017

Climate Data Sources (Lat/Lon): 41.806, -107.2

Design Structure

Layer type	Material Type	Thickness (in.):	Volumetric at Construction:	
Flexible	Default asphalt concrete	2.0	Effective binder content (%)	11.5
Flexible	Default asphalt concrete	10.0	Air voids (%)	5.5
NonStabilized	Crushed gravel	4.0		
Subgrade	A-6	Semi-infinite		

Traffic

Age (year)	Heavy Trucks (cumulative)
2017 (initial)	1,259
2027 (10 years)	2,348,680
2037 (20 years)	5,318,160

Design Outputs

Distress Prediction Summary

| Distress Type	Distress @ Specified Reliability		Reliability (%)		Criterion Satisfied?
	Target	Predicted	Target	Achieved	
Terminal IRI (in./mile)	170.00	118.33	85.00	99.88	Pass
Permanent deformation - total pavement (in.)	0.50	0.50	85.00	85.32	Pass
AC bottom-up fatigue cracking (percent)	15.00	3.52	85.00	100.00	Pass
AC thermal cracking (ft/mile)	1500.00	1036.51	85.00	99.46	Pass
AC top-down fatigue cracking (ft/mile)	5000.00	210.29	85.00	100.00	Pass
Permanent deformation - AC only (in.)	0.50	0.18	85.00	100.00	Pass

Distress Charts
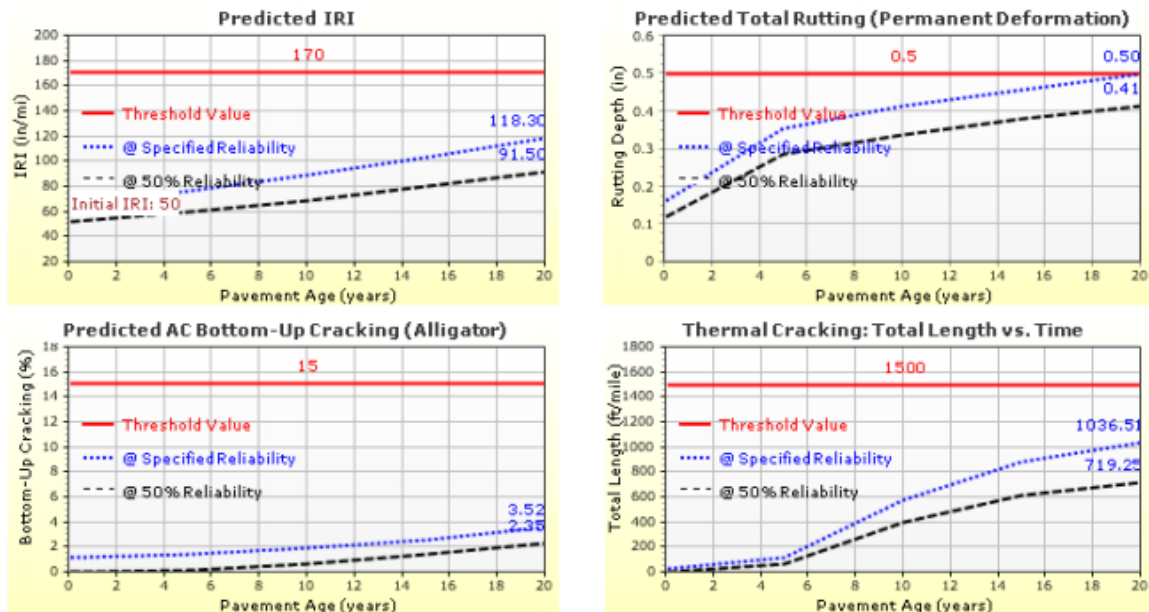
Figure 6.6 Pavement structure and predicted distresses for project#2 based on modified Design Approach 1 using PG 70-34 and PG 70-28 as the upper and lower AC layers

60

6.3.2 Design Approach 2: Based on Locally Calibrated Material Properties

Design Approach 2 was conducted based on the following adjustments made to the WYDOT 2012 user design guide:

1. Like Project#1, ARA constitutive M_r model was employed for determining the M_r value of the subgrade. The asphalt and base thicknesses were assumed to be 7 inches and 12 inches, respectively. Following the procedure described in project#1, the M_r of the subgrade was estimated as 9,476 psi.
2. Since the project was located in Carbon County, the measured M_r value of the base material obtained from Carbon County of 22,388 psi was used in this design for the base and subbase materials.
3. The locally calibrated coefficients updated in the WYDOT 2015 report (Byattacharya, et al., 2015) were used in addition to the calibrated coefficients documented in WYDOT 2012 user design guide.

Figure 6.7 shows the design outcome of pavement layers and predicted distresses based on the Design Approach 2. PG 70-28 asphalt binder was used for the 1.5-inch upper asphalt layer, while PG 64-28 was used for the seven-inch lower asphalt layer. All distresses satisfy the target limits except thermal cracking. Hence, the modified design outcome shown in Figure 6.8 indicates that the asphalt binder for the upper layer was changed to PG 64-40 to achieve the design limit of thermal cracking. Overall, cost estimation analysis of the modified Design Approach 2 is summarized in Table 6.5.

Table 6.5 Material and cost estimation for the pavement structure given in Figure 6.8

Pave-Layers thickness	Vol. per sy (yd²)	Materials	Cost per cf (ft³)	% of total mix	Vol. per material	Cost per Vol. of material	Cost per layer
A	B	C	D	E	F= E × B	G= D × f	H
2 in (0.167 ft)	1.5	Asphalt (PG 64-40)	14.25	11.5	0.173	2.47	6.37
		Hot plant mix	2.93	88.5	1.33	3.9	
6.5 in (0.54 ft)	4.86	Asphalt (PG 64-28)	14.18	10.2	0.5	7.09	19.88
		Hot plant mix	2.93	89.8	4.36	12.79	
10 in (0.83ft)	7.5	Crushed base	1.2	100	7.5	9	9
Total cost per square yards for the overall pavement structure							**$35.2**

sy – square yards, and cf – cubic foot

Design Inputs

Design Life: 20 years
Design Type: Flexible Pavement

Base construction: May, 2016
Pavement construction: June, 2017
Traffic opening: September, 2017

Climate Data Sources (Lat/Lon): 41.806, -107.2

Design Structure

Layer type	Material Type	Thickness (in.):	Volumetric at Construction:	
Flexible	Default asphalt concrete	1.5	Effective binder content (%)	11.5
Flexible	Default asphalt concrete	7.0	Air voids (%)	5.5
NonStabilized	Crushed gravel	9.0		
Subgrade	A-6	Semi-infinite		

Traffic

Age (year)	Heavy Trucks (cumulative)
2017 (initial)	1,259
2027 (10 years)	2,348,680
2037 (20 years)	5,318,160

Design Outputs

Distress Prediction Summary

Distress Type	Distress @ Specified Reliability		Reliability (%)		Criterion Satisfied?
	Target	Predicted	Target	Achieved	
Terminal IRI (in./mile)	170.00	124.65	85.00	99.66	Pass
Permanent deformation - total pavement (in.)	0.50	0.40	85.00	98.90	Pass
AC bottom-up fatigue cracking (percent)	15.00	14.86	85.00	87.54	Pass
AC thermal cracking (ft/mile)	1500.00	2741.20	85.00	29.35	Fail
AC top-down fatigue cracking (ft/mile)	5000.00	512.17	85.00	100.00	Pass
Permanent deformation - AC only (in.)	0.50	0.24	85.00	100.00	Pass

Distress Charts

Figure 6.7 Pavement structure and predicted distresses for project#2 based on Design Approach 2 using PG 70-28 as the upper AC layer.

62

Design Inputs

Design Life: 20 years
Design Type: Flexible Pavement

Base construction: May, 2016
Pavement construction: June, 2017
Traffic opening: September, 2017

Climate Data Sources (Lat/Lon): 41.806, -107.2

Design Structure

Layer type	Material Type	Thickness (in.):	Volumetric at Construction:	
Flexible	Default asphalt concrete	2.0	Effective binder content (%)	11.5
Flexible	Default asphalt concrete	6.5	Air voids (%)	5.5
NonStabilized	Crushed gravel	10.0		
Subgrade	A-6	Semi-infinite		

Traffic

Age (year)	Heavy Trucks (cumulative)
2017 (initial)	1,259
2027 (10 years)	2,348,680
2037 (20 years)	5,318,160

Design Outputs

Distress Prediction Summary

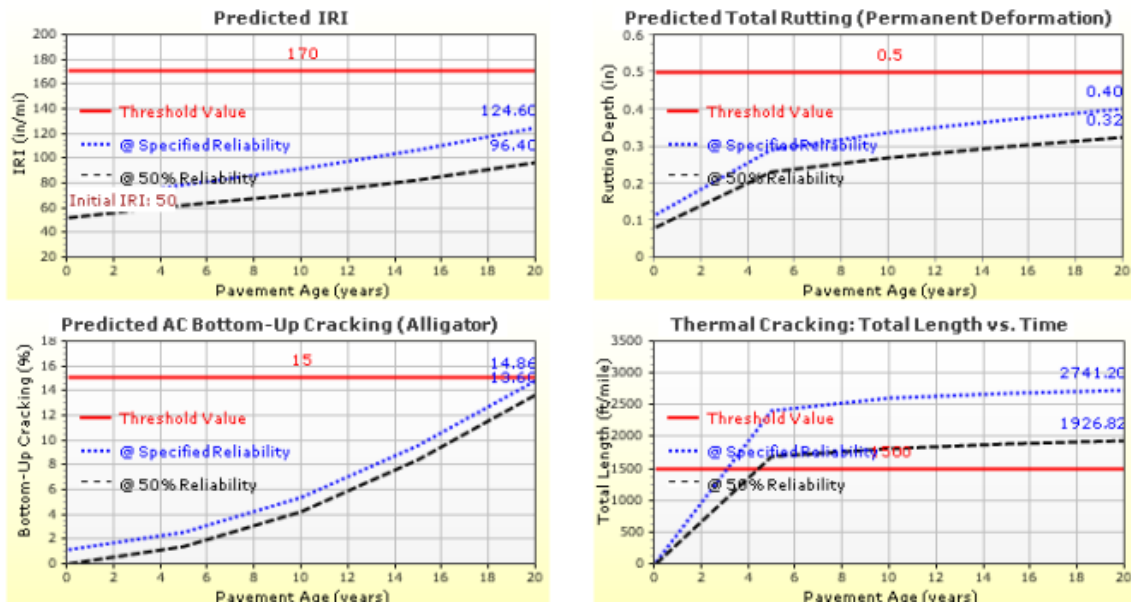| Distress Type	Distress @ Specified Reliability		Reliability (%)		Criterion Satisfied?
	Target	Predicted	Target	Achieved	
Terminal IRI (in./mile)	170.00	120.07	85.00	99.84	Pass
Permanent deformation - total pavement (in.)	0.50	0.40	85.00	99.13	Pass
AC bottom-up fatigue cracking (percent)	15.00	14.76	85.00	89.22	Pass
AC thermal cracking (ft/mile)	1500.00	22.75	85.00	100.00	Pass
AC top-down fatigue cracking (ft/mile)	5000.00	527.71	85.00	100.00	Pass
Permanent deformation - AC only (in.)	0.50	0.24	85.00	100.00	Pass

Distress Charts
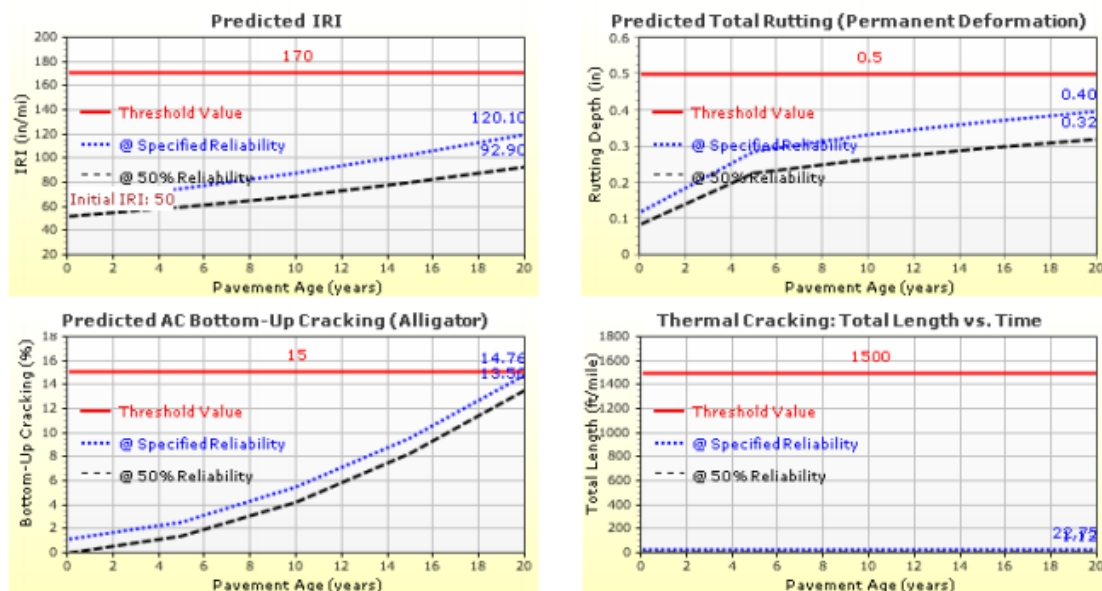
Figure 6.8 Pavement structure and predicted distresses for project#2 based on modified Design Approach 2 using PG 64-40 as the upper AC layer.

63

6.4 Project #3: New Flexible Pavement Design on Roadway WY 352 (JCT US 191)

Project #3 represents a secondary road with a new flexible pavement design in Sublette County, WY. The project is located in section JCT ROUTE 13 (US 191) and has 0.00 starting and 4.183 ending mile posts. According to WYDOT 2014 mile book, this project has AADT of 844 and AADTT of 119.

6.4.1 Design Approach 1: Fully Based on WYDOT 2012 User Design Guide

This project was designed for 20 years of design life, and the design criteria are 25% alligator cracking, 0.75 in total rutting, 2,500 ft/mi transverse (thermal) cracking, and 220 in/mile IRI as specified in the WYDOT 2012 user design guide for secondary roads. The design reliability of 75% was used for this project. Climate station positioned in Big Piney was employed for inputting the climate data for this project.

The subgrade soil for this project was assumed A-4, and the default M_r value is 6,085 psi. The M_r value of the subbase material was taken as 18,255 psi, which is three times the subgrade M_r value. In this design process, the old calibrated distress coefficients were used.

Figure 6.9 shows the design outcome of pavement structure and predicted distresses for project #3 based on the Design Approach 1 using the WYDOT 2012 user design guide. According to the commonly used asphalt grades, PG 64-28 and PG 64-22 were used for the upper and lower asphalt layers, respectively. Subsequently, the asphalt grade of the upper layer was changed to PG 64-40 to satisfy the required design limit of thermal cracking. Figure 6.10 shows the design outcome of pavement structure and modified predicted distresses for project#3 based on the WYDOT 2012 user design guide. The cost estimates for the modified Design Approach 1 of this project is summarized in Table 6.6.

Table 6.6 Material and cost estimation for the pavement structure given in Figure 6.10

Pave-Layers thickness	Vol. per sy (yd²)	Materials	Cost per cf (ft³)	% of total mix	Vol. per material	Cost per Vol. of material	Cost per layer
A	B	C	D	E	F= E × B	G= D × f	H
1 in (0.083 ft)	0.75	Asphalt (PG 64-40)	14.25	10.2	0.0765	1.09	3.06
		Hot plant mix	2.93	89.8	0.674	1.97	
3.5 in (0.292 ft)	2.63	Asphalt (PG 64-22)	12.14	10.2	0.268	3.25	10.15
		Hot plant mix	2.93	89.8	2.36	6.9	
7.5 in (0.625 ft)	5.63	Crushed base	1.2	100	5.63	6.76	6.76
Total cost per square yards for the overall pavement structure							**$19.9**

sy – square yards, and cf – cubic foot

Design Inputs

Design Life:	20 years
Design Type:	Flexible Pavement

Base construction:	May, 2017
Pavement construction:	June, 2017
Traffic opening:	September, 2017

Climate Data Sources (Lat/Lon)   42.584, -110.108

Design Structure

Layer type	Material Type	Thickness (in.):
Flexible	Default asphalt concrete	1.0
Flexible	Default asphalt concrete	3.5
NonStabilized	Crushed gravel	7.5
Subgrade	A-4	Semi-infinite

Volumetric at Construction:

Effective binder content (%)	10.2
Air voids (%)	7.0

Traffic

Age (year)	Heavy Trucks (cumulative)
2017 (initial)	119
2027 (10 years)	123,331
2037 (20 years)	279,261

Design Outputs

Distress Prediction Summary

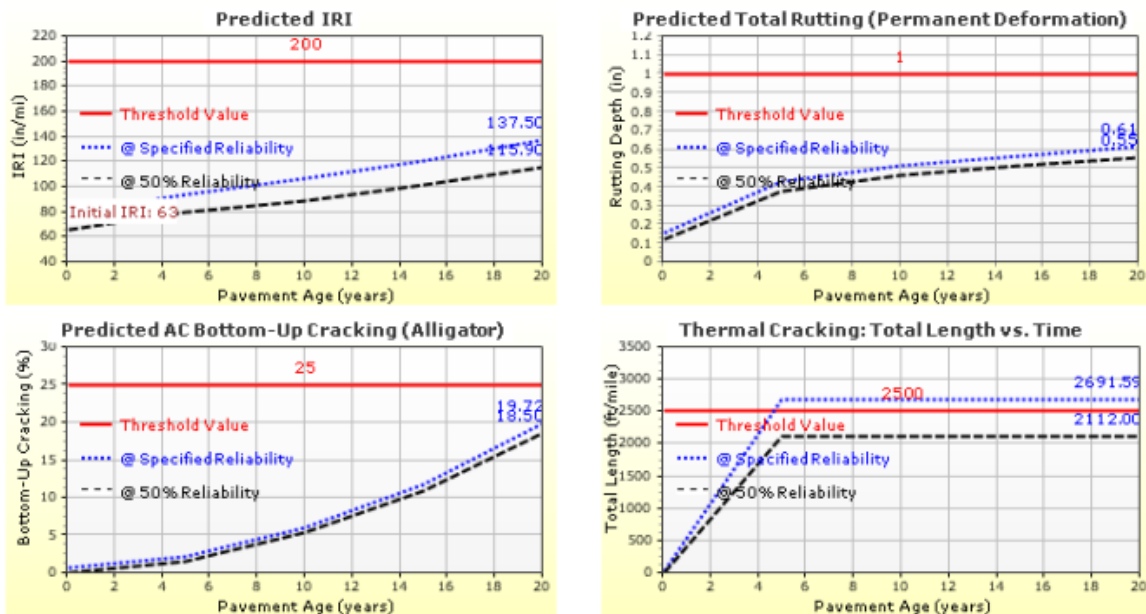| Distress Type	Distress @ Specified Reliability		Reliability (%)		Criterion Satisfied?
	Target	Predicted	Target	Achieved	
Terminal IRI (in./mile)	200.00	137.50	75.00	99.57	Pass
Permanent deformation - total pavement (in.)	1.00	0.61	75.00	100.00	Pass
AC bottom-up fatigue cracking (percent)	25.00	19.72	75.00	99.98	Pass
AC thermal cracking (ft/mile)	2500.00	2691.59	75.00	67.42	Fail
AC top-down fatigue cracking (ft/mile)	5000.00	1084.70	75.00	99.95	Pass
Permanent deformation - AC only (in.)	0.50	0.06	75.00	100.00	Pass

Distress Charts

Figure 6.9 Pavement structure and predicted distresses for project#3 based on Design Approach 1 using PG 64-28 as the upper AC layer.

65

Design Inputs

Design Life: 20 years
Design Type: Flexible Pavement

Base construction: May, 2017
Pavement construction: June, 2017
Traffic opening: September, 2017

Climate Data Sources (Lat/Lon): 42.584, -110.108

Design Structure

Layer type	Material Type	Thickness (in.):
Flexible	Default asphalt concrete	1.0
Flexible	Default asphalt concrete	3.5
NonStabilized	Crushed gravel	7.5
Subgrade	A-4	Semi-infinite

Volumetric at Construction:

Effective binder content (%)	10.2
Air voids (%)	7.0

Traffic

Age (year)	Heavy Trucks (cumulative)
2017 (initial)	119
2027 (10 years)	123,331
2037 (20 years)	279,261

Design Outputs

Distress Prediction Summary

| Distress Type	Distress @ Specified Reliability		Reliability (%)		Criterion Satisfied?
	Target	Predicted	Target	Achieved	
Terminal IRI (in./mile)	200.00	135.09	75.00	99.69	Pass
Permanent deformation - total pavement (in.)	1.00	0.62	75.00	100.00	Pass
AC bottom-up fatigue cracking (percent)	25.00	21.18	75.00	99.44	Pass
AC thermal cracking (ft/mile)	2500.00	789.20	75.00	100.00	Pass
AC top-down fatigue cracking (ft/mile)	5000.00	1183.59	75.00	99.89	Pass
Permanent deformation - AC only (in.)	0.50	0.06	75.00	100.00	Pass

Distress Charts
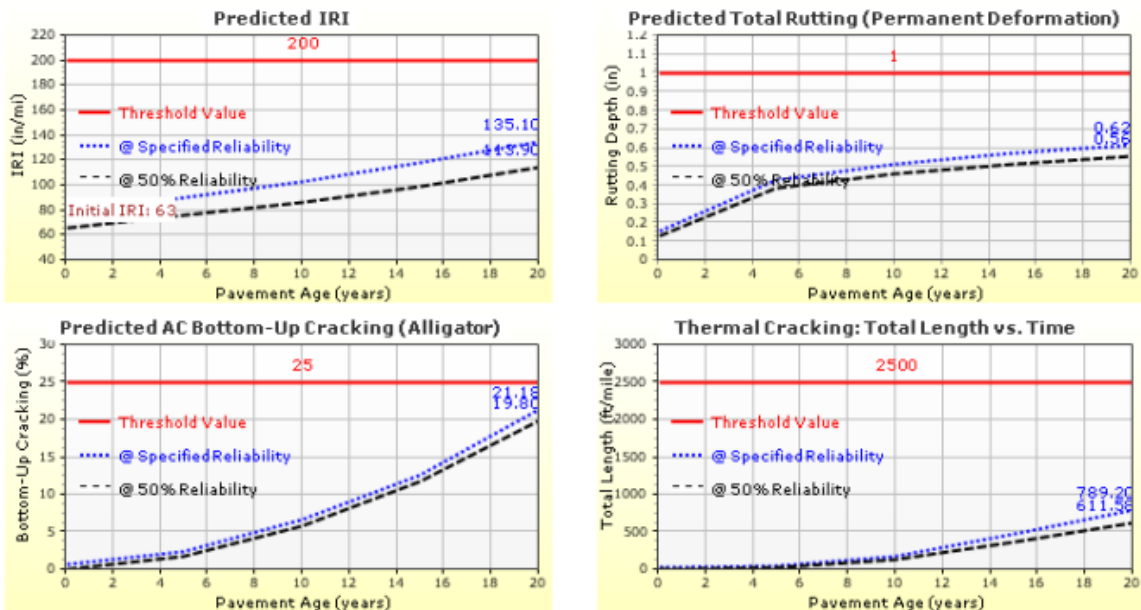
Figure 6.10 Pavement structure and predicted distresses for project#3 based on modified Design Approach 1 using PG 64-40 as the upper AC layer.

66

6.4.2 Design Approach 2: Based on Locally Calibrated Material Properties

The Design Approach 2 was conducted following adjustments made to the Design Approach 1:
1. The M_r of the subgrade was determined using the ARA constitutive model. The asphalt and base thicknesses were assumed to be 5 inches and 4 inches, respectively, for this pavement structure. M_r value of the subgrade was estimated to be 10,526.8 psi.
2. The nearest source of base material to this project was from Fermont County. Hence, the laboratory-measured M_r value of the base material taken from Fermont County, at optimum moisture, of 28,479 psi was used for the M_r value of the base in this design.
3. The locally calibrated coefficients updated in the WYDOT 2015 report (Byattacharya, et al., 2015) were used in addition to the calibrated coefficients documented in WYDOT 2012 user design guide.

Figure 6.11 shows the pavement structure and predicted distresses for the Design Approach 2. Applying the commonly used asphalt grades, PG 64-28 and PG 64-22 were used for the upper and lower asphalt layers, respectively. Subsequently, the asphalt grade of the upper layer was modified to 64-40 to satisfy the required design limit of thermal cracking. Figure 6.12 shows the design outcome based on the modified Design Approach 2 for Project#3. The cost estimates for the modified design of this project are summarized in Table 6.7.

Table 6.7 Material and cost estimation for the design strategy given in Figure 6.12

Pave-Layers thickness	Vol. per sy (yd²)	Materials	Cost per cf (ft³)	% of total mix	Vol. per material	Cost per Vol. of material	Cost per layer
A	B	C	D	E	F= E × B	G= D × f	H
1.5 in (0.125 ft)	1.125	Asphalt (PG 64-40)	14.25	10.2	0.103	1.47	4.46
		Hot plant mix	2.93	89.8	1.02	2.99	
3 in (0.25 ft)	2.25	Asphalt (PG 64-22)	12.14	10.2	0.23	2.79	8.71
		Hot plant mix	2.93	89.8	2.02	5.92	
4 in (0.333ft)	3	Crushed base	1.2	100	3	3.6	3.6
Total cost per square yards for the overall pavement structure							**$16.77**

Sy – square yards, and cf – cubic foot

Design Inputs

Design Life: 20 years
Design Type: Flexible Pavement

Base construction: May, 2017
Pavement construction: June, 2017
Traffic opening: September, 2017

Climate Data Sources (Lat/Lon): 42.584, -110.108

Design Structure
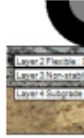
Layer type	Material Type	Thickness (in.):
Flexible	Default asphalt concrete	1.5
Flexible	Default asphalt concrete	3.0
NonStabilized	Crushed gravel	4.0
Subgrade	A-4	Semi-infinite

Volumetric at Construction:

Effective binder content (%)	10.2
Air voids (%)	7.0

Traffic

Age (year)	Heavy Trucks (cumulative)
2017 (initial)	119
2027 (10 years)	123,331
2037 (20 years)	279,261

Design Outputs

Distress Prediction Summary

| Distress Type	Distress @ Specified Reliability		Reliability (%)		Criterion Satisfied?
	Target	Predicted	Target	Achieved	
Terminal IRI (in./mile)	200.00	131.17	75.00	99.82	Pass
Permanent deformation - total pavement (in.)	1.00	0.31	75.00	100.00	Pass
AC bottom-up fatigue cracking (percent)	25.00	19.95	75.00	99.97	Pass
AC thermal cracking (ft/mile)	2500.00	2691.59	75.00	67.42	Fail
AC top-down fatigue cracking (ft/mile)	5000.00	1937.83	75.00	98.45	Pass
Permanent deformation - AC only (in.)	0.50	0.08	75.00	100.00	Pass

Distress Charts
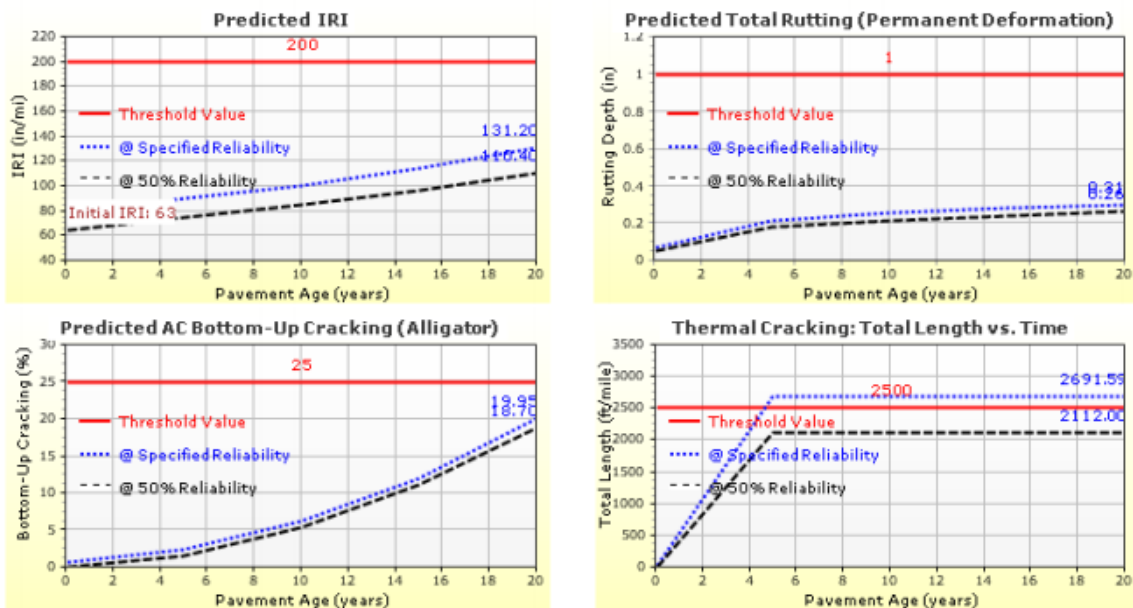
Figure 6.11 Pavement structure and predicted distresses for project#3 based on Design Approach 2 using PG 64-28 as the upper AC layer.

Design Inputs

Design Life: 20 years
Design Type: Flexible Pavement

Base construction: May, 2017
Pavement construction: June, 2017
Traffic opening: September, 2017

Climate Data Sources (Lat/Lon): 42.584, -110.108

Design Structure
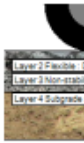
Layer type	Material Type	Thickness (in.):	Volumetric at Construction:	
Flexible	Default asphalt concrete	1.5	Effective binder content (%)	10.2
Flexible	Default asphalt concrete	3.0	Air voids (%)	7.0
NonStabilized	Crushed gravel	4.0		
Subgrade	A-4	Semi-infinite		

Traffic

Age (year)	Heavy Trucks (cumulative)
2017 (initial)	119
2027 (10 years)	123,331
2037 (20 years)	279,261

Design Outputs

Distress Prediction Summary

| Distress Type	Distress @ Specified Reliability		Reliability (%)		Criterion Satisfied?
	Target	Predicted	Target	Achieved	
Terminal IRI (in./mile)	200.00	130.70	75.00	99.83	Pass
Permanent deformation - total pavement (in.)	1.00	0.31	75.00	100.00	Pass
AC bottom-up fatigue cracking (percent)	25.00	21.98	75.00	97.98	Pass
AC thermal cracking (ft/mile)	2500.00	1709.42	75.00	98.25	Pass
AC top-down fatigue cracking (ft/mile)	5000.00	2273.82	75.00	97.38	Pass
Permanent deformation - AC only (in.)	0.50	0.08	75.00	100.00	Pass

Distress Charts
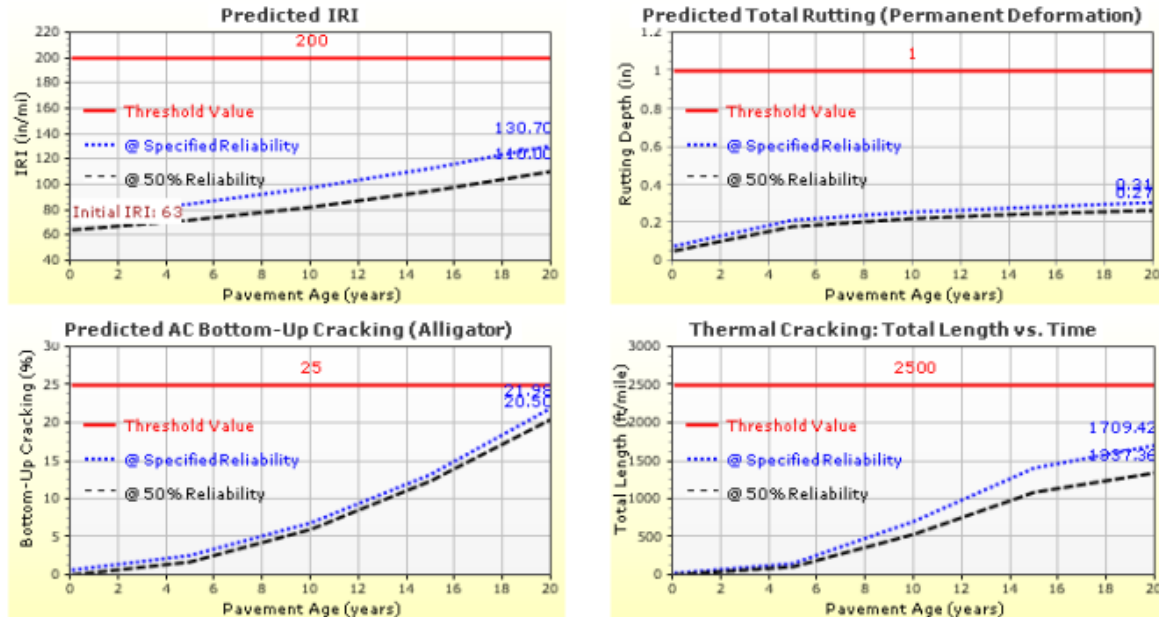
Figure 6.12 Pavement structure and predicted distresses for project#3 based on modified Design Approach 2 using PG 64-40 as the upper AC layer.

69

6.5   Pavement Design and Cost Comparison

- Most issues and problems associated with the WYDOT 2012 design guide were discussed and described in the design comparison report prepared by Ng et al. (2016). The comparison found that the predicted thermal cracking values based on all asphalt grades are greater than the threshold value of 1,000 ft/mi for interstate roads. Thus, Ng et al. (2016) suggested the need to increase the target design limit for interstate and primary roads in cold climates due to the large local calibration coefficient of 7.5 and the high standard error of the transfer function. Pavement design outcomes in all three projects possessed the same issue of satisfying thermal cracking.
- The overall material cost for the interstate roadway design (AADTT= 4199) based on the Design Approach 1 using the WYDOT 2012 user design guide was found to be $78.41 per square yard. The overall cost based on Design Approach 2 using the locally calibrated material properties was found to be $50.42 per square yard. This comparison clearly shows that Design Approach 2 reduces the overall cost by 35.7% or $27.99 per square yard.
- The overall material cost for the primary roadway design (AADTT= 1259) based the Design Approach 1 using the WYDOT 2012 user design guide was found to be $40.71 per square yard. The overall cost based on Design Approach 2 using the locally calibrated material properties was found to be $35.25 per square yard. This comparison clearly shows that the Design Approach 2 reduces the overall cost by 13.4% or $5.46 per square yard.
- The overall material cost for the local roadway design (AADTT= 119) based the Design Approach 1 using the WYDOT 2012 user design guide was found to be $19.97 per square yard. The overall cost based on Design Approach 2 using the locally calibrated material properties was found to be $16.77 per square yard. This comparison clearly shows that Design Approach 2 reduces the overall cost by 16.0% or $3.2 per square yard.

6.6   Summary

This section compares pavement designs for three pavement projects using two design approaches. The first design approach (denoted as Design Approach 1) follows design steps described in the WYDOT 2012 user design guide, and the second design approach (denoted as Design Approach 2) uses the locally calibrated M_r values for subgrade and base materials and locally calibrated distress coefficients. Cost analysis was performed to compare both design approaches. Design approach 2 resulted on average cost saving of 21% with pavement thicknesses less than that of Design Approach 1.

7. CONCLUSIONS AND RECOMMENDATIONS

7.1 Summary

WYDOT has been working on full implementation of the MEPDG in the state of Wyoming. To facilitate this implementation, many research works have been completed. Similarly, this report was completed to facilitate the full implementation of the MEPDG in the state of Wyoming.

Correlation studies on resilient modulus (M_r) of unbound subgrade layers and field measurements of DCP and SPT through a recently completed testing program were performed. Relationships between M_r value and Dynamic Cone Penetration Index (DCPI) and SPT N-values were investigated. Ten predictive models developed in previous research were evaluated to determine their relative accuracy on the estimation of flexible pavement performance using the software AASHTOWare. Three best M_r predictive models were identified and recommended for MEPDG implementation in Wyoming.

Sensitivity analyses were performed to evaluate the effects of input parameters on the MEPDG performance measures (cracking, rutting and smoothness). The influential variables to pavement performance were identified based on sensitivity study results by other agencies. The one at time (OAT) sensitivity analysis method was used, and this was conducted from varying each selected sensitive design parameter over a practical range to examine the change in the MEPDG predicted distresses. Finally, three new flexible pavement design comparisons were performed to evaluate and compare pavement design outcomes due to the locally calibrated M_r values of subgrade and base material, and updated distress coefficients. Additionally, cost analysis for Design Approach 1 and the Design Approach 2 was completed.

7.2 Conclusions

The following conclusions were drawn from this study:
1. A subgrade resilient modulus (M_r) predictive model with independent variables of Dynamic Cone Penetration Index (DCPI), optimum moisture content and maximum dry density was developed (Equation (3.1)). This model had coefficient of determination (R^2) of 0.67 and adjusted coefficient of determination (R^2-adj) of 0.59.
2. There was no linear relationship between M_r value and Standard Penetration Test N-value at significance levels of 0.05 and 0.1. Hence, no model was developed for M_r based on SPT N-value.
3. Among the 10 subgrade resilient modulus (M_r) predictive models developed for the state of Wyoming, three best models were selected based on a distress performance comparison. These three models are constitutive model by ARA (Model I), M_r design tables by Henrichs (Model D), and c-factor model by ARA (Model J).
4. Alligator cracking was hyper sensitive to AC air void, very sensitive to AC thickness, base thickness, base M_r, and AADTT, and sensitive to AC grade and climate. Thermal cracking was sensitive only to AC thickness. Total rutting was sensitive to AC thickness, AC air void, AADTT and climate, and non-sensitive to AC grade, base thickness, base M_r, and subgrade M_r. International Roughness Index (IRI) was sensitive to AC thickness, AC air void, subgrade M_r and AADTT, and non-sensitive to AC grade, base thickness, base Mr, and climate.
5. On average, the overall material cost for a new flexible pavement designed based on Design Approach 1 using the WYDOT 2012 design guide was 21% higher than the Design Approach 2 using the locally calibrated material properties and distress coefficients.

Although these findings and outcomes of this research are established for the Wyoming Department of Transportation (WYDOT), they can be adopted by other transportation agencies.

7.3   Recommendations

The following recommendations are suggested for future study and full implementation of MEPEDG in the state of Wyoming:
1. In this study, only one at a time (OAT) sensitivity studies were performed. Hence, global sensitivity analysis should be performed in the future so that the pavement designer can understand the interaction between the input variables.
2. The linear correlation between M_r and SPT-N value should be reevaluated when more data becomes available.
3. When the DCP data becomes available, accuracy of the M_r and DCPI correlation model should be re-evaluated.
4. The threshold value (design limit) for thermal cracking should be increased or the local calibrated coefficients of 7.5 of that thermal cracking should be reviewed.
5. The current WYDOT 2012 user design guide for pavement designs should be revised by incorporating recent research findings for subgrade and base materials.

Implementing the aforementioned recommendations would further facilitate full implementation of the MEPDG in the state of Wyoming, leading to more efficient and economical pavement designs.

REFERENCES

Ahammed, M.A., Kass, S., Hilderman, S., and Tang, W.K.S. (2011). MEDPG Implementation: Manitoba Experience. 2011 Annual Conference of the Transportation Association of Canada.

American Association of State Highway and Transportation Officials (AASHTO). (1993). AASHTO Guide for Design of Pavement Structures. Washington, D.C.

Applied Research Associates, Inc. (2012). MEPDG WYDOT Pavement Deign User Guide, Cheyenne, WY.

Applied Research Associates, Inc. (2004). Development of the 2002 Guide for the Design of New and Rehabilitated Pavement Structures. Final Report and Software (version 0.70) NCHRP Project 1-37A, Transportation Research Board, Washington, D.C., April.

Bhattacharya, B., Von Quintus, H., and Darter, M. (2015). Implementation and Local Calibration of the MEPDG Transfer Functions in Wyoming. Report No. FHWA 16/02F.

Carvalho, R., and Schwartz, C. (2006). Comparisons of Flexible Pavement Designs: AASHTO Empirical Versus NCHRP Project 1-37A Mechanistic-Empirical. Transportation Research Record: Journal of the Transportation Research Board, No. 1947, pp. 167-174.

Ceylan, H., Kim, S., Gopalakrishnan, K., and Ma, D. (2013). Iowa Calibration of MEPDG Performance Prediction Models. Report No InTrans Project. 58. pp 119.

Ceylan, H., Coree, B., and Gopalakrishnan, K. (2009). "Evaluation of the Mechanistic-Empirical Pavement Design Guide for Implementation in Iowa." The Baltic Journal of Road and Bridge Engineering, Vol. 4, No. 1, pp. 5-12.

Dzotepe, G.A. and Ksaibati, K. (2010). The Effect of Environmental Factors on the Implementation of the Mechanistic Empirical Pavement Design Guide. University of Wyoming, Laramie, WY.

Darter, M. I., Titus-Glover, L., and Von Quintus, H. L. (2009). Implementation of the Mechanistic-Empirical Pavement Design Guide in Utah: validation, calibration, and development of the UDOT MEPDG User's Guide. Report No. UT-09.11.

Farrar, M.J., and Turner, J.P. (1991). Resilient Modulus of Wyoming Subgrade Soils. Final report submitted to Mountain Plains Consortium, University of Wyoming, Civil and Architectural Engineering, Laramie, WY.

Glover, L. T., and Mallela, J. (2009). Guidelines for Implementing NCHRP 1-37A ME Design Procedures in Ohio: Volume 4-MEPDG Models Validation & Recalibration. Ohio Department of Transportation.

Hall, K.D., Xiao, D.X., and Kelvin Wang, C.P. (2010). Calibration of the MEPDG for Flexible Pavement Design in Arkansas. 90th Annual Transportation Research Board Meeting, Washington, D.C.

Hellrung, Daniel K. (2015). Back-calculation of Subgrade Resilient Modulus for Mechanistic-empirical Pavement Design in Wyoming. Master Thesis, University of Wyoming, Laramie, WY.

Henrichs, Zachary R. (2015). Measurement of the Resilient Modulus of Subgrade Materials for Mechanistic-Empirical Pavement Design Guide in Wyoming. Master Thesis, University of Wyoming, Laramie, WY.

Hutson, Zachary J. (2015) Characterization of Subgrade Properties for the Implementation of Mechanistic-Empirical Pavement Design Guide in Wyoming. Master Thesis, University of Wyoming, Laramie, WY.

Kang, M. and Adams, T. M. (2007). Local calibration for fatigue cracking models used in the 37 Mechanistic-Empirical Pavement Design Guide. Proceedings of the 2007 Mid-Continent Transportation Research Symposium, Ames, Iowa.

Kim, S., Ceylan, H., Gopalakrishnan, K., Smadi, O., Brakke, C. and Behnami, F. (2010). Verification of Mechanistic-Empirical Pavement Design Guide (MEPDG) Performance Predictions Using Pavement Management Information System (PMIS). 90th Transportation Research Board Annual Meeting, Washington D.C.

Kim, S., Ceylan, H., and Gopalakrishnan, K. (2007). "Effect of M-E Design Guide Input Parameters on Flexible Pavement Performance Predictions." Road Materials and Pavement Design, Vol. 8, Issue No. 3, pp. 375-397.

Li, J., Uhlmeyer, J.S., Mahoney, J.P., and Muench, S.T. (2011). Use of the 1993 AASHTO Guide,MEPDG and Historical Performance to Update the WSDOT Pavement Design Catalog. Washington State Department of Transportation, Tumwater, WA.

Li, J., Uhlmeyer, J.S., Mahoney, J.P., and Muench, S.T. (2010). Use of the AASHTO 1993 Guide, MEPDG and Historical Performance to Update the WSDOT Pavement Design Catalog. Transportation Research Record, No. 2776, pp. 15.

Li, J., Pierce, L. M. and Uhlmeyer, J. (2009). Calibration of Flexible Pavement in Mechanistic-Empirical Pavement Design Guide for Washington State. Journal of the Transportation Research Records, No. 2095, pp. 73-83.

Mallela, J., Titus-Glover, L., Sadasivam, S., Bhattacharya, B., Darter, M., and Von Quintus, H. (2013). Implementation of the AASHTO Mechanistic-empirical pavement design guide for Colorado. Report No. CDOT-2013-4.

Mebrahtom, Dawit. (2017). Characterization of Crushed Base in Wyoming. Master Thesis, University of Wyoming, Laramie, WY.

Mohammad, L. N., Gaspard, K., Herath, A., & Nazzal, M. D. (2007). Comparative evaluation of subgrade resilient modulus from non-destructive, in-situ, and laboratory methods (No. FHWA/LA. 06/417).

Muthadi, N. R. and Kim, Y. R. (2008). Local Calibration of Mechanistic-Empirical Pavement Design Guide for Flexible Pavement Design. Journal of the Transportation Research Record, No. 2087, pp. 131-141.

National Cooperative Highway Research Program (NCHRP) (2004). Guide for Mechanistic Empirical Design of New and Rehabilitated Pavement Structures. NCHRP Report 01-37A, Transportation Research Board, national Research council, Washington, D.C.

Ng, K., Hellrung, D., Ksaibati, K., and Wulff, S. S. (2016). Systematic Back-Calculation Protocol and Prediction of Resilient Modulus for MEPDG. International Journal of Pavement Engineering, pp. 1-13.

Ng, K., Von Quintus, H., Ksaibati, K., Hellrung, D., and Hutson, Z. (2016). Characterization of Material Properties for Mechanistic-Empirical Pavement Design in Wyoming. Report No. FHWA-WY-17/01F.

Ng, K., and Ksaibati, K. (2013). Characterization of Material Properties for Mechanistic-Empirical Pavement Design in Wyoming. University of Wyoming, Laramie, WY.

Rahim, A., and George, K. (2002). Automated Dynamic Cone Penetrometer for Subgrade Resilient Modulus Characterization. Transportation Research Record: Journal of the Transportation Research Board, No. 1806, pp. 70-77.

Schwartz, C. W., Li, R., Kim, S., Ceylan, H., and Gopalakrishnan, K. (2011). Sensitivity Evaluation of MEPDG Performance Prediction. Report No. NCHRP Project 1-47. Pp. 507.

Strategic Highway Research Program. (1993). Distress Identification Manual for the Long-Term Pavement Performance Project. National Academy of Sciences, Washington, D.C.

Sufian, Abu. (2016). Local Calibration of the Mechanistic Empirical Pavement Design Guide for Kansas. PhD Dissertation, Kansas State University.

Sun, X., Han, J., Parsons, R. L., Misra, A., Thakur, J. K., Turochy, R. E., and Meyer, H. (2015). Calibrating the Mechanistic-Empirical Pavement Design Guide for Kansas. Report No. KS-14-17. Kansas Department of Transportation.

Timm, D.H. (2006). Design Comparisons Using the New Mechanistic-Empirical Rigid Pavement Design Guide. Airfield and Highway Pavement, pp. 236-247.

Von Quintus, L. H. and Moulthrop, S. J. (2007). Mechanistic-Empirical Pavement Design Guide Flexible Pavement Performance Prediction Models for Montana. Montana Department of Transportation.

Wu, Z. and Xiao, D. X. (2016). Development of DARWin-ME Design Guideline for Louisiana Pavement Design. Report No. FHWA/LA. 11/551.

Wu, Z. and Yang, X. (2012). Evaluation of Current Louisiana Flexible Pavement Structures Using PMS Data and New Mechanistic-Empirical Pavement Design Guide. Report No. FHWA/LA. 11/482. Louisiana Transportation Research Center.

WYDOT 2016 weighted average bid prices. http://www.dot.state.wy.us/files/live/sites/wydot/files/shared/Contracts%20and%20Estimates/Weighted%20Average/2016%20English.pdf

APPENDIX A

Table A-1. Input values for Model B and Model C

Project No.	Sites	Soil Type	σc (psi)	σd (psi)	R-Value	γd	w	Pa (psi)	Rcat	Regression Coefficients		K4 for R>&R<50	Regression Coefficients	K4 for all soils
										R>50	R<50		for all soils	
0P11	C	A-7-6	0.8	3.8	15	105.9	17	14.696	1	b0 =4.16331	b0=2.877041	618.71	b0 =2.95733	4456.42
O601	A	A-2-4	0.8	3	67	117.2	8.3	14.696	0	b1= 0.00883	b1= -0.02638	14770.23	b1= 0.00895	4706.71
0N34	C	A-4	0.6	2.6	26	120	11.7	14.696	1	b2 =-22.45321	b2=4.001782	677.69	b2 = -0.02973	5652.05
0N30	A	A-6	0.4	9.9	14	113.8	14.7	14.696	1	b3 = 0.94778	b3 = 0.561017	946.47	b3 = 3.44703	4054.92
0N30	B	A-1-a	0.5	9.9	65	129.1	6.4	14.696	0	k5 = 1.55845	k5 = 0.098897	150596.56	b4 = -0.0254	5539.75
0N23	B	A-1-b	0.3	5.4	75	126.6	5.2	14.696	0	k6 = -0.95736	K = -0.353928	148283.68	b5 =-0.02341	7537.34
0P11	B	A-7-6	0.6	4.9	12	104.9	17	14.696	1			601.20	b6 = -9.57986	4667.16
O601	C	A-2-4	0.7	3.8	18	108.7	15.6	14.696	1			632.69	b7= 0.8153	4909.81
													k5 = 0.82712	
													k6 = -0.77521	

σc–confined pressure, σd–deviator stress, Pa– atmospheric pressure, wopt–optimum moisture content, γd– maximum dry density, Rcat– R value category.

Table A-2. Input values for Model D

Project No.	Sites	Soil Type	γ_d	W_{opt}	Asphalt Thickness (in)	Base Thickness (in)
0P11	C	A-7-6	105.9	17	6	12
O601	A	A-2-4	117.2	8.3	6	16
0N34	C	A-4	120	11.7	9	10
0N30	A	A-6	113.8	14.7	4	6
0N30	B	A-1-a	129.1	6.4	4	6
0N23	B	A-1-b	126.6	5.2	5	10
0P11	B	A-7-6	104.9	17	6.5	7
O601	C	A-2-4	108.7	15.6	6	12

w_{opt}–optimum moisture content, and γ_d– maximum dry density.

Table A-3. Input values for Model G

Project No.	Sites	Soil Type	R-Value	W_{opt}	Regression Coefficients for soils		
					β_i	U_i	α_i
0P11	C	A-7-6	15	17	-76.221	-573.156	22551
O601	A	A-2-4	67	8.3	-82.755	-558.42	22789
0N34	C	A-4	26	11.7	-95.003	-551.712	22729.6
0N30	A	A-6	14	14.7	-14.7855	-621.195	21062.3
0N30	B	A-1-a	65	6.4	-14.7855	-621.195	21062.3
0N23	B	A-1-b	75	5.2	-61.989	-595.273	22176.3
0P11	B	A-7-6	12	17	-66.67	-588.93	22289.05
O601	C	A-2-4	18	15.6	-76.221	-573.156	22551

w_{opt}– optimum moisture content

Table A-4. Input values for Model I

Project No.	Sites	Soil Type	σ_c (psi)	σ_d (psi)	Pa	Mr constitutive models Coefficients			Θ	τ
						K1	K2	K3		
0P11	C	A-7-6	0.8	3.8	14.696	520.4	0.264	0.651	6.2	3.103
O601	A	A-2-4	0.8	3	14.696	1131.2	0.483	-1.056	5.4	2.449
0N34	C	A-4	0.6	2.6	14.696	1000.6	0.52	-0.356	4.4	2.123
0N30	A	A-6	0.4	9.9	14.696	801.6	0.294	0.443	11.1	8.083
0N30	B	A-1-a	0.5	9.9	14.696	1544.8	0.626	0.527	11.4	8.083
0N23	B	A-1-b	0.3	5.4	14.696	1505.6	0.619	-1.063	6.3	4.409
0P11	B	A-7-6	0.6	4.9	14.696	520.4	0.264	0.651	6.7	4.001
O601	C	A-2-4	0.7	3.8	14.696	1131.2	0.483	-1.056	5.9	3.103

σ_c–confined pressure, σ_d–deviator stress, Pa– atmospheric pressure, Θ–bulk stress, and τ– octahedral shear stress

APPENDIX B

Table B-1. Comparison of distresses measured on site and predicted by ME-Software (AASHTOWare) using Model B

Project No	Sites	Longitudinal Crack (ft/mile)			Rutting Depth (inch)		
		Measured	Predicted	Error	Measured	Predicted	Error
0P11	C	965.49	1936.84	971.35	0.00	0.34	0.34
O601	A	0.00	361.10	361.10	0.50	0.28	0.22
0N34	C	0.00	857.14	857.14	0.00	0.42	0.42
0N30	A	0.00	1250.00	1250.00	0.00	0.57	0.57
0N30	B	0.00	1250.00	1250.00	0.00	0.47	0.47
0N23	B	0.00	2000.00	2000.00	0.00	0.52	0.52
0P11	B	445.00	984.13	539.13	0.00	0.33	0.33
O601	C	0.00	1326.3	1326.30	0.25	0.364	0.11
Total Sum of Errors				8555.02			2.98

Table B-2. Comparison of distresses measured on site and predicted by ME-Software (AASHTOWare) using Model C

Project No	Sites	Longitudinal Crack (ft/mile)			Rutting Depth (inch)		
		Measured	Predicted	Error	Measured	Predicted	Error
0P11	C	965.49	1777.77	812.28	0.00	0.37	0.37
O601	A	0.00	281.25	281.25	0.50	0.35	0.15
0N34	C	0.00	444.44	444.44	0.00	0.50	0.50
0N30	A	0.00	1388.88	1388.88	0.00	0.34	0.34
0N30	B	0.00	961.53	961.53	0.00	0.29	0.29
0N23	B	0.00	2187.50	2187.50	0.00	0.46	0.46
0P11	B	445	812.50	367.50	0.00	0.37	0.37
O601	C	0.00	1129.00	1129.00	0.25	0.42	0.17
Total Sum of Errors				7572.38			2.65

Table B-3. Comparison of distresses measured on site and predicted by ME-Software (AASHTOWare) using Model D

Project No	Sites	Longitudinal Crack (ft/mile)			Rutting Depth (inch)		
		Measured	Predicted	Error	Measured	Predicted	Error
0P11	C	965.49	1583.33	617.84	0.00	0.39	0.39
O601	A	0.00	285.70	285.7	0.50	0.34	0.16
0N34	C	0.00	500.00	500.00	0.00	0.50	0.50
0N30	A	0.00	1500.00	1500.00	0.00	0.33	0.33
0N30	B	0.00	1000.00	1000.00	0.00	0.29	0.29
0N23	B	0.00	2250.00	2250.00	0.00	0.41	0.41
0P11	B	445.00	843.00	398.00	0.00	0.34	0.34
O601	C	0.00	1125.00	1125.00	0.25	0.39	0.14
Total Sum of Errors				**7676.54**			**2.56**

Table B-4. Comparison of distresses measured on site and predicted by ME-Software (AASHTOWare) using Model E

Project No	Sites	Longitudinal Crack (ft/mile)			Rutting Depth (inch)		
		Measured	Predicted	Error	Measured	Predicted	Error
0P11	C	965.49	1583.33	617.84	0.00	0.391	0.39
O601	A	0.00	321.43	321.43	0.50	0.318	0.18
0N34	C	0.00	406.26	406.26	0.00	0.533	0.53
0N30	A	0.00	1388.88	1388.88	0.00	0.32	0.32
0N30	B	0.00	1066.66	1066.66	0.00	0.328	0.33
0N23	B	0.00	2158.73	2158.73	0.00	0.479	0.48
0P11	B	445.00	1000.00	555.00	0.00	0.322	0.32
O601	C	0.00	1125.00	1125.00	0.25	0.423	0.17
Total Sum of Errors				**7639.80**			**2.71**

Table B-5. Comparison of distresses measured on site and predicted by ME-Software (AASHTOWare) using Model F

Project No	Sites	Longitudinal Crack (ft/mile)			Rutting Depth (inch)		
		Measured	Predicted	Error	Measured	Predicted	Error
0P11	C	965.49	937.50	27.99	0.00	0.51	0.51
O601	A	0.00	410.71	410.71	0.50	0.27	0.23
0N34	C	0.00	185.70	185.70	0.00	0.70	0.70
0N30	A	0.00	1437.50	1437.50	0.00	0.43	0.43
0N30	B	0.00	1000.00	1000.00	0.00	0.32	0.32
0N23	B	0.00	2187.50	2187.50	0.00	0.48	0.48
0P11	B	445.00	1000.00	555.00	0.00	0.31	0.31
O601	C	0.00	870.96	870.96	0.25	0.51	0.26
Total Sum of Errors				6675.36			3.24

Table B-6. Comparison of distresses measured on site and predicted by ME-Software (AASHTOWare) using Model G

Project No	Sites	Longitudinal Crack (ft/mile)			Rutting Depth (inch)		
		Measured	Predicted	Error	Measured	Predicted	Error
0P11	C	965.49	1636.36	670.87	0.00	0.38	0.38
O601	A	0.00	321.43	321.43	0.50	0.3227	0.18
0N34	C	0.00	500.00	500.00	0.00	0.49	0.49
0N30	A	0.00	1587.30	1587.30	0.00	0.332	0.33
0N30	B	0.00	1021.00	1021.00	0.00	0.305	0.31
0N23	B	0.00	2187.50	2187.50	0.00	0.448	0.45
0P11	B	445.00	904.76	459.76	0.00	0.328	0.33
O601	C	0.00	1174.60	1174.60	0.25	0.41	0.16
Total Sum of Errors				7922.46			2.62

Table B-7. Comparison of distresses measured on site and predicted by ME-Software (AASHTOWare) using Model H

Project No	Sites	Longitudinal Crack (ft/mile)			Rutting Depth (inch)		
		Measured	Predicted	Error	Measured	Predicted	Error
0P11	C	965.49	1636.36	670.87	0.00	0.38	0.38
O601	A	0.00	321.43	321.43	0.50	0.32	0.18
0N34	C	0.00	500.00	500.00	0.00	0.49	0.49
0N30	A	0.00	1587.30	1587.30	0.00	0.33	0.33
0N30	B	0.00	1021.00	1021.00	0.00	0.31	0.31
0N23	B	0.00	2187.50	2187.50	0.00	0.45	0.45
0P11	B	445.00	904.76	459.76	0.00	0.33	0.33
O601	C	0.00	1174.60	1174.60	0.25	0.41	0.16
Total Sum of Errors				7922.46			2.62

Table B-8. Comparison of distresses measured on site and predicted by ME-Software (AASHTOWare) using Model I

Project No	Sites	Longitudinal Crack (ft/mile)			Rutting Depth (inch)		
		Measured	Predicted	Error	Measured	Predicted	Error
0P11	C	965.49	1116.28	150.79	0.00	0.48	0.48
O601	A	0.00	285.70	285.70	0.50	0.39	0.11
0N34	C	0.00	303.57	303.57	0.00	0.64	0.64
0N30	A	0.00	1460.32	1460.32	0.00	0.31	0.31
0N30	B	0.00	905.66	905.66	0.00	0.26	0.26
0N23	B	0.00	1937.50	1937.5	0.00	0.52	0.52
0P11	B	445.00	580.65	135.65	0.00	0.41	0.41
O601	C	0.00	966.67	966.67	0.25	0.47	0.22
Total Sum of Errors				6145.86			2.75

Table B-9. Comparison of distresses measured on site and predicted by ME-software
(AASHTOWare) using Model J

Project No	Sites	Longitudinal Crack (ft/mile)			Rutting Depth (inch)		
		Measured	Predicted	Error	Measured	Predicted	Error
0P11	C	965.49	1000.00	34.51	0.00	0.49	0.49
O601	A	0.00	392.85	392.85	0.50	0.28	0.22
0N34	C	0.00	500.00	500.00	0.00	0.50	0.50
0N30	A	0.00	1375.00	1375.00	0.00	0.31	0.31
0N30	B	0.00	1000.00	1000.00	0.00	0.30	0.30
0N23	B	0.00	2187.50	2187.50	0.00	0.43	0.43
0P11	B	445.00	857.14	412.14	0.00	0.34	0.34
O601	C	0.00	1238.10	1238.1.0	0.25	0.38	0.13
Total Sum of Errors				7140.10			2.72

Table B-10. Comparison of distresses measured on site and predicted by ME-Software
(AASHTOWare) using Model K

Project No	Sites	Longitudinal Crack (ft/mile)			Rutting Depth (inch)		
		Measured	Predicted	Error	Measured	Predicted	Error
0P11	C	965.49	1562.50	597.01	0.00	0.39	0.39
O601	A	0.00	328.13	328.125	0.50	0.31	0.19
0N34	C	0.00	419.35	419.35	0.00	0.53	0.53
0N30	A	0.00	1587.30	1587.3	0.00	0.35	0.35
0N30	B	0.00	1164.18	1164.18	0.00	0.34	0.34
0N23	B	0.00	2222.20	2222.2	0.00	0.45	0.45
0P11	B	445.00	888.80	443.8	0.00	0.34	0.34
O601	C	0.00	1086.96	1086.96	0.25	0.43	0.18
Total Sum of Errors				7848.92			2.77

APPENDIX C

Table C-1. Sensitivity analysis results

HMA Pavement Input	Distress types	Distress limits	lower value	Baseline value	Upper value	Distress due To lower value	Distress due to upper value	NSI	Level of Sensitivity
AC Thickness (in)	IRI (Roughness) (in/mi)	220	2	6	12	215.24	145.23	-0.2	S
	Total Rutting (in)	0.75	2	6	12	0.66	0.32	-0.3	S
	Alligator Cracking (%)	15	2	6	12	100	1.91	-3.9	VS
	Transverse cracking (ft/mi)	1500	2	6	12	3002.62	1837.03	-0.5	S
	Long. Cracking (ft/mi)	2000	2	6	12	2260.29	234.71	-0.6	S
AC Air void (%)	IRI (Roughness) (in/mi)	220	3	7	9	159.21	206.07	0.2	S
	Total Rutting (in)	0.75	3	7	9	0.44	0.51	0.1	S
	Alligator Cracking (%)	15	3	7	9	6.66	100	7.3	HS
	Transverse cracking (ft/mi)	1500	3	7	9	2695.8	2769.82	0.1	NS
	Long. Cracking (ft/mi)	2000	3	7	9	1600.07	7609.45	3.5	VS
AC PG Grade	IRI (Roughness) (in/mi)	220	1	2	3	195	188.3	0.0	NS
	Total Rutting (in)	0.75	1	2	3	0.51	0.45	-0.1	NS
	Alligator Cracking (%)	15	1	2	3	86.23	79.08	-0.5	S
	Transverse cracking (ft/mi)	1500	1	2	3	2629.98	2592.95	0.0	NS
	Long. Cracking (ft/mi)	2000	1	2	3	4947.59	3973.69	-0.5	S
Base Thickness (in)	IRI (Roughness) (in/mi)	220	3	7	12	202.78	184.31	-0.1	NS
	Total Rutting (in)	0.75	3	7	12	0.48	0.48	0.0	NS
	Alligator Cracking (%)	15	3	7	12	99.44	67.73	-1.6	VS
	Transverse cracking (ft/mi)	1500	3	7	12	2586.75	2750.52	0.1	NS
	Long. Cracking (ft/mi)	2000	3	7	12	9400.48	1550.48	-3.1	VS

NSI– normalized sensitivity index, S–Sensitive, NS–non- sensitive, VS–very sensitive, and HS–hyper sensitive.

Table C-2. Continued sensitivity analysis results

HMA Pavement Input	Distress types	Distress limits	lower value	Baseline value	Upper value	Distress due To lower value	Distress due to upper value	NSI	Level of Sensitivity
Base M_r (psi)	IRI (Roughness) (in/mi)	220	20000	30000	40000	199.59	184.96	-0.1	NS
	Total Rutting (in)	0.75	20000	30000	40000	0.49	0.47	0.0	NS
	Alligator Cracking (%)	15	20000	30000	40000	94.84	69.74	-2.5	VS
	Transverse cracking (ft/mi)	1500	20000	30000	40000	2664.79	2664.79	0.0	NS
	Long. Cracking (ft/mi)	2000	20000	30000	40000	6729.68	3200.27	-2.6	VS
Subgrade M_r (psi)	IRI (Roughness) (in/mi)	220	8000	12000	15000	197.51	174.28	-0.2	S
	Total Rutting (in)	0.75	8000	12000	15000	0.46	0.43	-0.1	NS
	Alligator Cracking (%)	15	8000	12000	15000	92.44	60.26	-3.7	VS
	Transverse cracking (ft/mi)	1500	8000	12000	15000	2643.67	2691.02	0.1	NS
	Long. Cracking (ft/mi)	2000	8000	12000	15000	2954.79	4640.88	1.4	VS
Traffic AADTT	IRI (Roughness) (in/mi)	220	250	2000	5000	154.14	208.8	0.1	S
	Total Rutting (in)	0.75	250	2000	5000	0.31	0.58	0.2	S
	Alligator Cracking (%)	15	250	2000	5000	7.88	100	2.6	VS
	Transverse cracking (ft/mi)	1500	250	2000	5000	2664.79	2664.79	0.0	NS
	Long. Cracking (ft/mi)	2000	250	2000	5000	1754.33	7701.23	1.3	VS
Climate	IRI (Roughness) (in/mi)	220	37.2	42.9	48.8	197.13	200.66	0.1	NS
	Total Rutting (in)	0.75	37.2	42.9	48.8	0.47	0.52	0.2	S
	Alligator Cracking (%)	15	37.2	42.9	48.8	86.83	89.24	0.6	S
	Transverse cracking (ft/mi)	1500	37.2	42.9	48.8	3002.62	3002.62	0.0	NS
	Long. Cracking (ft/mi)	2000	37.2	42.9	48.8	3919.28	4800.16	1.6	VS

NSI– normalized sensitivity index, S−Sensitive, NS−non- sensitive, VS−very sensitive, and HS−hyper sensitive.